

Proceedings of the

18th International Northern Research Basins Symposium and Workshop

Bergen-Geiranger-Loen-Fjærland-Voss, NORWAY
August 15-20, 2011



Organized by:
The Norwegian Council for Hydrology

Editors:
Oddbjørn Bruland, Knut Sand & Ånund Killingtveit

Table of Contents

Northern Research Basins preface	5
List of participants	9
Monitoring and Assessment Activities in the Arctic; Results from the 2011 AMAP assessments of climate change and pollution	
<i>Lars-Otto Reiersen</i>	13
Solid State Precipitation Comparison Study	
<i>Mareile Wolff, Eli Alfnes, Ragnar Brækkan, Ketil Isaksen, Asgeir Petersen-Øverleir and Erik Ruud</i>	14
Precipitation Phase Partitioning Based on Air Mass Boundary Identification	
<i>James Feiccabrino and Angela Lundberg</i>	20
SPA – Snow Pack Analyser	
<i>Wolfram Sommer and Reinhard Fiel</i>	21
Investigation of snowcover and melt patterns at Polar Bear Pass, Bathurst Island, Nunavut, Canada	
<i>Kathy L. Young, Jane Assini, Anna Abnizova and Elizabeth Miller</i>	24
Quantifying snow transport using snow fences and sonic sensors	
<i>Svetlana Stuefer, Matthew Sturm, Chris Hiemstra, Arthur Gelvin</i>	37
Development and testing of model updating techniques for the Hydropower industry in Norway	
<i>Oddbjørn Bruland, Knut Sand, Sjur Kolberg, Lena Tøfte, Kolbjørn Engeland, Glen Liston, Ashenafi Seifu Gragne, Knut Alfredsen</i>	38
Spatial distribution of snow depth at Hardangervidda Mountain, Norway, measured by airborne laser scanning	
<i>Kjetil Melvold and Thomas Skaugen</i>	39
Snow Accumulation studies in De Geer catchment, Spitsbergen	
<i>Ånund Killingtveit</i>	40
Evaluation of updating procedures for improving simulation of autumn flows	
<i>A. S. Gragne, K. Alfredsen, K. Engeland and S. Kolberg</i>	41
Automatic water quality measurements in the Baltic Compass project	
<i>Jari Koskiahho, Sirkka Tattari and Elina Jaakkola</i>	42
Ice impacts on behaviour and habitat choice in juvenile Atlantic salmon in steep rivers - summarizing results from the winter habitat project	
<i>Knut Alfredsen, Tommi Linnansaari and Morten Stickler</i>	43

Investigations of wintertime ice cover, circulation and water quality in Lake Vanajavesi	
<i>Matti Leppäranta, Onni Järvinen, Elina Jaatinen, Lauri Arvola, Anniina Kuiltomäki, and Kunio Shirasawa</i>	44
Hydropower Impact on Ice Regime	
<i>Netra Prasad Timalisina, Siri Almenning Stenhaug, Knut Alfredsen</i>	45
Subsurface hydrological carbon transport in the subarctic abiskoajokken catchment	
<i>Elin Jantze</i>	46
Ice problems on hydropower and implications of climate change	
<i>Solomon Gebre, Knut Alfredsen</i>	47
Recent fresh water fluxes from Arctic glaciers and ice caps	
<i>Jon Ove Hagen</i>	48
Nea-Nidelv Supersite	
<i>Ånund Killingtveit, Oddbjørn Bruland, Knut Alfredsen, Sjur Kolberg</i>	49
The consequence of permafrost change on hydrologic response across multiple scales	
<i>Johanna Mård Karlsson, Steve W. Lyon and Georgia Destouni</i>	50
An Improved Global Snow Classification Dataset for Hydrologic Applications	
<i>Glen E. Liston and Matthew Sturm</i>	51
Climate change impacts on snowmelt and runoff in a subarctic mountain basin	
<i>J. Richard Janowicz and John W. Pomeroy</i>	52
Comparison of streamflow simulations for a boreal mountainous basin using adjusted and multiple station data	
<i>Ming-ko Woo and Robin Thorne</i>	53
The effects of climate change on water bodies in the North European part of Russia	
<i>N. Filatov</i>	63
Jökulhlaups and sediment transport in Watson River, Kangerlussuaq, West Greenland	
<i>B. Hasholt, A.B. Mikkelsen, N.T. Knudsen</i>	64
A Satellite Perspective on Jökulhlaup in Greenland	
<i>Eva Mätzler, Bo Naamansen, Morten Larsen1, Christian Tøttrup, Dorthe Petersen and Kisser Thorsøe</i>	76
A Hydrology, Hydro-Climatology and Sediment Research Program related to the Canadian Oil Sands development	
<i>T.D. Prowse</i>	85
Multi-dataset time series of Arctic and sub-Arctic snow extent and snow water equivalent	
<i>Chris Derksen1* and Ross Brown2</i>	86

Preface

Welcome

It is an honor for the Norwegian Council for Hydrology to host the 18th International Northern Research Basins Symposium and Workshop. We warmly welcome all the symposium participants, keynote speakers and accompanying persons to interesting scientific sessions, fruitful discussions and friendly interaction during this week. During the symposium we will be visiting some of the most beautiful areas of the western coast of Norway. Hopefully the deep fjords, high waterfalls, steep mountains and glaciers will set the stage for a successful seminar and good memories from Norway.

Symposium Theme

The main theme of the 18th NRB symposium is **Methods for measuring, collecting and assimilating hydrological information in cold climate**. Technology development and innovation never stops, and the number of opportunities this gives grows exponentially. Both with regards to measurements, data collection, and methods of combining data from different sources we experience that horizons maybe more open now than ever before. Observations in the Northern regions are sparse. Thus it is important to exploit all sources for information available in these areas as efficiently and innovatively as possible. Alone one observation might not tell us much, but combined with information from other data sources the picture might become clearer. We hope by choosing this topic, that we have attracted presentations that give us an overview of how the hydrological community applies these opportunities in the northern regions.

For this meeting we are especially pleased to welcome:

- *Dr. Don Cline* as a keynote speaker for the main symposium theme: Methods for measuring, collecting and assimilating hydrological information in cold climate,
- *Dr. Lars Otto Reiersen* giving the introductory presentation on the Arctic Monitoring and Assessment Programme,
- *Dr. Knut Alfredsen* as a keynote speaker on the theme “Cold climate hydrology interactions with ecosystems”.
- *Prof. Terry Prowse* giving an invited talk on hydrological aspects related to the Canadian oil sands development.

NRB history and mandate

The NRB symposia was established in 1975 as part of the International Hydrologic Programme (IHP) by the National Committees of Canada, Denmark (Greenland), Finland, Norway, Sweden, the USA and the USSR. The Regional Working Group on Northern Research Basins was set up to foster research of river basins in northern latitudes and, unlike other snow and ice conferences, NRB is intended specifically for Arctic environments. Iceland joined the Working Group in 1992 and Russia has since taken over the role of the USSR. Countries with polar research programmes are eligible for associate membership; current associate members are the UK and Japan. Symposia are held every two years and alternate between North America and Europe.

Each member country can send up to 10 delegates to an NRB meeting, and the host country

can nominate additional participants as observers. Attendance is also open to observers from associate member countries and occasionally non-member countries. The chief delegate of the host country acts as the Chair for the interval from the conclusion of the previous meeting until the end of the current meeting.

Most NRB participants are hydrologists or glaciologists, however, participants have also included climatologists, geomorphologists, biologists, ecologists and now oceanographers. The objectives of the Northern Research Basins Working Group are:

- (1) to gain a better understanding of hydrologic processes, particularly those in which snow, ice, and frozen ground have a major influence on the hydrological regime and to determine the relative importance of each component of the water balance.
- (2) to provide data for the development and testing of transposable models which may be applied to regional, national and international water and land resource programmes;
- (3) to relate hydrologic processes to the chemical and biological evolution of northern basins;
- (4) to assess and predict the effect of human activities on the hydrologic regime in northern environments;
- (5) to encourage the exchange of personnel (technicians, scientists, research officers and others) among participating countries;
- (6) to provide information for the improvement and standardization of measurement - techniques and network design in northern regions;
- (7) to encourage exchange of information on a regular basis and
- (8) to set up task forces to promote research initiatives on topics of special interest to northern research basins.

NRB Task Forces

NRB fosters research between symposia by initiating taskforces which ask specific questions about the Arctic environment. Past task forces have included Prediction for Ungauged Basins (PUB) and Thermal Lake Regimes. One present task forces include Measurement of solid precipitation.

The following terms of reference for research taskforces is reprinted from the Proc. 9th International Northern Research Basins Symposium/Workshop, Canada, 1992. NHRI Symposium No. 10, T.D. Prowse, C.S. L. Ommanney and K.E. Ulmer (editors), p. 891-892.

- (1) The objective of an NRB Task Force is to continue liaison among member countries between NRB meetings, through investigation of an area of mutual concern.
- (2) A Task Force is constituted for two years, with the possibility of renewal for a maximum of two additional years. The Task Force is created during an NRB meeting, with a minimum participation of four member countries.
- (3) The Chair of the Task Force is appointed by the member country which proposed the subject for the Task Force. The Chair will confirm membership from supporting countries within one month of the NRB meeting.
- (4) A work plan should be formulated the Task Force within one month of its creation.

The plan is to include the objectives, the investigation approach and tangible outputs of the Task Force.

- (5) Membership and work plan of the Task Force must be approved by the Chief Delegates of the participating countries.
- (6) A progress report is to be distributed to the Chief Delegates at the end of the first year. Modifications are to be made to the work plan as appropriate.
- (7) A final report is to be delivered to the Chief Delegates one month before the next NRB meeting so that it may be distributed to the delegates in advance of the meeting.
- (8) A summary presentation is to be made by the Chair of the Task Force at the NRB meeting.
- (9) It is highly desirable that a proposed Task Force be identified and the concept circulated among Chief Delegates prior to an NRB meeting.

Acknowledgements

The organizers of the 18th NRB Symposium and Workshop would like to thank the following for their kind sponsorship, without which this meeting would not have occurred:

- The Research Council of Norway
- Statkraft
- CEDREN Centre for Environmental Design of Renewable Energy
- Norsk Hydrologiråd
- Sommer Mess-Systemtechnik
- Geonor
- ITAS - Instrumenttjenesten AS
- BKK
- SFE - Sogn og Fjordane Energi
- Sunnfjord Energi

We wish everyone a successful and enjoyable 18th NRB meeting!

The 18th NRB Organizing Committee:



Dr. Oddbjørn Bruland Statkraft
(chairman)



Dr. Knut Sand Statkraft



Prof. Ånund Killingtveit Department of Hydraulic and Environmental Engineering
Norwegian University of Science and Technology



Dr. Knut Alfredsen Department of Hydraulic and Environmental Engineering
Norwegian University of Science and Technology



Prof. Jon Ove Hagen Department of geosciences, University of Oslo



Dr. Kjetil Melvold Norwegian Water Resources and Energy Directorate

List of Participants

Austria:

Sommer, Wolfram Sommer Mess-Systemtechnik
Straßenhäuser 27
A-6842 Koblach, AUSTRIA
wsommer@sommer.at

Canada:

Derksen, Chris Environment Canada
4905 Dufferin Street
M3H5T4 Toronto, CANADA
chris.derksen@ec.gc.ca

Janowicz, Richard Yukon Water Resources
Box 2703
Y1A2C6 Whitehorse, CANADA
richard.janowicz@gov.yk.ca

Prowse, Jennifer 1620 Nelles Place
V8N 6L7 Victoria, BC, CANADA
prowset@uvic.ca

Prowse, Terry Water & Climate Impacts Research Centre
EC/W-CIRC, University of Victoria, P.O.Box 3060 STN CSC
V8W 3R4 Victoria, British Columbia, CANADA
prowset@uvic.ca

Woo, Caroline 902-1093 Kingston Road
M1N4E2 Scarborough, Ontario, CANADA
woo@mcmaster.ca

Woo, Ming-ko McMaster University
902-1093 Kingston Road
M1N4E2 Scarborough, Ontario, CANADA
woo@mcmaster.ca

Young, Kathy York University
N415 Ross, 4700 Keele Street
M3J 1P3 Toronto, CANADA
klyoung@yorku.ca

Denmark/Greenland:

Hasholt, Bent Department of Geography and Geology , University of Copenhagen
Øster Voldgade 10
DK1350 Copenhagen, DENMARK
bh@geo.ku.dk

Larsen, Morten Asiaq
P.O.Box 1003
3900 Nuuk, GREENLAND
mol@asiaq.gl

Petersen, Dorthé Asiaq
P.O.Box 1003
3900 Nuuk, GREENLAND
dop@asiaq.gl

Finland:

Järvinen, Onni University of Helsinki/Department of Physics
Erik Palmenin aukio 1, P.O. Box 48
FIN-00014 Helsinki, FINLAND
onni.jarvinen@helsinki.fi

Koskiaho, Jari Finnish Environment Institute
POBox 140
FIN-00251 Helsinki, FINLAND
jari.koskiaho@ymparisto.fi

Norway:

Alfredsen, Knut Norwegian University of Science and Technology
Dept. of hydraulic and environmental engineering
N- 7031 Trondheim, NORWAY
knut.alfredsen@ntnu.no

Bruland, Anne Loholtbakken 1A
N-7049 Trondheim, NORWAY
oddbjorn.bruland@statkraft.com

Bruland, Oddbjørn Statkraft Energi AS
Sluppenveien 6
N-7005 Trondheim, NORWAY
oddbjorn.bruland@statkraft.com

Fredriksen, Ivar GEONOR AS
PO Box 99 Røa
N-0701 Oslo, NORWAY
if@geonor.no

Gebre, Solomon Norwegian University of Science and Technology
Dept. of hydraulic and environmental engineering
N- 7031 Trondheim, NORWAY
solomon.gebre@ntnu.no

Gragne, Ashenafi Norwegian University of Science and Technology
Dept. of hydraulic and environmental engineering
N- 7031 Trondheim, NORWAY
ashenafi.gragne@ntnu.no

Haga, Oddvar Instrumenttjenesten AS
Frederik A. Dahls vei 20
N-1432 Ås, NORWAY
oddvar.haga@it-as.no

Hagen, Jon Ove University of Oslo, Department of geosciences
N-0316 Oslo, NORWAY
joh@geo.uio.no

Killingtveit, Liv Kirsti Roosevelts veg 16D
N-7058 Jakobsli, NORWAY
aanundk@c2i.net

Killingtveit, Ånund Norwegian University of Science and Technology
Dept. of hydraulic and environmental engineering
N- 7031 Trondheim, NORWAY
aanund.killingtveit@ntnu.no

Melvold, Kjetil Norwegian Water Resources and Energy Directorate/Department of
Hydrology
POBox 5091 Majorstua
N-0301 Oslo NORWAY
kjme@nve.no

Moen, Elisabeth Åsland Statkraft Energi AS
POBox 200 Lilleaker
N-0216 Oslo, NORWAY
elisabeth.aasland.moen@statkraft.com

Reiersen, Lars-Otto Artic Council
AMAP Secretariat, P.O.Box 8100 Dep.
N-0032 Oslo, NORWAY
amap@amap.no

Sand, Evalena
Ehrenpohl Thorvald Erichsens v.11
N-7020 Trondheim, NORWAY
knut.sand@statkraft.com

Sand, Knut Statkraft Energi AS
Sluppenveien 6
N-7005 Trondheim, NORWAY
knut.sand@statkraft.com

Timalsina, Netra Prasad Norwegian University of Science and Technology
Dept. of hydraulic and environmental engineering
N- 7031 Trondheim, NORWAY
netra.timalsina@ntnu.no

Wolff, Mareile The Norwegian Meteorological Institute
Henrik Mohns plass 1
N-0131 Oslo, NORWAY
mareile.wolff@met.no

Russia:

Filatov, Nikolay Northern Water Problems Institute, Karelian Research Center
Nevskogo 50
185030 Petrozavodsk, RUSSIA
nfilatov@rambler.ru

Sweden:

Bengtsson, Lars Lund University, Dept. of Water Resources Engineering
PO Box 118
S-22100 Lund, SWEDEN
lars.bengtsson@tvrl.lth.se

Destouni, Georgia Stockholm University, Dept. of Physical Geography and Quaternary
Geology
S- 10691 Stockholm, SWEDEN
georgia.destouni@natgeo.su.se

Jantze, Elin Stockholm University, Dept. of Physical Geography and Quaternary
Geology
Ola Hanssonsgatan 9
S- 11252 Stockholm, SWEDEN
elin.jantze@natgeo.su.se

Lundberg, R. Angela C. Luleå University of Technology LTU, Division of Geosciences &
Environmental Engineering
S- 97187 Luleå, SWEDEN
angela.lundberg@ltu.se

Mård Karlsson,
Johanna Stockholm University, Department of Physical Geography and Quaternary
Geology
Svante Arrhenius väg 8c
S- 10691 Stockholm, SWEDEN
johanna.maard@natgeo.su.se

Westerström, Göran Luleå University of Technology, Dept of Civil, Mining and Environmental
Engineering
S- 97187 Luleå, SWEDEN
goran.westerstrom@ltu.se

United States of America:

Cline, Don National Weather Service, NOAA, Office of Hydrologic Development
1325 East West Highway
Silver Spring MD 20910, USA
donald.cline@noaa.gov

Feiccabrino, James Luleå University of Technology / USAF Weather
PSC 3 Box 747
APO-AE 9021, USA
james.feiccabrino@gmail.com

Liston, Glen Colorado State University
CIRA-1375
FORT COLLINS, CO 80523-1375, USA

Stuefer, Sveta University of Alaska Fairbanks
PO Box 755860
Fairbanks, AK 99775, USA

**Monitoring and Assessment Activities in the Arctic;
Results from the 2011 AMAP assessments of climate change and pollution**

Lars-Otto Reiersen
Executive Secretary AMAP

AMAP was established in 1991 by ministers from the eight Arctic countries (Canada, Denmark, Finland, Iceland, Norway, Russia, Sweden and USA) and is today one of the working groups under the Arctic Council. The main task for AMAP has been to perform monitoring and assessment of the pollution of the Arctic, including documentations of effects on biota and humans. In 1993 AMAP was asked to include assessment of climate change and UV/ozone. In 1997 the first comprehensive circumpolar AMAP assessment was presented covering issues like persistent organic pollutants (POPs), heavy metals, radionuclides, oil and gas, climate and UV and human health. Since then several scientific based assessments have been prepared by AMAP - alone or as joint products with other international organizations. In 2004 the Arctic Climate Impact Assessment (ACIA) was presented as a joint work between AMAP and CAFF (Conservation of Arctic Fauna and Flora) and IASC (International Arctic Science Committee). In May this year, AMAP in cooperation with IASC, WCRP/CliC (World Climate Research Programme/Climate and Cryosphere Project) and IASSA (International Arctic Social Science Association) presented a new assessment of the effect of climate change on the Arctic Cryosphere - SWIPA – Snow, Water, Ice and Permafrost in the Arctic. In addition to this report, AMAP presented an assessment about the status for the mercury pollution of the Arctic and an assessment about the combined effects of climate change and persistent organics on Arctic ecosystems and humans.

This presentation will give an introduction to the Arctic Council and AMAP, results from the latest assessments regarding climate change (SWIPA) and pollutions - levels, trends and effects on Arctic ecosystems and humans. Finally, the presentation will cover some information about actions taken to reduce the threat to the Arctic ecosystems and humans and the initiative taken to improve the research and monitoring activities and access to data in the Arctic – the SAON process – Sustaining Arctic Observing Networks.

Solid State Precipitation Comparison Study

Mareile Wolff^{1*}, Eli Alfnes², Ragnar Brækkan¹, Ketil Isaksen¹, Asgeir Petersen-Øverlei² and Erik Ruud²

¹ Norwegian Meteorological Institute, Blindern, 0313 Oslo, NORWAY

² Statkraft, Lilleaker, 0216 Oslo, NORWAY

*Corresponding author, e-mail: mareile.wolff@met.no

ABSTRACT

Precipitation measurements have a well documented mostly wind dependent bias which is especially apparent during solid precipitation events. The resulting inaccuracy in precipitation data are a remaining area of concern in quantifying regional and global trends induced by climate change.

Norway, as a high-latitude country, has many solid precipitation events often combined with high wind speed, where the currently recommended adjustment functions have only limited validity. As a cooperation of The Norwegian Meteorological Institute, Statkraft and other Norwegian energy companies, this study aims to improve the quality of solid precipitation data.

In an extended field experiment, one minute data of two standard automatic precipitation gauges are compared with data of a reference precipitation gauge. The reference gauge is surrounded by an octagonal double fence construction which minimizes wind impact. Numerous instruments are measuring other important meteorological parameters at several locations at the test site, allowing for an in-depth analysis of recorded precipitation events. The goal is to develop a new set of adjustment functions for solid precipitation measurements that accounts for Norway's typical climate and is suitable for automated measurements.

After a one-year long pre-study, a location in the southern Norwegian mountain area was chosen as the test site. Measurements started in winter 2010/2011 and will continue during the following 1-2 winters. In this paper we'll describe the technical aspects of the instrumentation on site, present data and preliminary results from the test period and first winter.

KEYWORDS

solid precipitation; wind correction of precipitation; DFIR; precipitation measurements

INTRODUCTION

It is well known that gauge measurements of precipitation have a systematic undercatch mainly depending on wind-speed. The error is higher for snowfall than for rain observations. A large international solid precipitation intercomparison by the World Meteorological Organization (WMO) resulted in a quantification of these errors and a recommended set of empirically derived adjustment formulas for precipitation measurements (Goodison *et al.*, 1998). Since the standard gauges in most countries were manual during the intercomparison period, the WMO-study was focused on 12 hour manual precipitation measurements.

Today, various automated gauges are widely spread, most of them providing precipitation data every hour. The adjustment functions from Goodison *et al.* (1998) can not just be transferred to higher frequent measurements. Shorter accumulation periods result in less total precipitation and higher wind averages, both likely to change the adjustment curve. Acknowledging that new adjustment functions need to be determined, Smith and Yang (2010)

proposed and assessed a Geonor gauge inside a double fence construction (Geonor-DF) as a new reference for automated measurements. The resulting wind adjustment functions for the Geonor-DF will be used and further tested in this study for determining the reference precipitation.

The objectives of this study are to improve the data quality of Norwegian precipitation measurements and thus improving regional climate models and providing a better data base for budget and production calculation of the countries hydroelectric power plants. This will be achieved by comparison measurements between the Norwegian standard precipitation gauge Geonor plus Alter wind shield with the reference Geonor-DF at our test site in the southern Norwegian mountains. Numerous additional meteorological parameters will be monitored to support the analysis and development of a set of adjustment functions for wind induced undercatch of automated precipitation measurements.

OBSERVATION SITE

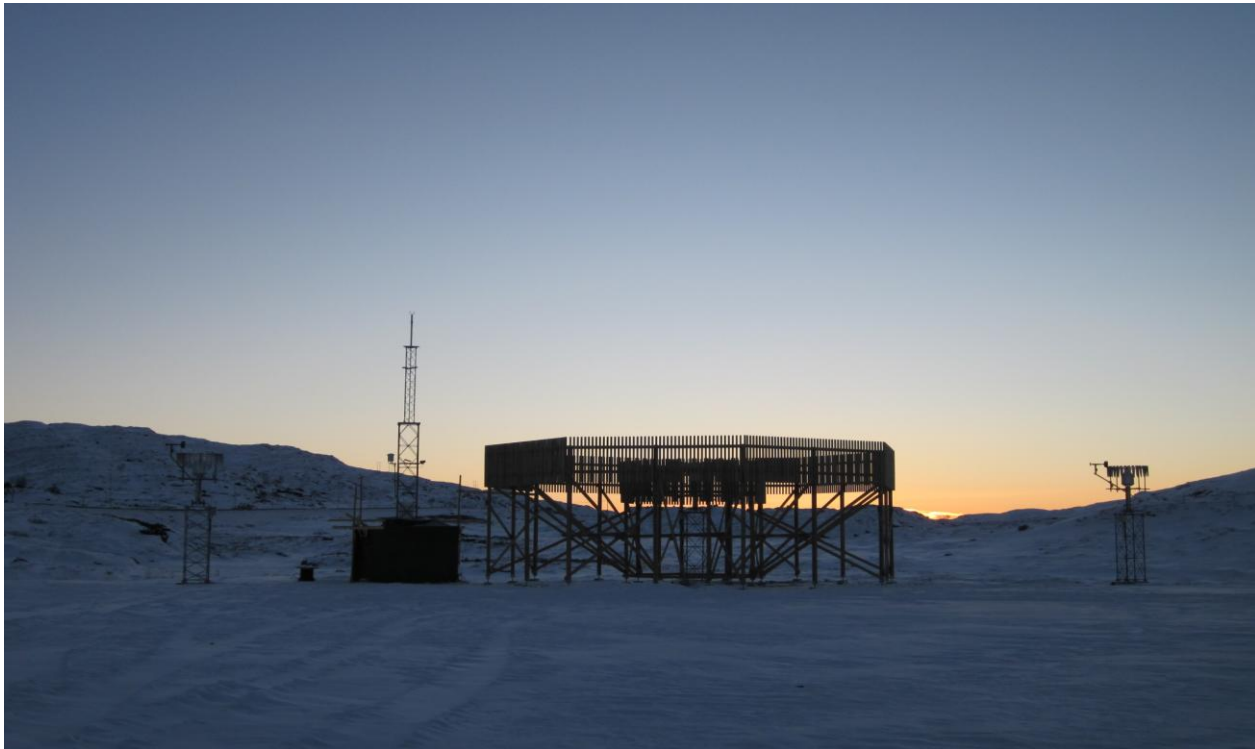


Figure 1: Photograph of the test site on Haukeli (990 m a.s.l.), southern Norway.

The test site “Haukeli” is located on a mountain plateau at 990m altitude close to the European Road E134, in the municipality Telemark (59.81°N, 7.21°E), photograph in Figure 1.

Three similar precipitation gauges (type Geonor with Alter wind shield, the standard automatic gauge in Norway) are placed along a line, vertical to the main wind direction with a distance of about 15m between them. To measure true precipitation, the gauge in the middle is surrounded by a double fence (DF) construction. The specifications of the double fence are the same as for the WMO recommended Double Fence Intercomparison Reference (DFIR) which uses a manual Tretyakov gauge in the centre, described by Goodison et al. (1998). The orifice height of all gauges is at 4.5m over ground, to assure enough clearing below, even when maximal expected snow depth of 3 m is reached. It furthermore prevents drifting snow from reaching the orifice.

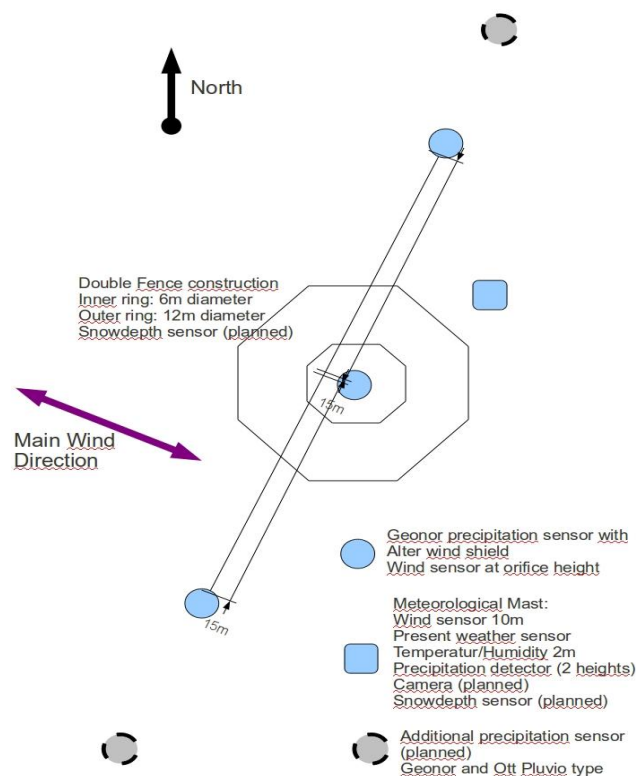


Figure 2: Schematic illustration of the test site

At each precipitation gauge a wind sensor is measuring wind speed and direction. A temperature sensor is directly mounted to each of the gauges. The measured temperature is used for controlling the heating system, which prevents snow blocking of the precipitation sensor. At a close-by meteorological mast, additional data are recorded: 10 m wind, 2m air temperature and humidity, precipitation detectors (yes/no) at 4 and 8 m and two present weather detectors at 6 m. Figure 2 shows a schematic overview of the test site and its instrumentation.

All data are recorded with one minute time resolution. Data are transferred hourly via a broadband Internet connection from the local storage to a server for further processing.

Completion/Extension of the instrumentation is planned for this summer. Two additional precipitation sensors are to be installed, extending the line of gauges on both ends, allowing for tests of additional sensor types and/or windshields. Snow depth sensors will be mounted at two locations. The meteorological mast will be equipped with one additional present weather sensors and a camera. An additional meteorological mast upstream will provide wind measurements in 4.5m and 10m. Two of the wind sensors on the test site will be upgraded from 2D to 3D sensors.

Precipitation measurements at the site started in the beginning of 2011. Additional sensors for several meteorological parameters have been applied during the following months. Table 1 gives the status of the actual instrumentation on site.

Table 1: Description and status of instrumentation at test site.

Sensor	Location	Parameter	Status
Geonor T200-BM (1000mm, 3str) Alter wind shield	North sensor	accum. precipitation	installed, data since Jan 2011
Geonor T200-BM (1000mm, 3str) Alter wind shield	South sensor	accum. precipitation	installed, data since Jan 2011
Geonor T200-BM (1000mm, 3str) Alter wind shield	double fence	accum. precipitation, reference	installed, data since Jan 2011
Pt100	North sensor	Geonor temperature	installed, data since Feb 2011
Pt100	South sensor	Geonor temperature	installed, data since Feb 2011
Pt100	double fence	Geonor temperature	installed, data since Feb 2011
Pt100	met. mast	air temperature	installed, data since Jan 2011
Gill WindObserver extreme	double fence	wind inside double fence, orifice height	installed, data since Feb 2011
Young Wind Monitor-SE	North sensor	wind North sensor, orifice height	installed, data since Feb 2011
Young Wind Monitor-SE	South sensor	wind South sensor, orifice height	installed, data since Feb 2011
Gill WindObserverII	met. mast	wind 10m height	installed, data since Feb 2011
Vaisala HMP155	met. mast	relative humidity	installed, data since Feb 2011
Thies precipitation sensor	double fence (4m)	precipitation yes/no	installed, data since Mar 2011
Thies precipitation sensor	met. mast (8m)	precipitation yes/no	installed, data since Mar 2011
Vaisala PWD21	met. mast (6m)	precipitation type, present weather	installed, data since Mar 2011
Thies LPM extended heating	met. mast (6m)	precipitation type, present weater	installed, data since May 2011
Ott Parsivel	met. mast (6m)	precipitation type, present weather	to be installed
SR50A	met. mast	snow depth	to be installed
SR50A	double fence	snow depth	to be installed
videocamera	met. mast	photo monitoring	to be installed

During the current summer season the test site will be upgraded with two additional precipitation gauges and possibly a meteorological mast northwest of the main instruments for undisturbed measurements of the 3D wind field.

RESULTS AND DISCUSSION

The homogeneity of the test site was assessed by Wolff et al. (2010) during a pre-study with data from two similar precipitation gauges and additional wind measurements at each sensor. The results testified a sufficient homogeneity of the site. Evaluation of the homogeneity will continue during the whole period of the study.

Data are manually quality checked and all measured parameter feature stability and high regularity. Preliminary analysis was done for a data period from February to April 2011. During that period about 100 hours precipitation was detected, from which 75 hours belong to 21 events with duration longer than 1 hour. The remaining 25 hours arise from separated

shorter precipitation events. In February and March, most precipitation was snow, whereas April precipitation was dominated by rain and mixed precipitation.

Total accumulation during this time was 336 mm in the Geonor-DF, whereas South and North sensor accumulated only 200 ± 8 mm, which is about 40% less than the reference (Figure 3). As expected, both single-event and a very limited statistical analysis reveal a significant correlation between undercatch and wind speed.

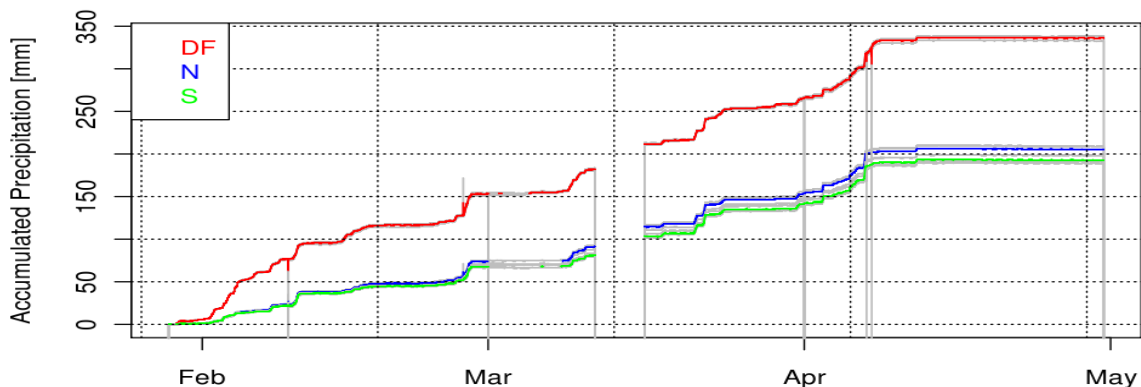


Figure 3: Total accumulated precipitation of precipitation gauges North (N), South (S), and inside double fence (DF) for the period February til April 2011.

The derivation of new adjustment functions, however, requires a larger dataset than half a winter of measurements could provide. Events need to be characterized by average and variation of meteorological parameters which might influence the catch efficiency of the precipitation sensor as wind speed, wind direction, temperature, precipitation type and intensity. Statistical analysis will be resumed next winter and continuously updated with the growing data set over the project period.

CONCLUSIONS

The Norwegian Meteorological Institute has started in cooperation with Statkraft AS and other Norwegian energy companies an initiative for the improvement of solid precipitation measurements. A pre-study attested the chosen test-site in the Southern Norwegian mountains sufficient homogeneity.

Instruments for the main period of the study were installed during autumn and winter 2010. The test site is operational since beginning of 2011, recording one minute data from 2 Norwegian standard gauges (Geonor and Alter wind shield) and a reference gauge in a double fence construction, as well as from several additional meteorological instruments. During the current summer period, the site will be extended with more instruments and is expected to be fully operational with at the beginning of next winter.

As expected, preliminary analysis of individual solid precipitation events and statistical examinations, based on data from February to April 2011, show that the standard gauges measure significantly less precipitation than the reference gauge, mainly depending on wind

speed and precipitation type. A complete statistical analysis needs more data than currently available and will be resumed during the coming winter. We expect to gain a solid data base over the course of the study (currently prospected over 2 more winters) for an in-depth analysis.

The test site provides, beside the named national interests in this study, the possibility for the Norwegian Meteorological Institute to actively participate in the currently planned WMO led intercomparison of methods and instruments for automatic snowfall/snow depth/precipitation measurements, proposed by Nitu and Wang (2010).

ACKNOWLEDGEMENT

This study is registered as project nr. SyPD-2.4_09 at Energi Norge AS and funded from the following Norwegian energy companies: Statkraft, Norsk Hydro, BKK, Agder Energi Prod., Lyse Energi, E-CO Energi, NTE, GLB and Trønder Energi.

The authors like to thank Eirik J. Førlund for his encouragement and support of this work.

REFERENCES

- Goodison, B.E., Louie, P.Y.T., Yang, D. 1998 *WMO Solid Precipitation Measurement Intercomparison - Final Report*. Instruments and Observing Methods Report No. 67, WMO/TD-No. 872, World Meteorological Organization, Geneva.
- Nitu, R., Wong, K. 2010 *CIMO Survey on National Summaries of Methods and Instruments for Solid Precipitation Measurement at Automatic Weather Stations*. Instruments and Observing Methods Report No. 102, WMO/TD-No. 1544, World Meteorological Organization, Geneva.
- Smith, C.D, Yang, D. 2010 An Assessment of the GEONOR T-200B Inside a Large Octagonal Double Fence Wind Shield as an Automated Reference for the Gauge Measurement of Solid Precipitation. In: *Proceedings of the 90th AMS Annual Meeting*. American Meteorological Society, Atlanta, GA.
- Wolff, M., Brækkan, R., Isaaksen, K., Ruud, E. 2010 A new Testsite for Wind Correction of Precipitation Measurements at a Mountain Plateau in Southern Norway. In: *Proceedings of WMO Technical Conference on Meteorological and Environmental Instruments and Methods of Observation (TECO-2010)*. Instruments and Observing Methods Report No. 104, WMO/TD-No. 1546, World Meteorological Organization, Geneva.

Precipitation Phase Partitioning Based on Air Mass Boundary Identification

Abstract

Hydrological models that apply the same surface-air temperature-based precipitation phase identification scheme for all precipitation events neglect the fact that surface precipitation phase is dependent on energy exchanges between falling hydrometers and air in the lower troposphere. Air mass boundaries change lower tropospheric conditions and therefore have diverse precipitation phase probabilities. However, similar air mass boundary passages also undergo comparable changes in surface conditions which are distinguishable from other precipitation causing events. Therefore, by identifying surface air mass boundaries, hydrological models can without measurement account for different lower tropospheric conditions. Manual 20 year precipitation observations from eight US weather stations were used to compare the number of misclassified precipitation events when all events were analyzed together and when analyzing cold-air-mass boundary (CAMB) events (recognized by rapid surface air temperature decrease) separately from non-CAMB events. A two temperature threshold precipitation phase identification scheme was used with a threshold for only snow (T_S) and another for only rain (T_R) and a linear snow fraction decrease between thresholds. These thresholds were found to be 1°C warmer for CAMB (0°C; 4°C) than for non-CAMB (-1°C; 3°C). When CAMB and non-CAMB events were analyzed separately, the number of misclassified precipitation events was reduced by 23%.

Key words: air mass boundary, modeling, precipitation phase, rain, snow.

PhD student James Feiccabrino¹⁾

Assistant Professor Angela Lundberg¹⁾

Dr. David Gustafsson²⁾

¹⁾ Division of Geosciences

Department of Civil, Mining and Environmental Engineering and Geosciences

Luleå University of Technology

SE- 971 87 Luleå, Sweden

²⁾ Department of Land and Water Resources Engineering,

Royal Institute of Technology KTH,

SE-100 44, Stockholm, Sweden

Corresponding author:

Angela Lundberg

Angela.Lundberg@ltu.se

Phone: 46-929-491207

SPA - Snow Pack Analyser

Reinhard Fiel¹, Wolfram Sommer¹ ¹ Sommer Mess-Systemtechnik, Koblach, Austria

ABSTRACT: The Snow Pack Analysing System is an automatic in-situ measurement system to determine the characteristics of snow covers. Measurements of the complex impedance along flat ribbon sensors in combination with a snow depth sensor result in the snow density, the snow water equivalent and the contents of ice and liquid water in the snow. The data values are recorded during the complete snow cover cycle from the accumulation until the melt off.

KEYWORDS: Snow density, snow water equivalent, liquid water content, on-line measurement.

1 INTRODUCTION

Obtaining information about snow by measurements is a difficult task. A multiplicity of parameters have to be registered to make reliable statements about the snow pack. Additionally, snow has an enormous variability in space and time. Up to now mainly punctual measurements are available for the relevant parameters. The Snow Pack Analyser (SPA) constitutes a revolutionary innovation in snow measurement. It is a world unique system for automatic and continuous measurement of all the relevant snow parameters like snow depth, snow density, snow water equivalent and contents of liquid water and ice. The SPA offers a modern and highly time delayed data gathering. There are several possibilities to install the system, depending on demand. Moreover, the system helps to reduce dangerous and expensive adoption of human resources in the wintry area.

2 PRINCIPLES OF MEASUREMENT

Snow consists out of the three components ice, water and air. Referring to different measurement frequencies, these components show different dielectric constants. Measuring the complex impedance along a flat ribbon sensor (SPA-sensor) with at least two frequencies allows to estimate the volume contents of the individual components. These specific volume contents equate the liquid water, ice and air content in the snow pack, which consequently results in the snow density. Combining the snow density

Corresponding author address: Reinhard Fiel,
Sommer Mess-Systemtechnik, Koblach, Austria;
tel: +43 5523 55989; fax: +43 5523 55989-19;
email: office@sommer.at

with the snow depth defines the snow water equivalent.

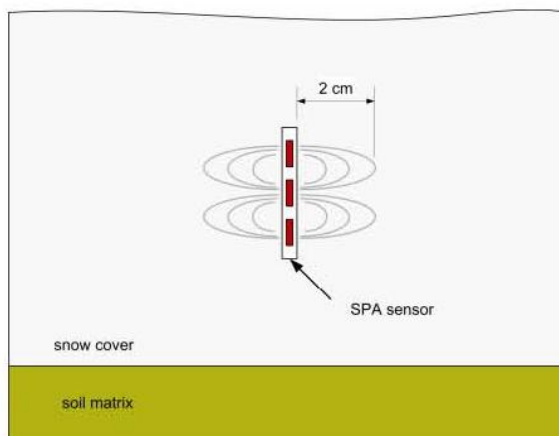


Figure 1. Principle of measurement of the SPA-sensor.

3 SYSTEM CONFIGURATION

The SPA-sensor is a 6 cm wide flat ribbon sensor including three copper wires. The length varies between 3 and 10 m. The sensor is installed with a suspension to ensure a tight and upright position. The snow depth sensor is based on transit-time measurements of an ultrasonic pulse between the sensor and the snow surface. Optional temperatures are measured at the ground level, at defined levels in the snow cover and the snow surface. A control unit performs all measurements, switches between multiply sensors and calculates the snow parameters. The data is transferred via a RS-232 interface for example to a data logging device.

The SPA-system can operate with up to four SPA-sensors. Their quantity and assembly is related to the desired measurement demands. The sensors are either installed sloping through the complete snow cover, or they are spanned horizontally in the snow at defined levels.

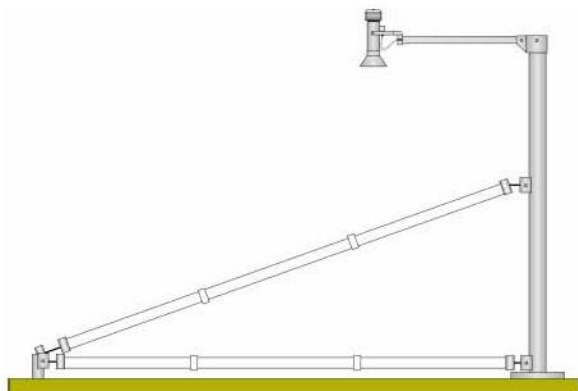


Figure 2. Combined assembly.

Combinations of sloping and horizontal sensors (Figure 2) increase the information content of the measurements. The sloping sensor determines the snow density, the snow water equivalent and the ice and liquid water contents of the complete snow cover. The horizontal sensor supplies additional information about the snow conditions close to the ground layer.

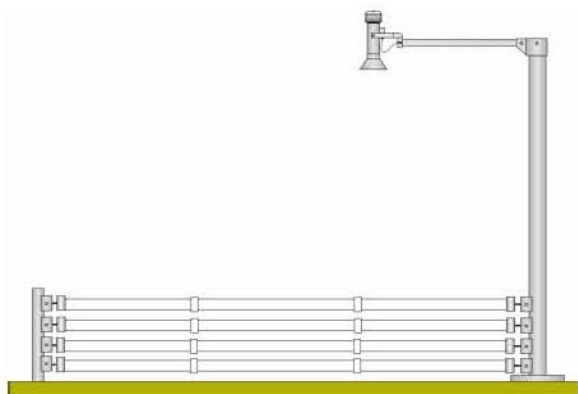


Figure 3. Profile assembly.

The horizontal installation of SPA-sensors with increasing levels (Figure 3) results in a profile of snow densities and liquid water contents. With this arrangement it is possible to detect the transit of snowmelt water through the snow pack and to generate a snow profile.

A further assembly is the installation of four sloping sensors in a star shape. The measurements of the individual sensors are averaged. This results in a high areal resolution, that corresponds to the pixel size of remote sensing data.

5 EXAMPLES

SPA-systems have been installed at various locations, including alpine sites in Switzerland, arctic sites in Sweden, and low mountain range sites in Germany. In the following examples of measurements are presented.

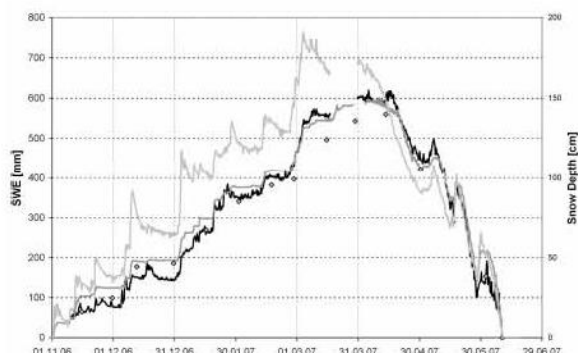


Figure 4. SWE of a 10 m sloping sensor, of a snow pillow and from manual probes at Weissfluhjoch test site (Switzerland) in the winter season 2006/2007.

In Figure 4 a comparison of different SWE measurements is shown. The black curve indicate the SWE data from the SPA-system and the dark gray curve SWE data from a 3x3 m snow pillow. The points are SWE samples from manual probes. For orientation the snow depth is displayed as a light gray curve. The SWE measured by the SPA-system shows a good correlation with the compared data during the complete snow cover cycle.

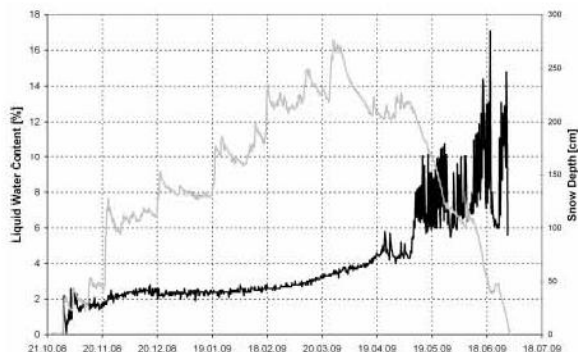


Figure 5. Liquid water content of a 5 m horizontal sensor situated in the ground layer at Weissfluhjoch test site (Switzerland) in the winter season 2008/2009.

The liquid water content in Figure 5 is a unique parameter of the SPA-system and represents the volume content of liquid water along the SPA-sensor in the snow cover. It has a significant increase at the beginning of the water run-off and can show a daily variation during the melting process.

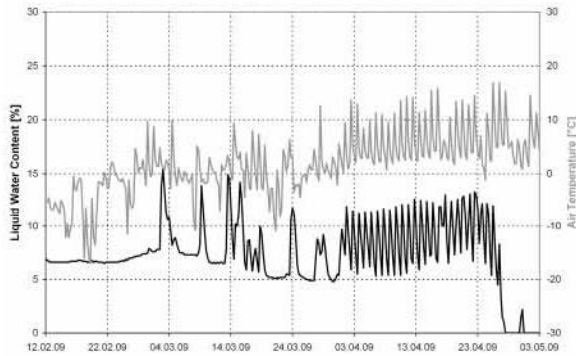


Figure 6. Liquid water content of a 5 m horizontal sensor at Hindelang test site (Germany) in the winter season 2008/2009.

The data of Figure 6 is from a low mountain range in Germany. The liquid water content is high at the beginning of March. A slight increase of the liquid water above saturation causes a sudden further rise of the liquid water, that is reduced by run-off. The daily variation in the melting period correlates with the daily temperature but the maximum has a slight shift into the evening.

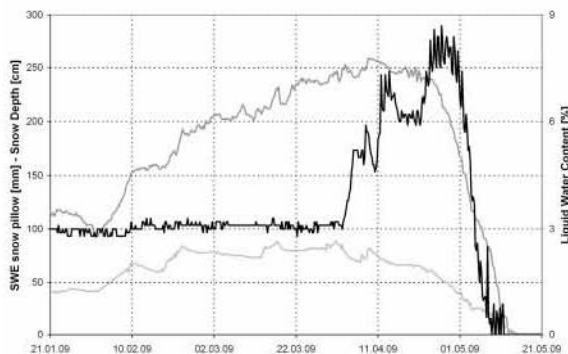


Figure 7. SWE of a snow pillow and liquid water content of a 5 m horizontal sensor at Korsvattnet test site (Sweden) in the winter season 2008/2009.

At the beginning of April the water content increases in Figure 7. The snow depth and the SWE of the snow pillow do not show significant changes at that time. The melting process has started. At a liquid water content of about 7-8 % the SWE starts to decrease, the run-off of the water from the snow cover has started.

In Figure 8 a compression of the snow occurs at the beginning of April while the SWE stays constant. The start of the run-off is defined by the decrease of the SWE. A significant increase of the liquid water content can be seen prior to the starting of the run-off. Therefore the liquid water content can provide a forecast of the point in time of the water run-off.

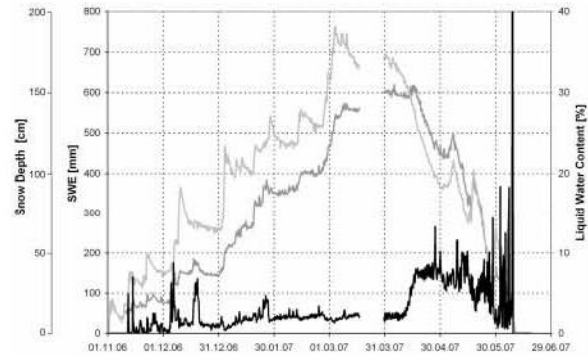


Figure 8. Liquid water content, SWE and snow depth of a 10 m sloping sensor at Weissfluhjoch test site (Switzerland) in the winter season 2006/2007.

5 FIELDS OF APPLICATION

For hydropower companies and flood prevention authorities the precise monitoring of water resources on catchment scales is indispensable for the prognosis of snowmelt run-off, which in return is relevant for flood prevention. In agriculture and mining estimations of the infiltration of melting water into the soil or underground are of basic interest. The information about the liquid water content of the snow pack makes it possible to estimate the point of saturation and snowmelt run-off. Thereby the system offers an important upgrading information for hydrological models. Furthermore these information is also important for snowmelt models, referring to remote-sensing data. The SPA can be a ground control for calibration. Snow density and liquid water content are fundamental parameters for the risk assessment of wet snow avalanches. The SPA helps to improve the quality and density of data for the responsible authorities. Thereby the systems contributes to increase the security of alpine villages and skiing-regions.

6 CONCLUSION

The SPA-system is an in-situ measurement system for snow density and snow water equivalent. The unique determination of the liquid water content enables a wide field of new applications. The possibility to arrange up to four SPA-sensors in sloping or horizontal installation enables to optimize the information depending on demands. The system can be simply installed even at hillsides and is not influenced by ice layers in the snow cover. The unique principle of measurement fulfils all the needs regarding to accuracy and reliability and will set new standards in the future.

Investigation of snowcover and melt patterns at Polar Bear Pass, Bathurst Island, Nunavut, Canada

Kathy L. Young*, Jane Assini, Anna Abnizova and Elizabeth Miller

Dept. Geography, York University, Toronto, Ontario, M3J 1P3, CANADA

*Corresponding author, e-mail: klyoung@yorku.ca

ABSTRACT

Extensive wetlands are important ecosystems in the Canadian High Arctic but little is known of their hydrology and future sustainability to climate warming. Here we examine the present (2008 - 2010) and future seasonal snowcover and melt of an extensive low-gradient wetland at Polar Bear Pass (PBP) (75° 40'N, 98° 30'W). This wildlife sanctuary (100 km²) is characterized by two large lakes and numerous tundra ponds and is bordered by rolling hills with incised hillslope stream valleys.

In arctic environments, snow remains one of the most important sources of water for wetlands. Terrain based end-of winter snowcover measurements (snow, depth, density, SWE) together with direct and modelled estimates of snowmelt allowed the temporal and spatial patterns to be evaluated. In addition, we explore how the snowmelt pattern at PBP could be modified (*e.g.* timing, duration) in response to future climate change (*e.g.* rising air temperature, end-of winter snowcovers). Inter-annual variability in spatial snowmelt patterns is evident at PBP and can be attributed to a non-uniform snowcover distribution and local microclimatic conditions. In the future, in response to warmer spring temperatures, snowmelt could be advanced by two weeks.

KEYWORDS

Arctic Snowcover; Arctic Wetland; Snowmelt

1 INTRODUCTION

Wetlands are critical landscapes in the High Arctic, providing food for migratory birds and larger fauna such as caribou and muskox. They also serve to store and replenish freshwater supplies and recently they have been the focus of interest in terms of their role in up-taking and releasing greenhouse gases such as carbon dioxide (CO₂), methane (CH₄) and water vapour (H₂O). Snow remains an important source of water into these ecosystems, often replenishing ponds and lakes and re-saturating wet meadow areas at the end of a cold winter season. Since the mid 1990's, we have investigated the hydrologic processes, including snowcover distribution and snowmelt, in a range of wetlands from the small patchy type (local scale - 1 to 10 km²), up to the meso-scale (*ca.* 25 km²), and we have a reasonable understanding of the hydrologic dynamics of these ecosystems and their water budgets. In 2008, our studies shifted attention to much larger wetland systems existing in the Canadian High Arctic. Up until then we knew little about their hydrology and role in the broader landscape, *i.e.*, carbon movement, runoff into polar seas, influence, or uptake/loss of greenhouse gases. The objectives of this study are to first present our knowledge concerning the snowcover and melt pattern processes for a three year period at Polar Bear Pass, an extensive low-gradient wetland situated in the middle of Bathurst Island. Secondly, we will

investigate the future snowcover and melt conditions for this site as predicted by climate change scenarios (ACIA 2005), and discuss the implications of such changes.

2 STUDY AREA

The study took place at Polar Bear Pass (PBP), located in the middle of Bathurst Island (75° 40'N, 98° 30'W) from 2008 to 2010 (Figure 1). Polar Bear Pass (20 km long x 5 km wide) is a designated wildlife sanctuary and is classified as a Ramsar site. As is typical of wetland complexes, it comprises wet meadows, dry and wet ground, two large lakes and a mosaic of ponds of varying shapes and sizes situated on a range of substrate types (coarse to fine-grained), and has a low gradient (*ca.* 0.002, <0.1% slope). In July 2010, Terra-SarX imagery revealed about 4800 ponds here (Sina Muster, personal communication). The Pass runs east-west and is bordered by low-lying hills to the north and south with an elevation rising from about 23 m up to 150 m. The slopes themselves are dissected by a series of v-notched valleys (about 50 of varying order) which are effective in transferring water and nutrients to the low-lying wetland (Young *et al.* 2010).

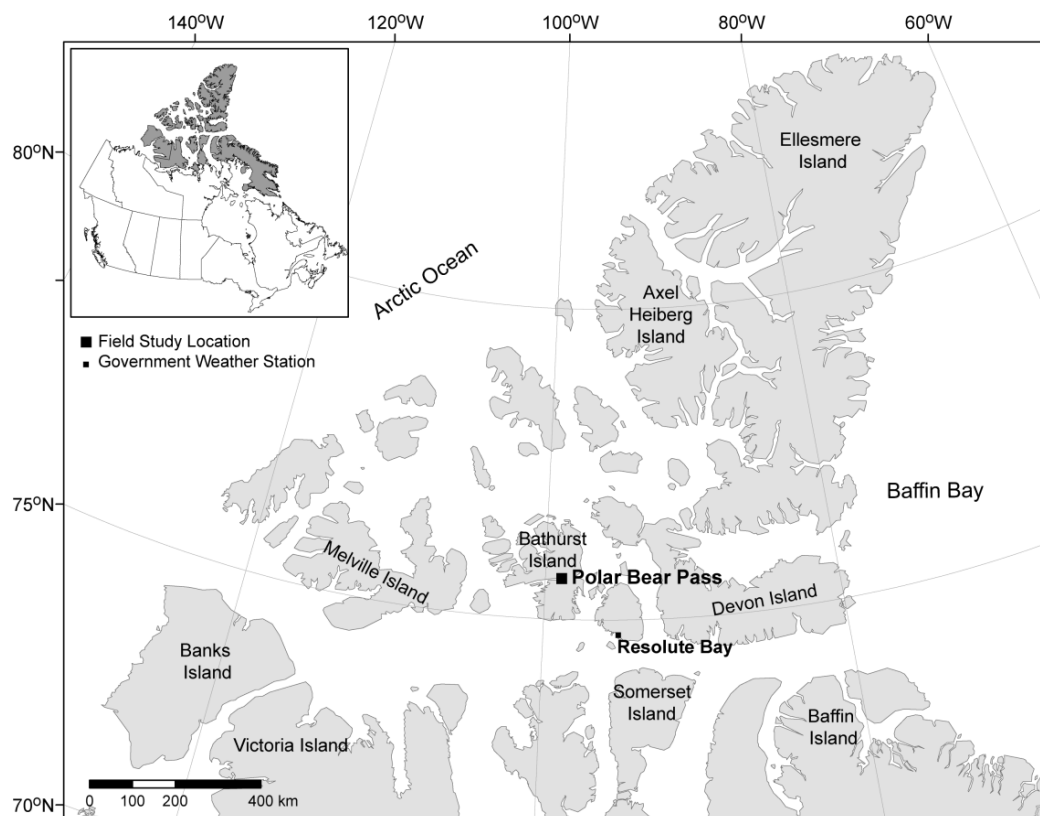


Figure 4 Location of Polar Bear Pass (75° 40'N, 98° 30'W), Bathurst Island, Nunavut, Canada (map modified after Young *et al.* 2010).

3 METHODOLOGY

3.1 Snowcover

Detailed end-of winter snowcover measurements (depth, density) were carried out from mid-to late May (2008-2010). A terrain-based snow survey of representative sites (plateau, wet meadow, pond, lake, late-lying snowbed, stream valley, etc) was followed (see Woo 1997).

The results of the local snow survey were then up-scaled to the regional scale utilizing two topographical maps covering the area (Caledonian River, 1985, 68H/11, 1:50 000 and McDougall Sound, 1994, 68H, 1:250 000). A 10 × 10 m grid was applied over the digitized maps, and each 10 m² grid cell (based on typical size of ponds) was classified as one of the main terrain types. There were 18 possible values, based on terrain type and geographical location in the Pass. This allowed snow survey estimates to be interpolated across the entire low-lying wetland.

3.2 Snowmelt

Snowmelt measurements at PBP consisted of both direct measurements of surface ablation of key terrain types (e.g. pond, wet meadow, late-lying snowbed, plateau, etc) using the approach outlined by Heron & Woo (1978) and employment of a physically-based snowmelt model (see Woo & Young 2004). Specifically, direct measurements of ablation were made daily at four sites: pond, wet meadow, late-lying snowbed and plateau. This involved measuring the distance (± 5 mm) from the top of the snowpack to a stable reference point (*i.e.* a string held taut between two dowels). An average of 10 height measurements at each site was recorded daily. Daily surface density was also recorded in order to determine surface melt in snow water equivalent units (mm/day).

The physically-based snowcover model (Woo & Young 2004) was useful in distributing the snowcover and melt across the Pass for 2008-2010. Initially, this model builds up the snowcover at varying terrain units with respect to a base station; here, a centrally - located wet meadow site. It considers slope, aspect and lapse rates when determining initial snowcover depth and cold content. Meteorological inputs into the model include hourly inputs of incoming solar radiation (K_{\downarrow} , W/m²), air temperature (T_{air} , °C), relative humidity (%), precipitation (mm), and pressure (Pa). Radiation is adjusted for aspect, temperatures and relative humidity and melt will only occur once the daily cold content is fulfilled. Adjustments can be made to the albedo algorithm for different snowpacks (seasonal vs. persistent) and the wind function (sheltered vs. exposed landscapes). Meteorological information for the model came from a centrally located station in the middle of the wetland and two roving meteorological stations across the Pass (see Young & Labine 2010 for details on the instrumentation used). A Hobo pressure transducer provided pressure data, and in the case of missing data, pressure data from Resolute Bay was substituted. The model outputs daily melt for various terrain units. The model's reliability in High Arctic wetlands, and at this specific wetland site has been well documented (*e.g.* Young 2008; Abnizova & Young 2010; Young *et al.* 2010; Assini & Young submitted).

To investigate the impact of future alterations in air temperature and precipitation (*i.e.* late-winter snowcover), we adjusted the snowmelt model inputs (snow, temperature) based on the ACIA future climate change scenarios (ACIA 2005) (see Table 1). No changes to rain-on-snow events were attempted at this time, though recent studies have remarked on its importance (Floyd & Weiler 2008; Ye *et al.* 2008).

Table 2 Climate change scenarios (*after* ACIA 2005) examined in the snowmelt sensitivity study at Polar Bear Pass.

Scenario	Air Temperature °C	End-of-winter Snowcover: % Change from 2008 levels
<i>Conservative</i>	↑ 0.08°C	↑ 2%
<i>Moderate</i>	↑ 1.12°C	↑ 5%
<i>Extreme</i>	↑ 4.00°C	↑ 15%

Table 2 Climatic data for Polar Bear Pass and Resolute Bay, May-July, 2008 to 2010.

		May ¹			June			July			Energy Fluxes ²	
		Tair	PPT	U	Tair	PPT	U	Tair	PPT	U	Q*	Q _T
		°C	mm	m/s	°C	mm	m/s	°C	mm	m/s	(MJ/m ²)	(MJ/m ²)
PBP	2008	-8.3	0	4.4	2.6	19.5	4.3	6.9	44.1	4.2	260	141
	2009	-10.5	0	5.8	1.9	2.1	4	5	61.7	4.4	235	121
	2010	-8.4	2.0	11	2.6	0	4	7.7	35.8	3.7	235	167
Resolute Bay	2008	-7.1	5.3	6.1	2.2	21.6	7	5.3	33	6.3		
	2009	-10.3	1.2	5.1	1	3.4	5.7	5.3	64.3	6.1		
	2010	-8.7	9	5.5	2.2	3.4	4.9	5.4	36.4	3.8		
	1971-2002	-10.9	9.5	5.6	-0.1	14.7	5.7	4.3	20.2	5.8		

Precipitation measurements at Polar Bear Pass were collected during 25-31 May, 19-31 May, and 14-31 May in 2008, 2009 and 2010, respectively. ²The total energy fluxes at the main wetland site during the snowmelt season June 2–30. Note Q_M , energy available for melt = Q^*+Q_T , where Q^* is net radiation and Q_T is the turbulent fluxes (Q_H+Q_E).

4 RESULTS & DISCUSSION

Weather conditions at Polar Bear Pass (PBP) during the period from 2008-2010 are comparable to those of Resolute Bay confirming a polar desert climate designation (Table 2). During the snowmelt period at PBP (June and July) average air temperatures were slightly warmer in 2010 (5.2 °C) than in 2008 (4.8 °C) and 2009 (3.4 °C). Precipitation at Polar Bear Pass was negligible during snowmelt but increased during the summer season with above average levels in 2008 and 2009. Overall, summer precipitation at Polar Bear Pass was comparable to Resolute Bay (Table 2).

In 2008 and 2009, turbulent energy comprised 35% and 34% of the net energy required for melt (Q_M) where $Q_M=Q^*+Q_T$ given that PPT inputs were small during melt. In 2010, turbulent energy was slightly higher at 41% (Table 2). At PBP, Q^* can be considered the most important energy flux for snowmelt, as occurs elsewhere in the High Arctic (Woo and Guan 2006; Abnizova and Young 2010).

4.1 End-of Winter Snowcover

Figure 2 illustrates the end-of winter snowcover results for the various years 2008-2010 and includes snow depth (cm), snow density (kg/m^3), and snow water equivalent (mm) for typical terrain units comprising the wetland. As expected, wind-blown terrain (plateau, ponds, lakes) tend to accumulate less snow than sheltered valleys and the lee of slopes where winds are dampened. Variability in snowcover remains the norm with the deepest snow occurring in 2010. Like other environments including temperate ones, snowcover variability in terms of water equivalent units (see Figure 2c) largely depends on the variation in snow depth (see Figure 2a) which ranges from 6 to 91cm. Snow density is more uniform, ranging from 200 to 300 kg/m^3 for the terrain units in most years (Figure 2b). Higher densities occurring in deep snow (valleys, lee of slopes) or shallow snowpacks where strong winds enhance wind slab. Dashed lines in Figure 4.1 illustrate the areally weighted snow water equivalent for the low-lying wetland area. Snowcover varies slightly from year to year (46-65 mm) with deeper snow occurring in 2010. Surprisingly, these estimates are akin to a wetland having a polar oasis-type climatic regime (Woo & Guan 2006) rather than one influenced by a polar desert climate (Abnizova & Young, 2010).

Pooled snowcover results for 2008 to 2010 (not shown) indicate that a good relationship exists for SWE (mm) in relation to snow depth (cm) for a range of terrain units ($y=3.06x$, $R^2=0.96$, $n=36$, $p<0.001$). Similarly, a good agreement exists for ponds located across the Pass (north, south, east and west sectors) ($y=2.76x$, $R^2=0.89$, $n=25$, $p<0.001$).

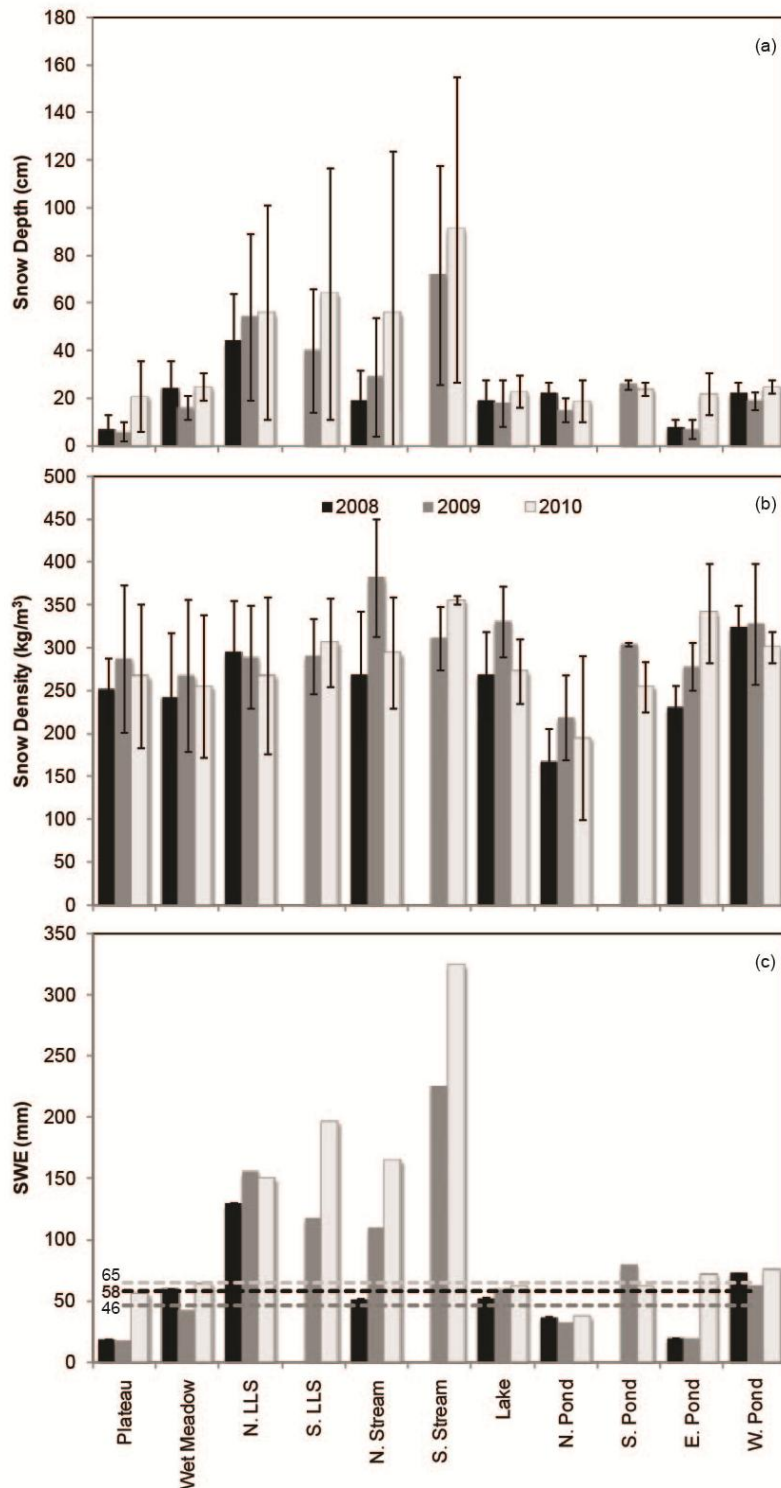


Figure 2 End-of-winter snow survey (depth, density and SWE) of terrain and ponds of Polar Bear Pass (PBP) for 2008, 2009 and 2010. Dashed lines in the SWE diagram indicate basin averaged SWE values for the three years of study. Standard deviations are given by error bars.

4.2 Snowmelt

4.2.1 Terrain units

Figure 3 indicates the measured snowmelt pattern for the different terrain units in 2008-2010. Comparable climate and snowpack conditions between the three year periods created similar melt timing and duration, especially for the shallower snowpacks. For the plateau, wet meadow, and pond sites (shallow snow), active melt occurred in the first week of June, and most of the melt was effectively over by the middle of June. Plateau areas melted out earlier than the ponds and the wet meadows (Figure 3a). In 2008-2010, the average late-lying snowpack (value obtained from snow survey) melted out by June 19. Deeper parts of the hillslope snowpack persisted past the main melt period (see LLS-P lines in Figure 3b). In 2008 and 2010 it lingered until June 25 but in 2009, due to a colder spring and summer, it lasted well into July. No measured values were made of the deep snowpacks in the hillslope stream valleys which bordered the low-lying wetland.

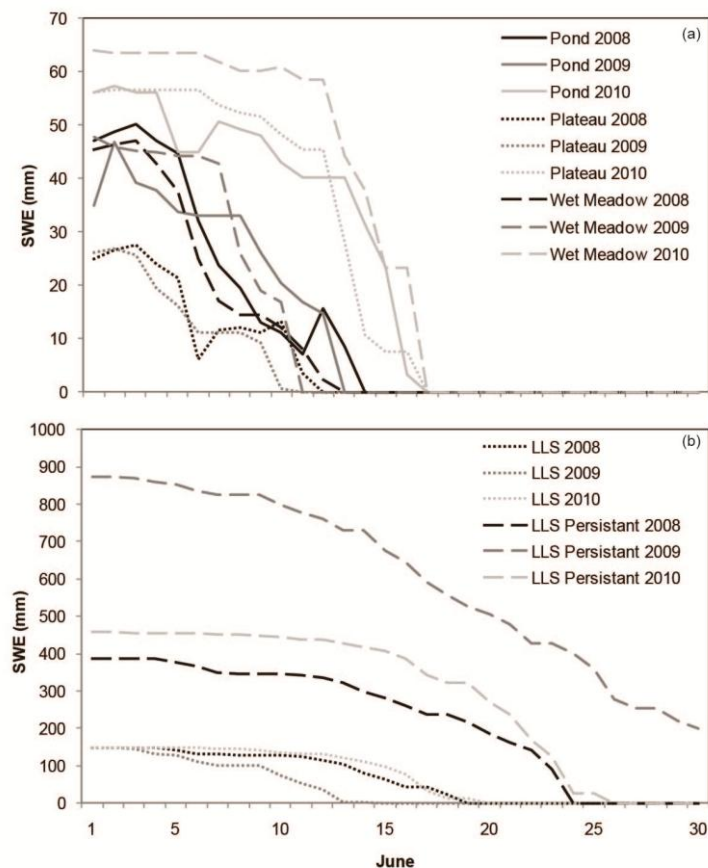


Figure 3 Measured daily snowmelt (mm) of four terrain types typical of PBP: plateau, wet meadow, and pond (a); and a south-facing late-lying snowbed (b), June 2008-2010. Initial values are from the end-of-winter snow survey. Persistent refers to the snowcover which remains after the average hillslope snowpack has depleted.

4.2.2 Low-lying wetland

To assess the spatial and temporal variability of melt over the wetland, the end of winter snowpack information and snowmelt pattern was upscaled to the entire low-lying wetland (about 20 km x 5 km) for 2008-2010 (Figure 4) using modelled melt and GIS. The various

terrain units were identified to a resolution of 10 m² (typical size of pond). These maps reveal a number of patterns. First, due to deeper snow and cooler conditions in 2010, active snowmelt was delayed by a few days (June 17) in comparison to 2008 (June 13) and 2009 (June 15). Snowmelt was generally over by the third week in June spanning from June 19 (2008) to June 23 (2010). In a shallow snow year (2009) the eastern part of the Pass melted out quicker than the western edge; the reasons for this remain unclear. Aspect plays a role in the Pass, i.e., the snowpack is slower to disappear in the southern part of the Pass (north-facing). In 2009, observations indicated that sediment windswept off the Plateau onto the northern half of the Pass served to accelerate melt, while the southern part of the Pass remained relatively clean. Delivery of sediment did not occur in 2010 (deeper, more extensive snowpack on the upland), suggesting that this phenomenon only occurs in low snow years, when adjoining plateaus are relatively barren, or else blown free of snow during periodic wind storms. The acceleration of melt due to aeolian erosion and deposition has been found elsewhere in the High Arctic (Lewkowicz & Young 1991; Woo *et al.* 1991).

Depletion curves are uniform for the three years (2008-2010) and show two distinct legs (data not shown). During the early melt season, the snowcover is nearly 100% across the Pass, and then it disappears quite rapidly. By the time 10% of the initial snowpack remains only about 20% of the area is snow covered. These depletion curves differ from other basins, such as hilly catchments where the number and types of terrain-types may be more diverse leading to variable end-of winter snowcover and non-uniform melt (Woo & Young 2004).

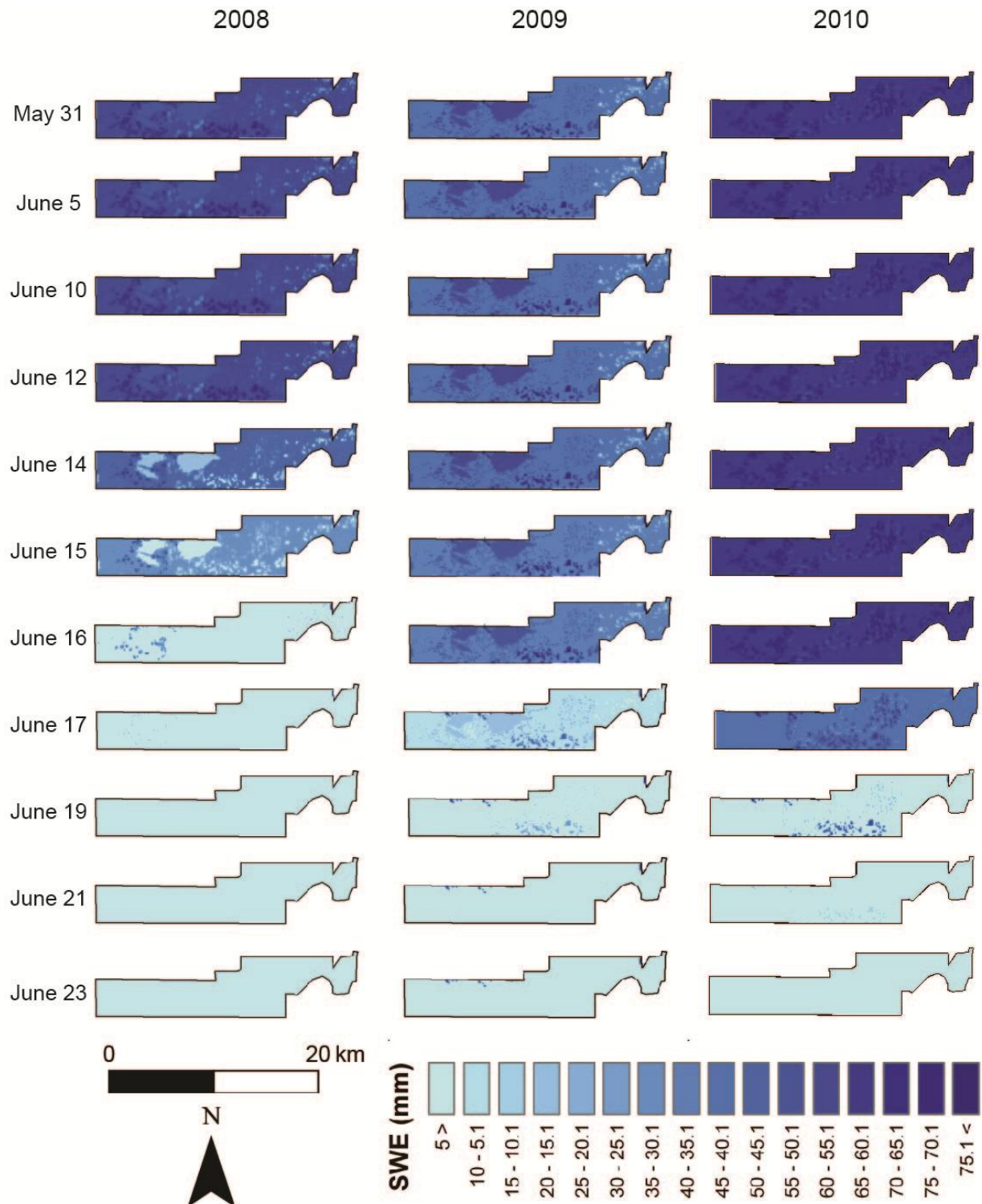


Figure 4 Time series of melt simulations for the low-lying wetland at PBP during the main snowmelt periods (2008, 2009 and 2010).

4.3 Future Snowcover and Melt at PBP

Climate change scenarios predict a much different climate for high latitude sites. Employing recent climate change scenarios reported in the ACIA (2005) report (see Table 1), we simulate

future conditions of enhanced air temperature and snowcover for PBP using 2008 initial conditions (Figure 5). The results clearly reveal that slight increases in the snowpack and spring air temperature (Conservative Scenario) will not affect the timing of melt and its duration by much, perhaps only by a day or two. Nevertheless, despite a 5% increase in the snowpack, a rise in air temperature of 1°C will accelerate melt and the melt period will be shortened by about a week. The greatest change is expected for years with a rise in air temperature of 4°C, even despite a deeper snowpack (15% higher), snowmelt could be advanced by 2 weeks. In this situation, the thaw season could begin in early June, which would enhance evapotranspiration losses and accelerate ground thaw for this wetland. Analysis using 2009 and 2010 initial conditions revealed similar patterns (data not shown). Given that we are already observing pond desiccation and sizeable drops in pond water tables during warmer and drier seasons (e.g. 2007-Young & Labine 2010), we speculate that PBP might become drier, and small, shallow tundra ponds will dry out for extended periods, especially ponds lying in coarse substrates or having no reliable hydrological linkages to their catchments (Abnizova and Young, 2010). Moreover, landscape transitions from ponds to wet meadows, and/or wet meadows to drier meadows are entirely possible and this transformation in the landscape might eventually impact migratory birds and the grazing patterns of muskox and caribou. Finally, our sensitivity study, while simplistic, does support the modelling efforts of others. For instance, Pohl et al. (2007) indicated that the date of peak runoff (associated with snowmelt) in Trail Valley Creek, Northwest Territories, Canada would be advanced by 6 - 25 days under similar climate changes in temperature and precipitation.

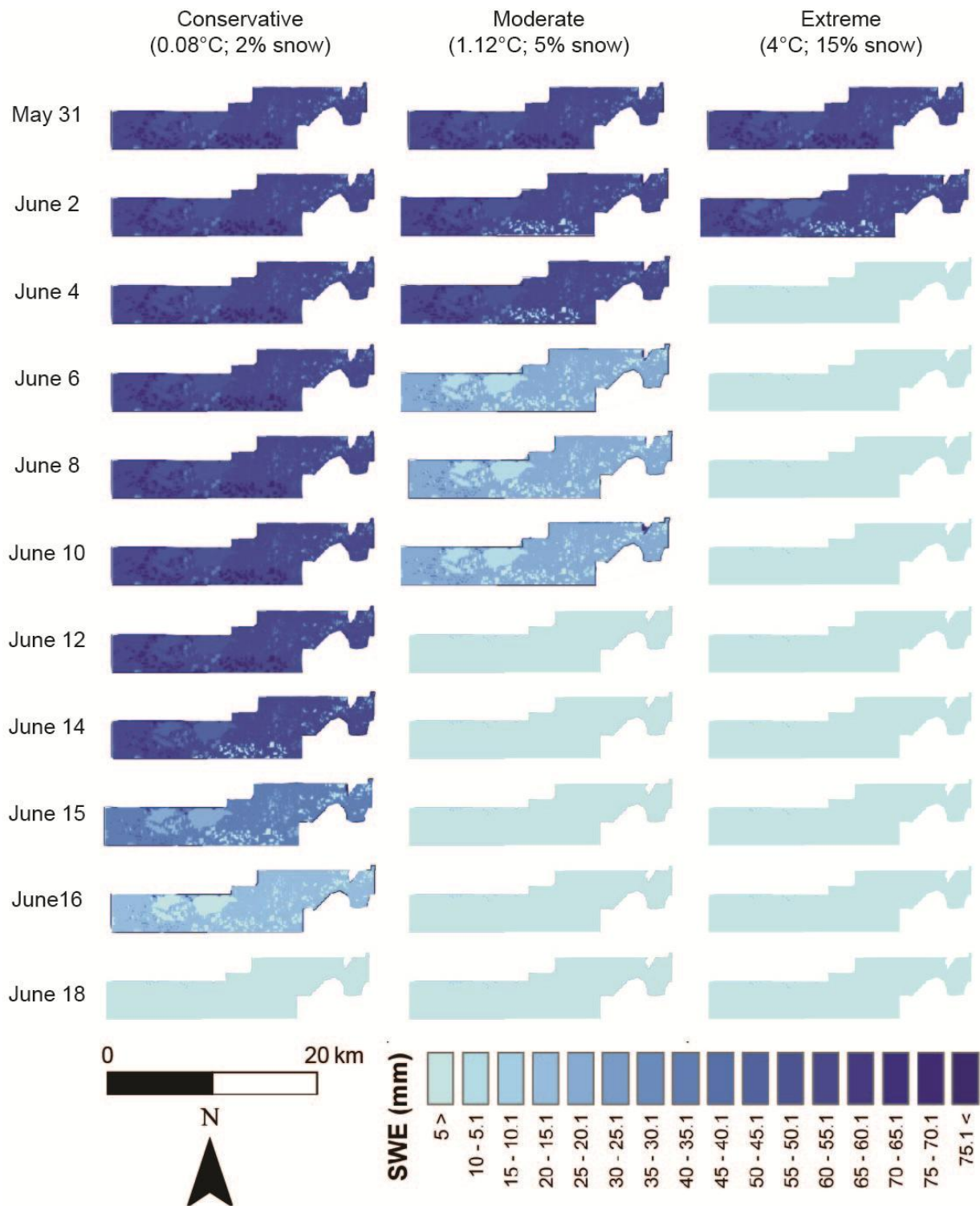


Figure 5 Sensitivity analysis simulations for the low-lying wetland using 2008 snow and climate data. The three scenarios: conservative, moderate and extreme are represented (see Table 1 for conditions). Similar findings were found for 2009 and 2010.

5 CONCLUSIONS

Snow is an important source of water to arctic ecosystems, allowing ponds, lakes, and wet meadows to be refreshed and recharged. Our results suggest that snowcover across the Pass (58-65 mm) is generally low, and more typical of wetlands experiencing a polar oasis-type environment (Woo and Guan 2006) than a polar desert one (Abnizova and Young 2010). Our snow survey results suggest a strong relationship between SWE (mm) and snow depth (cm), which is encouraging for future validation of remote sensing imagery for northern sites (Derksen *et al.* 2010). Snowmelt begins in June and is slow for a few days until air temperatures rise above 0°C, at which time active melt occurs and the snowcover is depleted by the third week in June. Deeper snow can linger in the lee of slopes or incised valleys providing additional meltwater and nutrients to nearby ponds and wet meadows. Future climate change scenarios suggest that the wetland snowpack at PBP could be depleted by early June if spring air temperatures were to rise by 4°C, even despite deeper snowcover. Direct impacts on this low-lying wetland complex might be accelerated thaw, enhanced evaporation losses, and a transition from wetter to drier ground.

ACKNOWLEDGEMENT

This research is supported by the Natural Sciences and Engineering Research Council (NSERC) of Canada, the Federal Government of Canada-International Polar Year program (IPY) and the Network Centre of Excellence - ArcticNet. We are grateful for the excellent logistical support from Polar Continental Shelf Program (PCSP) and Northern Student Training Program (NSTP). Many thanks to A. Croft, A.H. McGregor, N. DeMiranda, J. Siferd and A. Swidzinski for their assistance in the field. We would like to thank J. Siferd for his help in editing the manuscript.

REFERENCES

- Abnizova, A. & Young, K.L. 2010 Sustainability of High Arctic ponds in a polar desert environment. *Arctic* **63**, 67-84.
- Abnizova, A. & Young, K.L. 2008 Hillslope hydrological linkages: Importance to ponds within a polar desert High Arctic wetland. *Hydrol. Res.* **39**, 4, 309-321.
- ACIA. 2005 *Arctic Climate Impact Assessment*. Cambridge University Press, New York, 1042 pp.
- Assini, J. & Young, K.L. Snowcover and snowmelt of an extensive High Arctic wetland: spatial and temporal patterns. *Hydrol. Sci. J.* submitted Oct. 31, 2010.
- Derksen, C., Toose, P., Rees, A., Wang, L., English, M., Walker, A. Sturm, M. 2010 Development of a tundra-specific snow water equivalent retrieval algorithm for satellite passive microwave data. *Remote Sensing of Environ.* **114**, 1699-1709.
- Floyd, W. & Weiler, M. 2008 Measuring snow accumulation and ablation dynamics during rain-on-snow events: innovative measurement techniques. *Hydrol. Process.* **22**, 4805-4812.
- Heron R. & Woo, M.K. 1978 Snowmelt computations for a high arctic site. 35th Eastern Snow Conference. Hanover, New Hampshire, p. 162-172.
- Lewkowicz, A.G. & Young, K.L. 1991. Observations of Aeolian transport and niveo-aeolian deposition at three lowland sites, Canadian Arctic Archipelago. *Perm. and Perigl. Process.* **12**, 197-210.

- Pohl, S., Marsh, P. & Bonsal, B.R. 2007. Modeling the impact of climate change on runoff and annual water balance of an Arctic headwater basin. *Arctic*, **60**, 173-186.
- Woo, M.K. 1997 A guide for ground based measurement of the arctic snow cover. Canadian Snow Data CD, Meteorological Service of Canada, Downsview, Ontario.
- Woo, M.K. & Guan, X.J. 2006 Hydrological connectivity and seasonal storage change of tundra ponds in a polar oasis environment, Canadian High Arctic. *Perm. and Perigl. Process.* **17**, 309-323.
- Ye, H., Yang, D. & Robinson, D. 2008 Winter rain on snow and its association with air temperatures in northern Eurasia. *Hydrol. Process.* **22**, 2728-2736.
- Young, K.L. 2008 Role of snow in the hydrology of a High Arctic riparian wetland. *Hydrol. Res.* **39**, 277-286.
- Young, K.L. & Labine, C. 2010 Summer hydroclimatology of an extensive low-gradient wetland: Polar Bear Pass, Bathurst Island, Nunavut Canada. *Hydrol. Res.* **41.6**, 492-502.
- Young, K.L. & Abnizova, A. 2011 Hydrologic thresholds of ponds in a polar desert wetland environment, Somerset Island, Nunavut, Canada. *Wetlands*, in press, Mar. 8, 2011.

QUANTIFYING SNOW TRANSPORT USING SNOW FENCES AND SONIC SENSORS

Svetlana Stuefer¹, Matthew Sturm², Chris Hiemstra², Arthur Gelvin²

¹ *University of Alaska Fairbanks, USA*

² *Cold Region Research Engineering Laboratory, Fairbanks, USA*

*Corresponding author, e-mail: sveta.stuefer@alaska.edu

ABSTRACT

Accurate assessment of snow transport (T) during wind events is a prerequisite to reliable estimation of snow loads on infrastructure and prediction of avalanche danger in the mountains. It is also a critical term in the winter water balance, affecting snow sublimation. To assess T we constructed two snow fences in northern Alaska, and used an existing municipal fence near Barrow, Alaska, to trap the wind-blown flux of snow. On the leeward side of each fence, we installed a line of SR50 sonic ranging sensors that could be used to track the increase in snow height with time. We also installed web-cameras to monitor changes in drift shape. Periodic snow surface elevation surveys using a DGPS system provided more detailed drift profiles during the winter. Wind speed and direction were monitored near the fences. The sonic sensor results have been combined with the DGPS surveys to produce a time series of drift cross-section from which the flux has been computed. We have related this flux to individual wind events in an effort to identify the optimal conditions for blowing snow transport and to derive an empirical expression for T from weather measurements.

KEYWORDS

Arctic, snow transport, snow fence

Development and testing of model updating techniques for the Hydropower industry in Norway

Oddbjørn Bruland^{1*}, Knut Sand¹, Sjur Kolberg², Lena Tøfte², Kolbjørn Engeland², Glen Liston³, Ashenafi Seifu Gragne⁴, Knut Alfredsen⁴

¹Statkraft, Sluppen, 7035, Trondheim, NORWAY

²SINTEF Energy Research, Trondheim, NORWAY

³Cooperative Institute for Research in the Atmosphere, Colorado State University, Fort Collins, Colorado

⁴Department of Hydraulic and Environmental Engineering, NTNU, Trondheim, NORWAY

*Corresponding author, e-mail: Oddbjorn.Bruland@Statkraft.no

Abstract

Nationally it is attempted to improve the feedback and update methodology in today's operating modeling tools. Conclusions from these has been that the effect is not necessarily significant in terms of better simulations, but the probability for large errors is reduced by one or more states are physically more correct. However the results are not implemented in the operational tools. The reason for this has largely been that the system is not designed for automation of such processes. This is necessary with the scope and time requirements related to operations in the hydro power industry.

The term update (updating) of hydrological models is not widely used internationally, the best option is English "data assimilation". Often treated with general uncertainty analysis, data assimilation has been a rapidly increasing attention over the past decade, in many cases related to Bayesian techniques. Examples of methods that have been suggested are "generalized likelihood uncertainty estimation, Bayesian recursive estimation and Dynamic identifiability analysis (DYNIA). More methods estimate the different variable types simultaneously, eg the parameters and conditions using the particle filter, Ensemble Kalman Filter or a combination of EnKF and a Metropolis search algorithm and the Differential Evolution Adaptive Metropolis (DREAM) to analyze input uncertainty with parameter-estimation.

In this study different methods are combined and studied and related to observations and modeled states. This study presents how SnowTran, Dream, Dynia and a likelihood method are applied for updating hydrological models preliminary results of tests carried out in the distributed hydrological model ENKI.

Keywords

ENKI; model updating; data assimilation, Dream, Dynia, SnowTran

Spatial distribution of snow depth at Hardangervidda Mountain, Norway, measured by airborne laser scanning

Kjetil Melvold¹ and Thomas Skaugen¹

¹*The Norwegian Water Resources and Energy Directorate (NVE), Norway*
e-mail: kjme@nve.no

ABSTRACT

It is difficult to obtain measurements of snow depth distribution over a large area at a resolution that approximates the scale of its true variability. Such measurements are needed in order to validate spatially distributed snow simulations or observations from satellites. Manual data collection using snow stakes or probes, is labour intensive, expensive, and potentially dangerous in steep mountain environments. These issues call for new technology such as airborne laser scanning, which is a powerful tool for surveying large area within a short period. This study presents laser scanner mapping of snow depth in the mountain plateau Hardangervidda, Norway, in two different years (2009 with less snow than normal and 2008 with more snow than normal) at the peak time of snow accumulation during the winter. The extent of the survey area is more than 240 square kilometres.

We present the distribution of snow depth as derived from the laser scanning data and the results of a comparison of the measured snow depth and snow water equivalent (based on additional snow density measurements) derived from the laser scanning data with simulations using a snow model used for producing the Snow Maps for Norway available at <http://senorge.no>, which is run on a 1 km and 1 day resolution. The analysis showed that (1) the large scale spatial pattern of snow distribution of is well captured by the seNorge model and (2) that relatively large differences in amount (volume and depth) of snow between the measured and modelled snow were present.

Snow Accumulation studies in De Geer catchment, Spitsbergen

Ånund Killingtveit¹

*¹Department of Hydraulic and Environmental Engineering
Norwegian university of Science and Technology (NTNU)
N-7491 Trondheim, Norway
aanund.killingtveit@ntnu.no*

The spatial distribution of snow at the end of the accumulation season (usually in early May) in the De Geer-catchment in Spitsbergen has been studied in a measurement program running for most of the years from 1992 to 2005. Due to logistical problems a few years are missing. The De Geer catchment is 79.1 km², ranging from 40 m.a.s.l. up to 987 m.a.s.l., it is located about 15 km NE of Longyearbyen. The measurement program for snow distribution was planned in 1991 and started in 1992, in a project financed by Norwegian Hydrological Committee. The measurements were organized as 5 permanent Snow Courses with lengths of 500 or 600 meters, with snow depths measured at 10 meters interval. Snow density was also measured, usually at 3-5 different depths along each course. The location of the 5 snow courses were fixed and kept exactly the same for all years, and also the position of individual depth measurements along the courses. This was done in order to be able to isolate the effect of spatial distribution from temporal variations. For three years (2000, 2001 and 2005) the manual snow depth measurements were also duplicated by snow radar measurements. The presentation will give an overview of the measurement program, present some of the data collected and a few results regarding snow distribution statistics including the relation between elevation and snow storage.

Evaluation of updating procedures for improving simulation of autumn flows

A. S. Gragne¹, K. Alfredsen^{1,2}, K. Engeland² and S. Kolberg²

¹Department of Hydraulic and Environmental Engineering, Norwegian University of Science and Technology, Trondheim, Norway; ²SINTEF Energy A.S., Trondheim, Norway

Inflows simulated using the HBV conceptual hydrologic model were assessed against observed inflows into three hydropower reservoirs in Norway. The assessment revealed significant discrepancies between simulated and observed inflows at different periods over a hydrologic year. Such discrepancies result from uncertainties in the modeling process that can generally be attributed to uncertainty related to: data/observations, model parameters and/or model structure. This can cause major problems when using hydrological models for operational purposes without inclusion of a specific updating procedure. One issue observed in the data is repeated errors in autumn flows. A plausible explanation to the observed autumn differences is errors in the model's ability to correctly handle the snow/rain transition. With emphasis on deviations noticed in autumn flows, a temperature based updating procedure is developed in this study. At every simulation time interval, simulated and observed flows are evaluated and if differences are detected the model updating procedure is invoked to reduce the errors. Updating is done by evaluating threshold temperature, temperature gradient and snow accumulation, and then adjusting temperature through an iterative procedure. The strategy chosen is evaluated against an alternative particle filtering based updating approach to remove the simulation error.

Keywords: HBV model; updating; autumn flow.

Title: Automatic water quality measurements in the Baltic Compass project

Authors: Jari Koskiaho, Sirkka Tattari and Elina Jaakkola.
Finnish Environment Institute, PO Box 140 FIN-00251 Helsinki, Finland

Abstract:

The overall objective of the Baltic COMPASS (BC) project is to implement the Baltic Sea Action Plan as a means for sustainable development and increased competitiveness in the bio-economy of the Baltic Sea region. One sub-activity within BC is to implement necessary pilot investments in automatic water quality monitoring in selected river basins in Finland and Poland. In the project, water quality monitored by turbidity sensors in a 2000-km² lake-rich watershed discharging into the Gulf of Finland was scrutinized and compared with traditional, water sampling -based monitoring with respect to suspended solids and phosphorus loading. Not only did automatic monitoring improve the accuracy of the estimated loading from the watershed, but it also proved its usability in exploring spatial differences and lake retention within the watershed. In October 2010, a new automatic water quality measurement station was established in the river Vantaa, also discharging into the Gulf of Finland. A similar monitoring station will be installed in the river Narew, Poland, in spring 2011. The first results from Vantaa showed high sensitivity of the hourly-recorded turbidity and nitrate concentrations to the fluctuations of the river flow induced by heavy autumn rains. As a new feature for 2011, detection of organic carbon was added to the measuring station. The station is maintained every 2–3 weeks.

Keywords: watershed, automatic monitoring, turbidity sensor, sediment, phosphorus, loading

Ice impacts on behaviour and habitat choice in juvenile Atlantic salmon in steep rivers -
summarizing results from the winter habitat project

Knut Alfredsen¹, Tommi Linnansaari² and Morten Stickler³

¹Department of Hydraulic and Environmental Engineering, NTNU, 7491 Trondheim. email: knut.alfredsen@ntnu.no

²Canadian Rivers Institute, University of New Brunswick, Fredericton, Canada

³Statkraft AS, Oslo, Norway

Winter conditions can prove a challenging time for juvenile Atlantic salmon inhabiting steep streams. Dynamic ice formation causes rapid changes in available habitat and influences both behaviour and habitat selection. Compared to studies carried out during summer there are few winter studies, probably due to the inherent challenges in working with juvenile fish in the river environment during winter. Between 2003 – 2008 winter habitat conditions for juvenile Atlantic salmon were studied in several Norwegian and Canadian rivers, contrasting both natural and regulated flow and ice regimes. All rivers can be considered steep with dynamic ice regimes. Fish data were collected using radio telemetry and PIT technology. Using PIT, fish were followed from autumn to spring in several rivers. This paper summarizes findings across all rivers and tries to draw outline some findings regarding fish behaviour and habitat choices in winter.

The studies shows interesting contrasts between activity patterns between the natural and the regulated flow regimes, with no clear diurnal activity pattern and longer movements in the regulated river compared to natural conditions. A far more severe frazil and anchor ice production in the regulated river may contribute to this. Across all rivers, shelter is found to be important for habitat use and winter survival, and anchor ice formation did not necessarily lead to extra movement or changes in behaviour. Apparent survival decreased most during the autumn period leading up to the winter period and remained stable over winter.

Investigations of wintertime ice cover, circulation and water quality in Lake Vanajavesi

Matti Leppäranta¹, Onni Järvinen¹, Elina Jaatinen¹, Lauri Arvola², Anniina Kiiltomäki^{1,2},
and Kunio Shirasawa³

¹ Department of Physics, University of Helsinki, Finland

² Lammi Biological Station, University of Helsinki, Lammi, Finland

³ Institute of Low Temperature Science, Hokkaido University, Sapporo, Japan

Keywords ice cover, ice thickness, light conditions, circulation oxygen

Abstract

A wintertime research program of Lake Vanajavesi, southern Finland has been performed in 2009–2011. The lake is eutrophic, mean depth is 8 m and area is 150 km². The objectives were to examine the structure and thickness of ice cover, light transfer, geochemistry and circulation of the water body beneath the ice, and the influence of ice on ecological conditions. The ice cover consists of snow-ice and congelation ice. The snow cover protects the lake ice underneath by reducing warming and deterioration of the ice sheet. Even a thin dry snow cover is a very good protector. This reduction is both due to high albedo and high light extinction coefficient of snow. In the course of melting season, albedo and extinction coefficient both decrease when liquid water content in snow increases, and therefore the melting front catches ice surface where there is still a thin layer of snow left. Optical properties of snow cover on the lake ice are critical factors for the growth and deterioration of ice and primary production inside and below ice. The depth- and time-dependency of these properties need to be considered in parameterization of numerical models. Albedo decreased from 0.8 for dry snow to 0.2 for wet bare ice, and e-folding depth of light level was 50–70 cm for congelation ice and 10–20 cm for snow-ice and snow. When snow was thin or absent, euphotic depth was 1–2 m beneath the ice. Wintertime circulation is fairly stable forced by inflow of the main river and heat fluxes from the lake bottom. The key geochemical parameters have been conductivity, pH, oxygen, colour and nitrate. Incoming river water flows under ice towards the outflow, with fingerprint weakening along the way. In long ice seasons oxygen deficit becomes a major issue.

Hydropower Impact on Ice Regime

Netra Prasad Timalisina¹, Siri Almenning Stenhaug, Knut Alfredsen

Norwegian University of Science and University, Trondheim, Norway

Changing energy demand, climate change impacts and focus on renewable energy systems are important topics today. Hydropower often presents an attractive form of energy production in this respect since it is only renewable source so far with any storage potential. Hydropower also has an operational flexibility that can provide a potential for load balancing in a system with increasing use of non-storable renewable energy production. In cold regions, however, hydropower operation can be seasonally constrained by impacts of river ice. Warm water release from reservoirs due to hydropower production will influence downstream ice regimes. More fluctuation and increased flow during winter tends to aggravate ice problems until the surface of the river becomes ice covered, which may not happen at all in many northern regulated rivers. Variable production can also influence ice cover duration and break up. Therefore, operational strategies of hydropower can have a profound impact on water temperature and river ice regime, and river ice problems may lead to restrictions on operation.

In this paper, we focus on the implementation of models to identify impacts of hydropower production on the ice and temperature regime in a river. The models are implemented in the river Orkla south of Trondheim, Norway. The one-dimensional hydrodynamic model HEC-RAS from the US Army Corps of Engineers is used to simulate water temperature. The one-dimensional hydrodynamic model, MIKE 11 from DHI is used together with an ice module developed by Le Groupe- Conseil LaSalle for simulation of ice formation and breakup in Orkla. Simulations are carried out for the winter 2002-2003 and 2010-2011. The temperature model is validated with field data from temperature loggers in Orkla. The ice simulation is validated using data collected from ground based observations and aerial mapping.

Key words: River Ice, hydrodynamic, regulated, HEC- RAS, MIKE 11, Ice formation, Break-up

¹ Department of Hydraulic and Environmental Engineering, Norwegian University of Science and Technology, 7491 Trondheim, Norway, netra.timalisina@ntnu.no.

SUBSURFACE HYDROLOGICAL CARBON TRANSPORT IN THE SUBARCTIC ABISKOJOKKEN CATCHMENT

Elin J. Jantze, Steve W. Lyon, Georgia Destouni

Dept of Physical Geography & Quaternary Geology, Stockholm University

Correspondance to: elin.jantze@natgeo.su.se

Abstract

Warming and thawing of permafrost and deepening of the active layer related to climate change have been reported in arctic and subarctic environments. These changes may change the subsurface hydrological flow paths and advection rates through the landscape, and thereby also the quantity and timing of hydrological transport. Organic carbon is dissolved into soil water by the decomposition of soil organic matter. The carbon amount available for dissolution increases with thawing of ground frost and ice. Inorganic carbon is also dissolved into soil water by the weathering of mineral rich soils. Dissolved carbon of both types is further transported by soil water and groundwater from the terrestrial systems into streams and lakes, and finally to the ocean. This study investigates how the distribution of subsurface hydrological pathways and travel times through the landscape affects the transport of dissolved carbon to streams. The subsurface transport of dissolved carbon and the resulting downstream stream loading is specifically studied in the subarctic Abiskoajokken catchment (68°21'N, 18°49'E), which is underlain by discontinuous permafrost. We find the stream concentration of dissolved inorganic carbon (DIC) to be relatively constant in time and the stream load [MT^{-1}] of DIC to be highly correlated with stream flow. In contrast, both the concentration and the load of dissolved organic carbon (DOC) are flow-independent. We hypothesize, test and show with a consistent mechanistic approach to both the DIC and the DOC transport modeling that: a) The high flow-dependence of DIC load is due to a relatively slow average DIC (weathering) release rate from its essentially constant geogenic source, implying a large characteristic dissolution time in relation to the average advective travel time of DIC to the stream, which keeps the DIC concentration essentially constant in time. b) The flow-independence of both the concentration and the load of DOC is instead due to the annual renewal of the soil source of DOC, in conjunction with a characteristic relation of about similar average (respiration) release rate (or dissolution time) and advection rate (or advective travel time). These results show that, and facilitate further quantification and projection of how, the magnitude and dynamics of DIC and DOC export to streams are likely to be affected in quite different ways by the same, climate-driven and hydrologically mediated and propagated changes in permafrost. Carbon export from Arctic catchments should be monitored and modeled based on an understanding of these fundamental DOC and DIC transport differences, in order to accurately detect, interpret and project how permafrost-related changes in subsurface flow rates and pathways, as well as in production and decomposition of organic carbon combine to affect current and future carbon fluxes and budgets in permafrost regions.

Ice problems on hydropower and implications of climate change

Solomon Gebre¹, Knut Alfredsen²

*^{1,2}Norwegian University of Science and Technology, NTNU
Department of Hydraulic and Environmental Engineering
7491 Trondheim, Norway*

¹solomon.gebre@ntnu.no, ²knut.alfredsen@ntnu.no

Hydropower is a major power source in northern countries including Norway where it accounts for about 95% of the electricity production. To meet winter demands storage schemes are employed to a large extent in the Norwegian hydropower system. Ice may create operational constraint during winter leading to reduction in power production, and sometimes even complete shutdowns. The problems occur mainly due to frazil ice, ice runs and ice jams. Counteracting these ice problems is usually a difficult task which involves expensive measures and possibly lost production. Climate-induced changes to river ice processes and river hydrologic regimes can have considerable impact on the ice-hydropower interaction we observe today. In Norway, climate models predict an increase in average annual temperature of between 2°C and 4°C in 2071-2100 and a more fluctuating temperature with more mild spells during winter. Precipitation is also expected to increase in most parts of Norway by between 5 and 25 percent. Hydrological simulations show a marked increase in winter flows in the future climate. This will have significant influence in the ice regime and thereby for the hydropower industry. This paper reviews existing problems of ice on hydropower and analyses how climate change predictions for Norway will impact in either exacerbating or alleviating the problems.

Recent fresh water fluxes from Arctic glaciers and ice caps.

Jon Ove Hagen,

Department of geosciences, University of Oslo, Oslo, Norway.

ABSTRACT

The glaciers and icecaps in the world are main contributors to sea level changes. In the last IPCC-report from 2007 it was stated that the glacier contribution to sea level was about 1.8 mm/yr and that 1.1 mm or about 60% stems from melting glaciers and ice caps.

The Arctic (Alaska, Canada, Iceland, Svalbard, Russian Arctic) has about 55% of all glaciers and ice caps in the world. During the International Polar Year (IPY) selected target ice caps have been studied in the Arctic. There are large regional variations in the development of the mass loss over the last 20-30 years. Alaska and the Canadian Arctic has shown accelerating mass loss, while Svalbard and the Russian Arctic have had more stable conditions. Accelerated total mass loss from pan-Arctic glaciers including Greenland has doubled; in the period 1961-2004 we see an increase from -91 to -141 Gt/yr, while from 1995-2005 we see an increase from -170 to -280 Gt/yr.

Recent remote sensing data from ICESat giving time series of volume change data and GRACE gravity data giving time series of direct mass changes has improved the accuracy of the mass balance data over the years since 2003. The current overall data combining remote sensing and direct in situ measurements, indicates that the Arctic overall mass balance is strongly negative (giving an extra fresh water runoff to the oceans), of about 160 ± 30 Gt/yr for the last years 2003-2009. This is equivalent to a yearly contribution to sea level rise of 0.44 ± 0.08 mm/yr. In comparison the Greenland ice sheet, that has experienced accelerating mass loss over the last decade, now has a mass loss of about 200 ± 50 Gt/yr or 0.54 ± 0.14 mm/yr. The Arctic glaciers are thus still very important contributors to the increased fresh water fluxes to the Arctic oceans. However, in many parts of the Arctic, climate warming should cause glacier runoff to increase for a few decades or longer, but glacier area reduction will ultimately cause glacier runoff to decline (SWIPA, 2011).

Reference:

Snow, Water, Ice and Permafrost in the Arctic (SWIPA), 2011. AMAP, Arctic Monitoring and Assessment Program, Oslo, 2011.

Nea-Nidelv Supersite

Ånund Killingtveit¹, Oddbjørn Bruland², Knut Alfredsen¹, Sjur Kolberg³

*¹Department of Hydraulic and Environmental Engineering
Norwegian university of Science and Technology (NTNU)
N-7491 Trondheim, Norway*

aanund.killingtveit@ntnu.no

²Statkraft, POB 200 Lilleaker, N-0216 Oslo, Norway

³SINTEF, POB 4760 Sluppen, N-7465 Trondheim, Norway

The concept of a Hydrological Supersite, as introduced for example in ICARP II, has been used to describe an integrated system where observations, process studies, modelling, synthesis and studies of future climate scenarios are combined within a certain geographical region, for example a river catchment. The purpose could be to meet multi-disciplinary research needs for water in cold regions, for example to give input to the Terrestrial Cryosphere and Hydroclimatology of Cold Regions (TCHM). Norway has proposed to use the Nea-Nidelv catchment in Mid-Norway as a Supersite for TCHM. We will here give a description of the geography of the catchment, the institutions who are cooperating in research there, hydrological and meteorological measurement programs, some examples of integrated research programs and some results. Further, we want to invite to a discussion on how the Nea-Nidelv Supersite can be best used and integrated in TCHM and other International research programs, and what type of new measurement and research programs that should be introduced there.

The consequence of permafrost change on hydrologic response across multiple scales

Johanna Mård Karlsson^{1,2}, Steve W. Lyon^{1,2} and Georgia Destouni^{1,2}

¹ Department of Physical Geography & Quaternary Geology, Stockholm University, Sweden

² Bert Bolin Centre for Climate Research, Stockholm University, Sweden

Abstract

Permafrost position and extent determines the terrestrial hydrology in northern latitudes. As such, large-scale changes in permafrost should be manifested in the hydrological response of a landscape. In this study, we assess the capacity for existing hydrological monitoring data to detect and monitor hydrological shifts due to changes in permafrost (particularly the net decrease in thermokarst lake abundance). The study focuses on the Nadym, Taz and Pur river drainage basins in northwestern Siberia. These basins are characterized by tundra and taiga landscapes underlain with continuous to discontinuous permafrost, and a high abundance of thermokarst lakes and wetlands. The permafrost in these drainage basins has been warming significantly during the recent decades and caused development of new thermokarst lakes as well as drainage of existing ones across large scales. We use the temporal evolution of observed rainfall-runoff ratios based on long-term monthly precipitation and discharge data as a tool to investigate hydrological shifts in these basins. Namely, are these drainage basins undergoing a transition from surface water-dominated systems to groundwater-dominated systems (or visa versa)? Results indicate that there is variability in the hydrological shifts observed in these basins across different scales. This reflects the spatiotemporally dynamic nature of both permafrost thawing and thermokarst lake development/drainage in this Siberian landscape. These changes in permafrost extent and the coupled distribution of terrestrial water have large impacts on the vegetation patterns and biogeochemical cycling through changed rates of carbon and nutrient fluxes that ultimately could feed back to climate change.

Key words: northwestern Siberia, hydrological monitoring, permafrost, thermokarst lakes, carbon/nutrient cycling

An Improved Global Snow Classification Dataset for Hydrologic Applications

Glen E. Liston

Cooperative Institute for Research in the Atmosphere, Colorado State University, Fort Collins,
Colorado

and

Matthew Sturm

U. S. Army Cold Regions Research and Engineering Laboratory, Ft. Wainwright, Alaska

Out of a need to improve our description and understanding of snow covers found around the world, Sturm et al. (1995) introduced a seasonal snow cover classification system for local to global applications. It has seen considerable use since its initial development, but the original dataset describing the global distribution of snow classes was limited by its ~50 km spatial resolution. Consequently, it could not be used in high-resolution applications. The latest available fine-scale atmospheric forcing, topography, and land cover datasets were used to recalculate the snow classes on a global ~1 km grid. This new resolution greatly increases the accuracy of the system and opens the door for additional uses. Here we provide a summary of the new dataset and example applications that include: 1) defining snow parameter values for regional and global snow-process and climate modeling at fine spatial scales, 2) defining parameter values to enhance snow remote-sensing algorithms, 3) categorizing and/or stratifying field measurements and/or model outputs, and 4) defining parameter values for snow-property models such as depth-density relationships, again at real landscape scales. The new classification is available for use by contacting Glen Liston.

KEY WORDS: snow, snow classification, snow cover, remote sensing

**CLIMATE CHANGE IMPACTS ON SNOWMELT AND RUNOFF IN A
SUBARCTIC MOUNTAIN BASIN**

J. Richard Janowicz¹ and John W. Pomeroy²

**¹Water Resources Branch
Yukon Department of Environment
Whitehorse, YT
Canada**

**Centre for Hydrology
University of Saskatchewan
Saskatoon, SK
Canada**

Spring runoff is usually the most important hydrologic event of the year in streams draining subarctic regions. The magnitude and timing of the runoff event is controlled by the distribution of snow water equivalent over the basin, the rate of snowmelt and the delivery of water to the stream channel. Vegetation patterns have a dominant role in controlling the accumulation of snow as well as the energy available for the snowmelt process. In addition watershed flow pathways are largely determined by surface and soil conditions which are also controlled by vegetation through its effect on soil moisture. An analysis of snow accumulation and snowmelt runoff was carried out for Wolf Creek, a small (195 km²) watershed in the headwaters of the Yukon River. The basin has three distinct ecosystems, with the upper portion consisting of alpine tundra, middle elevations subalpine taiga and the lower portion boreal forest. Basin snow water equivalent and daily melt rates were estimated at three sites and extrapolated to the three corresponding ecosystems. Estimated snowmelt runoff from each ecosystem was compared to measured streamflow.

Temperature and precipitation projections based on several climate change scenarios are used as a base to estimate the change in vegetation patterns. The effects of these changes on variations in the rate of snowpack accumulation, snowmelt, and the infiltrability of frozen soils on the potential runoff and the errors in estimating the components of the spring water balance are examined.

Comparison of streamflow simulations for a boreal mountainous basin using adjusted and multiple station data

Ming-ko Woo* and Robin Thorne

School of Geography and Earth Sciences, McMaster University, Hamilton, Ontario, L8S 4K1,
CANADA

*Corresponding author, e-mail: woo@mcmaster.ca

ABSTRACT

Precipitation is usually underestimated in gauge records but hydrological models continue to use published data to simulate discharge. Additionally, few climate stations are found in mountainous areas. We explored the effects of using adjusted precipitation data or the inclusion of data from more than one station in streamflow simulation. A well tested hydrological model (SLURP) was used to simulate streamflow from the mountainous Pine River basin (area 12 100 km²) in northeastern British Columbia, Canada. Thirty years of daily data were simulated using (1) published, then (2) adjusted precipitation of one single station (Fort St. John), followed by (3) including input data from additional stations located in different parts of the basin. The adjusted precipitation only slightly improves the simulated result, as the underestimation in published precipitation is compensated by the optimized model parameters. However, when climatic data from additional stations (Mackenzie and Dawson Creek) are added to the model input, the simulation results are enhanced considerably. This improvement is attributed to the introduction of precipitation of different regimes to represent separate parts of the drainage basin. These results suggest that model parameterization can compensate the differences between published and adjusted precipitation but spatial variability in the occurrence of precipitation can only be depicted by the usage of data from climatic stations under different precipitation regimes.

KEYWORDS

Adjusted precipitation, streamflow simulation, parameterization, mountainous basin, northern river

1 INTRODUCTION

Hydrometric stations are too few and far between to match the hydrological diversity of northern mountainous regions and yet, streamflow information is important to hydro-power operation, fishery and flood management, as well as environmental impact investigations. The modelling approach is a common option to estimate flow with climatic data. Streamflow simulation of mountainous basins makes use of climatic records from limited available sites, mostly located at low elevations (Thorne & Woo 2006). The scarcity of data is highlighted in the present study with the aim that the methods and findings are applicable to mountainous basins elsewhere.

Precipitation undercatch is generally acknowledged to be a problem with conventional gauges, particularly serious in regards to snowfall (Goodison 1978). Recommendations have been made to adjust precipitation records to rectify the gauge undercatch (Metcalf *et al.* 1994) and to account for trace events which can be significant for some northern areas (Woo & Steer 1979). The usage of adjusted rather than unadjusted published precipitation data as

model input may (or may not) affect the outcome of streamflow simulation. Additionally, model parameterization is expected to play a significant role in the simulation of flow (van der Linden & Woo 2003).

Medium to large mountainous basins (area $>10^4$ km²) manifest considerable within-basin variability in the timing and magnitude of precipitation (Woo *et al.* 2006). Different parts of a basin may even have distinct regimes (e.g. one area is under maritime influence and another may be more continental, with attendant effects on precipitation). While most hydrological models have algorithms that adjust precipitation amount with topography (e.g. using empirical lapse rates to raise precipitation with elevation), the occurrence of events in different parts of a basin can be portrayed only by using data from auxiliary stations. The importance of such spatial information to hydrological modelling needs to be further examined.

To address these two questions pertaining to the amount and timing of precipitation, numerical experiments were conducted, specifically to examine (1) whether the usage of adjusted precipitation from a climate station can improve the performance of hydrological simulations, and (2) whether the inclusion of input data from more than one climate station from different parts of a medium-sized basin, in a complex mountainous environment, would improve the simulation results.

2 STUDY AREA, DATA AND METHODS

A case study was carried out to model streamflow of Pine River in British Columbia, Canada, which drains 12 100 km² at East Pine (55°43'12"N, 121°12'28"W) where it is gauged from 1970 to 1999. Pine River flows into Peace River at Fort St. John. The basin lies on the leeward side of the Western Cordillera but the headwater area, generally reaching 2600 m elevation, may still experience the influence of maritime airflow from the Pacific (Figure 1). Streamflow data for Pine River are available from Environment Canada through HYDAT. Air temperature and precipitation data for Fort St. John (56°13'54"N, 120°43'54"W, elevation 695 m) are published by Environment Canada through the Meteorological Service of Canada. Two stations in areas adjacent to the Pine River basin also provide temperature and precipitation data: Dawson Creek (55°44'24"N, 120°10'48"W, elevation 655 m) and Mackenzie (55°18'36"N, 123°08'24"W, elevation 690 m). The Mackenzie climate station has missing record in the first two years of the study period and this gap was filled by substituting data obtained from a nearby station 5 km away. Auxiliary precipitation data from Pine Pass station on the western side of the basin (56°33'N, 122°28'48"W, elevation 680 m, record started after 1975 with many years of data missing) permit a check on the Mackenzie station record. The mean monthly temperature and precipitation for the climate stations and mean monthly discharge of Pine River are shown in Figure 2.

In addition to the published data, the Climate Research Division of the Meteorological Service of Canada made available adjusted precipitation for the Fort St. John climate station. Precipitation was adjusted to generate a high quality precipitation time series designed for climate change analyses (Mekis & Hogg 1999). Depending on the rain gauge type, corrections were made to account for wind-induced undercatch, evaporation, and gauge-specific wetting losses, further described in Devine & Mekis (2008). For snowfall, adjustments were made to account for gauge undercatch due to wind and for wetting and sublimation losses, including density corrections to properly compute snow water equivalent from Nipher gauge measurements (Mekis & Hopkinson 2004). Finally, corrections for trace precipitation were made as described by Mekis (2005).

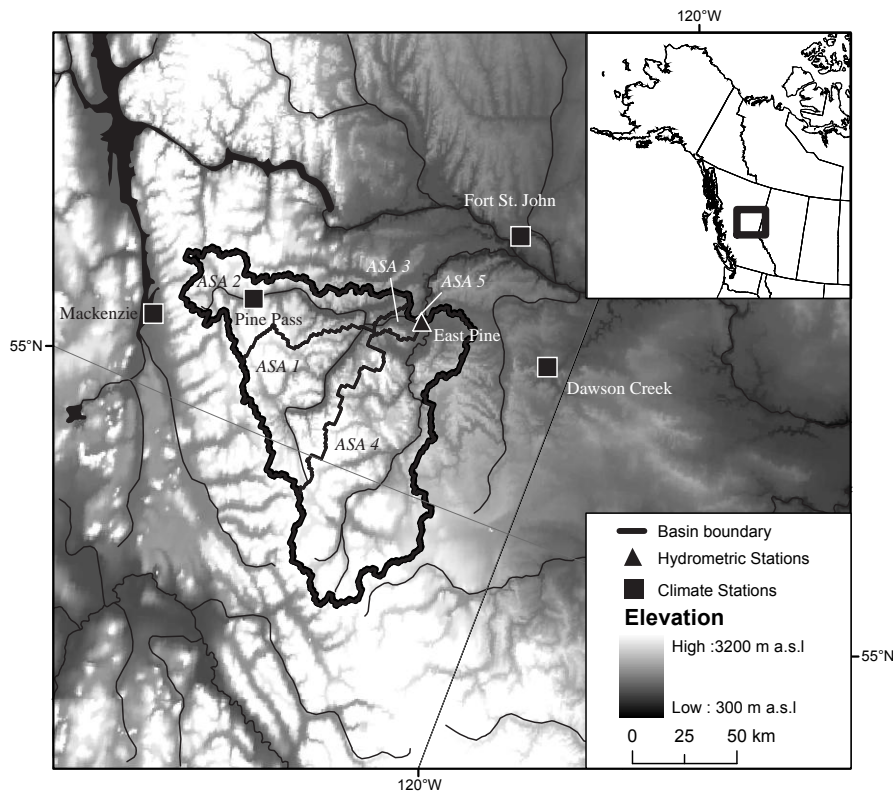


Figure 5 Topography of Pine River basin, British Columbia, Canada, showing the stream gauging station and climatic stations that provide temperature and precipitation data for this study. Black lines within the basin depict the boundaries of the aggregated simulation areas (ASAs). The land cover of various ASAs (numbered) is summarized in Table 1.

The Semi-distributed Land Use-based Runoff Processes (SLURP) Model was used for streamflow simulation (Kite *et al.* 1994). This model has been well tested in mountainous basins (Thorne & Woo 2006). It divides a large catchment into aggregated simulation areas (ASAs). The area of each ASA and the percentages of land cover types are given in Table 1, and the boundaries of the ASAs are delineated in Figure 1. Temperature and precipitation for each ASA are extrapolated by the model from the records of climate stations located within and around the basin, using a lapse rate of -0.75°C for temperature and a rate of precipitation increase of 5%, for every 100 m elevation rise. Clearly, there are limitations to the feasibility of such manipulations by the model: where there are few climatic stations available over a large area, the warming and cooling as well as the timing and amount of precipitation may not be realistically distributed over the basin.

Simulation by SLURP version 12.2 is based on (1) a vertical component consisting of daily surface water balance and flow generation from several storages, and (2) a horizontal component of flow delivery within each ASA and channel routing to the basin outlet. Daily time steps are used in streamflow simulation. The purpose of this study is not to investigate the performance of the model. Rather, the SLURP model is employed to perform several experiments that allow comparison of flows simulated with different datasets. Thus, we used the same sets of input data to derive model parameters as well as to simulate streamflow over the same time period.

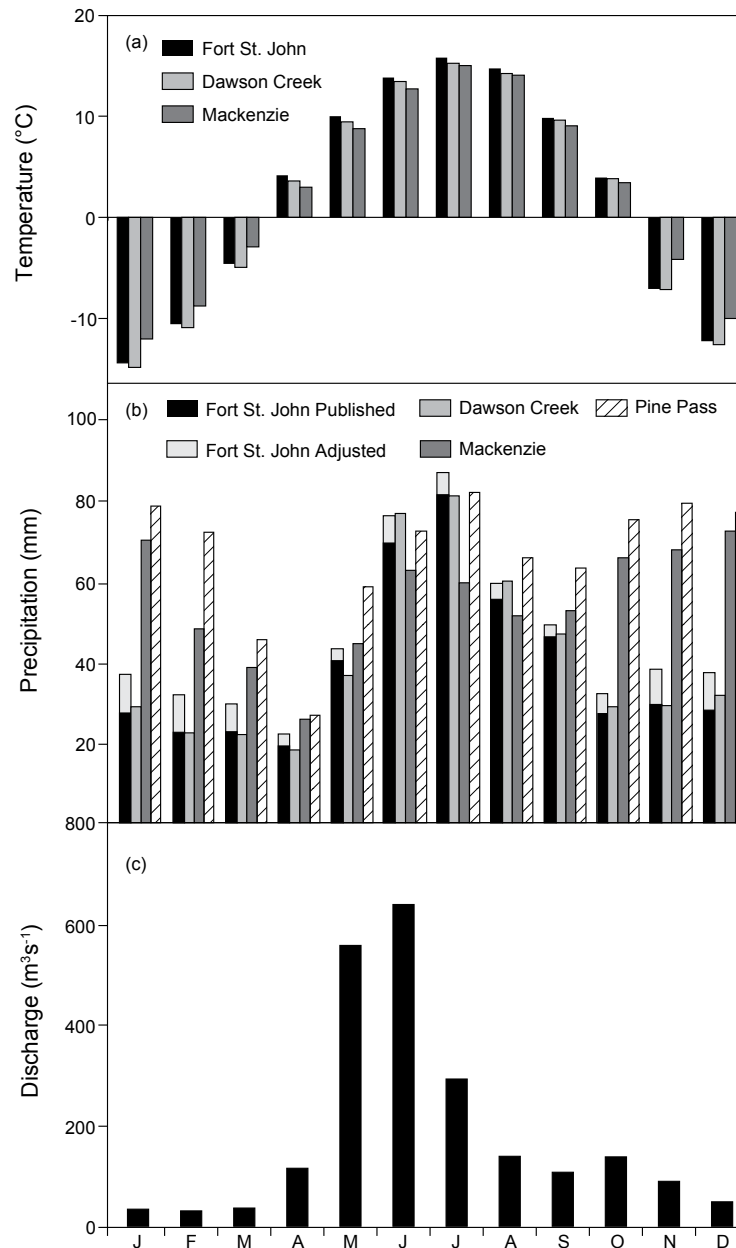


Figure 2 Mean monthly temperature and precipitation for four climatic stations (Fort St. John, Dawson Creek, Mackenzie and Pine Pass) and mean monthly discharge of Pine River (1970-99). For precipitation, the light grey coloured bars on top of the black bars indicate the amounts of adjusted precipitation for Fort St. John that exceed the published values (black bars).

Table 3 Area and percentage land cover of the five ASAs in Pine River basin.

ASA	Area (km ²)	Deciduous	Evergreen	Mixed forest	Water	Tundra
1	3010	8.1	13	60.7	5.1	13.1
2	2747	2.6	13	63.7	4.1	16.6
3	260	6.9	21.2	4.2	4.6	63.1
4	6618	15.0	13.3	55.3	4.2	12.2
5	7	0	0	14.3	0	85.7

For each simulation, the Nash-Sutcliffe (1970) coefficient is used as a measure of the goodness of fit between the observed and the simulated discharge. An ideal match between simulated and measured flow would yield a Nash-Sutcliffe coefficient of 1.0 and a root-mean-

square error of zero. These conditions are rarely met, but the simulation is considered to be better when the root-mean-square error diminishes and the Nash-Sutcliffe coefficient gets close to 1.0.

3 RESULTS

The model first obtains parameter values using temperature, precipitation and discharge records. The derivation of parameters was left to model optimization, except for snowmelt rates in which the parameter values were assigned manually. Four simulation experiments were carried out: (1) using only published temperature and precipitation from Fort St. John, (2) replacing the published precipitation by its adjusted counterpart, (3) employing published temperature and precipitation for Fort St. John as well as for Mackenzie, and (4) adding the data from Dawson Creek. Parameter values for these four experiments are listed in Table 2. Each set of parameter was used to simulate streamflow for the entire 30 year period (1970-99), using air temperature record together with published or adjusted precipitation data. SLURP outputs streamflow on a daily time scale, and daily flows were also averaged into monthly values to facilitate comparisons among the modelled results. Like many boreal rivers, the Pine exhibits a subarctic nival regime of streamflow (Woo *et al.* 2008). Winter is a low flow season and annual peak flow occurs in the snowmelt period. After the snow is depleted, the spring high flow recedes though summer low flow is occasionally interrupted by hydrograph rises due to rainfall events. Secondary peaks often follow in the fall due to precipitation associated with the passage of fronts.

3.1 Simulations using inputs from one single station

Simulation using published temperature and precipitation data from a single station in the basin is here considered as the baseline or the worse-case situation. While the temperature input remains the same, the published and adjusted precipitation datasets for Fort St. John were used for two separate simulations. Comparison of the precipitation datasets shows that the adjusted data are higher than the published record for all the months in a 30-year period (Figure 2). The differences are larger for every month in the winter than in the summer (Figure 3), suggesting that the undercatch of snow has a more pronounced effect on streamflow than the under-recording of rainfall.

Observed and simulated discharges of Pine River are presented in Figure 4. The data are averaged to monthly values for the ease of comparison (daily values have too many spikes and troughs that render comparison visually difficult to comprehend). Both simulation runs, using published and adjusted precipitation, perform poorly. Compared with observed daily flow, the simulated values yield Nash-Sutcliffe coefficients of 0.46 and 0.52 for the runs using published and adjusted precipitation of Fort St. John. Their respective root-mean-square errors are $186 \text{ m}^3\text{s}^{-1}$ (using published precipitation) and $177 \text{ m}^3\text{s}^{-1}$ (using adjusted precipitation).

Plotting the simulated against observed values indicates systematic departures from the 1:1 slope, indicating substantial bias in the simulated outputs (Figure 5). Winter low flows are over-estimated by both simulations. With the adjusted precipitation input, there is a slight reduction in and simulated high flows are conspicuously large, with the simulated outputs greatly underestimating the high flows. The adjusted precipitation marginally raises the high flows in the snowmelt runoff month of May, June and July (Figure 6), possibly due to the larger amount of snow produced by the higher winter precipitation in the adjusted data.

Table 4 Parameter values obtained through optimization of 1970-99 daily data, using (a) published temperature and precipitation data from Fort St. John, (b)

published temperature and adjusted precipitation from Fort St. John, (c) published temperature and precipitation of Fort St. John and Mackenzie. (d) same as (c) but with Dawson Creek added.

Parameter	Deciduous	Evergreen	Mixed forest	Water	Tundra
Max Infiltration Rate (mm/d)					
(a)	1	1	1	50	1
(b)	1	1	1	50	1
(c)	50	1	22.97	50	1
(d)	1	50	8.17	50	1
Manning roughness					
(a)	0.2	0	0.06	0	0
(b)	0.07	0.01	0	0	0.16
(c)	0.2	0	0	0	0
(d)	0.2	0.19	0	0	0
Retention constant Fast Store					
(a)	1	91.06	75.32	1	1
(b)	86.21	68.44	64.1	1	78.72
(c)	49.13	51.59	30.99	1	72.09
(d)	54.65	43.9	51.57	1	58.2
Max Capacity Fast Store (mm)					
(a)	505.1	1243	1615	0	1381
(b)	742	520	467.9	0	1646
(c)	1497	1058	85.26	0	1397
(d)	939.5	485	167.5	0	1027
Retention constant Slow Store					
(a)	5438	15100	41230	100000	20180
(b)	42270	66280	67140	100000	18400
(c)	61960	49360	4985	100000	21750
(d)	63360	58240	17770	100000	17130
Max Capacity Slow Store (mm)					
(a)	2514	7808	6234	6951	5759
(b)	5879	6325	2323	3151	6035
(c)	6651	2759	5321	8004	3288
(d)	5371	1541	7846	3993	5006
Snowmelt Rate for Jan (mm/d)					
(a)	0	0	0	0	0
(b)	0	0	0	0	0
(c)	0	0	0	0	0
(d)	0	0	0	0	0
Snowmelt Rate for Jul (mm/d)					
(a)	1.1	1.1	1.1	1.1	1.1
(b)	1.5	1.5	1.5	1.5	1.5
(c)	2.1	2.1	2.1	2.1	2.1
(d)	2.1	2.1	2.1	2.1	2.1

3.2 Simulations using data from more than one station

To assess the effect of adding the temperature and precipitation from another station as model input, the records of the Mackenzie climate station located just outside of the basin was included. Although some data have to be substituted from nearby stations to fill the missing gaps in the Mackenzie time series, it is the only available site near the western headwater areas of Pine basin with a sufficient length of record. Another station, Pine Pass, is located within the study basin but its records are too short (starting after 1975 and with many gaps) for use. On the other hand, the periods that its records overlap with those of the Mackenzie station allow comparison of their

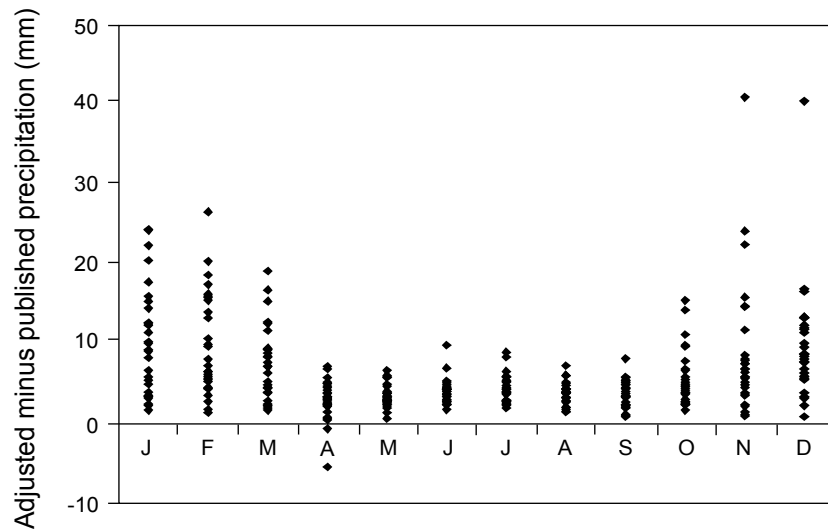


Figure 3 Differences between adjusted and published precipitation values for 30 years (1970-99) of monthly data, Fort St. John, showing underestimation of precipitation in published data, notably for winter months due to snow undercatch.

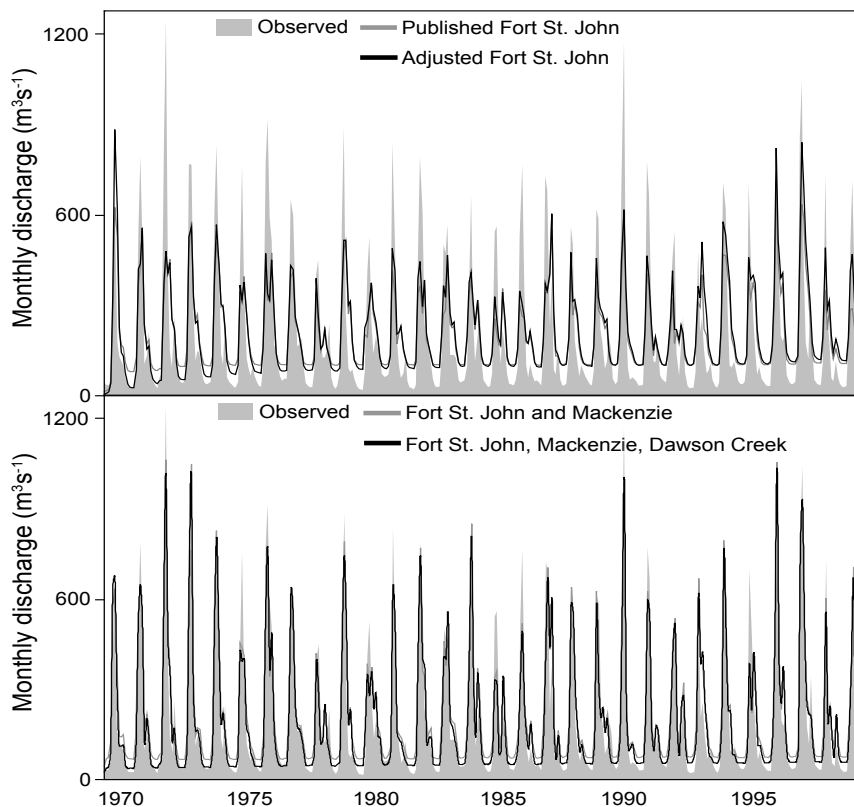


Figure 4 Hydrographs of monthly discharge obtained through simulations, compared with the monthly flow of Pine River measured at East Pine.

precipitation regimes. Figure 2 shows that though the magnitudes differ, as expected for an area of mountainous topography, their precipitation regimes are comparable.

Mackenzie station, apparently under stronger influence of the Pacific airflow, has a more uniform precipitation regime than Fort St. John, located on the eastern side of Pine basin. Mackenzie also has warmer winters but cooler summers than Fort St. John (Figure 2). With

larger winter precipitation as indicated by Mackenzie, the western part of the basin likely has higher snow accumulation than in the east.

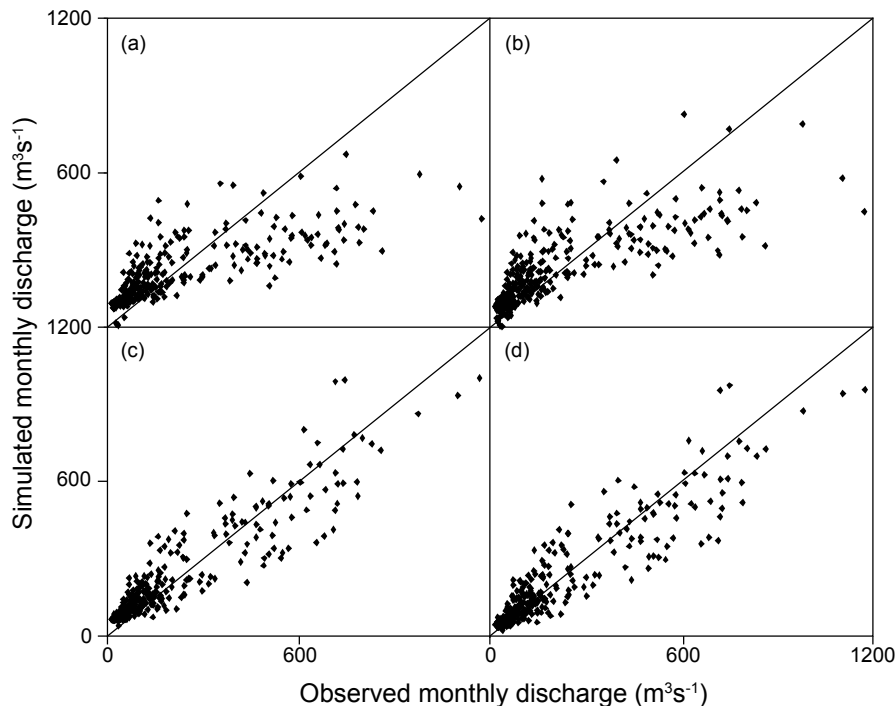


Figure 5 Scatter plots that compare observed with simulated discharge using different sets of input data: (a) published temperature and precipitation of Fort St. John, (b) published temperature and adjusted precipitation of Fort St. John, (c) published temperature and precipitation of Fort St. John and Mackenzie, and (d) published temperature and precipitation of Fort St. John, Mackenzie and Dawson Creek.

Daily discharge simulated using temperature and precipitation data of both Fort St. John and Mackenzie are averaged to monthly values and presented in Figure 4. Compared with the other simulations using single station data, the Nash-Sutcliffe coefficient increases to 0.69 and the root-mean-square error of the daily outputs is reduced to $141 \text{ m}^3\text{s}^{-1}$. In terms of bias, the winter flow bias is mostly eliminated. Spring peaks are higher than those obtained using inputs from a single climate station, possibly because the high winter precipitation in the western basin (represented by Mackenzie station) raises the snow storage to augment spring melt runoff. Nevertheless, snowmelt peaks are still underestimated. The flows of August and September are overestimated, but much less so than the outputs simulated using single station data.

Another station (Dawson Creek) near Fort St. John in the eastern basin offers 30 years of temperature and precipitation data that can be included in the simulation. With data from this added station, the simulated streamflow yields a Nash-Sutcliffe coefficient of 0.70 and a root-mean-square error of $139 \text{ m}^3\text{s}^{-1}$. Compared with the two-station inputs, the addition of this third station near Fort St. John only slightly improves the simulation results.

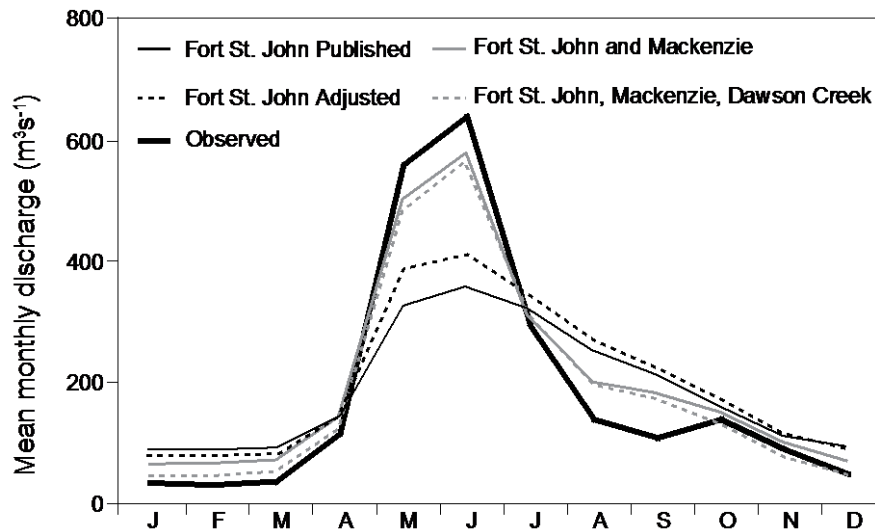


Figure 6 30-year mean monthly modelled discharge from four simulations, using published and adjusted precipitation of Fort St. John, published data from Fort St. John and Mackenzie, and additional data from Dawson Creek. Thick line shows measured flow of Pine River.

4 DISCUSSIONS AND CONCLUSIONS

The modelling experiments show that using temperature and precipitation data from only one climatic station performs poorly in the simulation of streamflow, and replacing the published by adjusted precipitation only marginally improves the Nash-Sutcliffe coefficient. However, using data from one or two additional stations in a different part of the basin considerably enhances the performance of the simulation.

Results do not support the postulation that by providing more accurate precipitation, the adjusted input data can produce more satisfactory simulated streamflow than with published records. The likely explanation is related to the construct of the hydrological model. Most climate stations are located in valleys where settlements are sited and there is a dearth of measured data from high elevations in mountainous terrain. Hydrologic models usually take heed of such shortcomings and extrapolate station temperature and precipitation information to high parts of a basin using empirical lapse rates. In so doing, underestimation of station precipitation is taken into account and is rectified to varying extents through the optimization of parameters to yield the best possible fit between precipitation and discharge.

Within a medium-size basin, spatial variability in the magnitude and the timing of precipitation events cannot be represented by a single station. In the case of Pine River basin, despite its geographical location on the leeward side of the Rocky Mountains, its western sector remains under some maritime influence spilled over across the continental divide. Adding a station (Mackenzie) in this part of the basin with a precipitation regime different from that of Fort St. John improves the representation of spatial variability, which gives rise to different timing of precipitation events. In turn, this information allows more rational simulation of runoff in a different part of the basin, thus improving the overall simulated outflow from the basin.

It is further noted that to be helpful to the simulation, an added climate station may represent a different precipitation regime. However, two stations in close proximity may be under the same precipitation regime and data provided by more than one station would add little to the information content. This is exemplified by the addition of Dawson Creek data to the

simulation. This station, being close to Fort St. John, yields meager additional information and therefore including its temperature and precipitation in the simulation does not substantially improve the modelled streamflow.

Based on the results of the experiments, several recommendations are advanced regarding the usage of climatic data for streamflow simulation. (1) Compared with published data, adjusted precipitation offers a better appreciation of the amount of winter snow accumulation, which is useful for operational and management applications. (2) Precipitation data from only one station in a basin with complex terrain is inadequate for modelling streamflow. Using adjusted instead of published data is insufficient to improve the performance of hydrologic simulation. (3) With data from one additional station under a separate precipitation regime, even though there are missing values in the record that have to be estimated, the simulation of streamflow can be considerably enhanced.

5 ACKNOWLEDGEMENT

We thank Dr. Éva Mekis of the Meteorological Service of Canada for providing the adjusted precipitation data of Fort St. John.

REFERENCES

- Devine, K.A. & Mekis, É. 2008. Field accuracy of Canadian rain measurements. *Atmos. Ocean* **46**(2), 213-227, doi:10.3137/ao.460202.
- Goodison, B.E. 1978. Accuracy of Canadian snow gage measurement. *J. Appl. Meteorol.* **27**, 1542-1548.
- Kite, G.W., Dalton, A. & Dion, A. 1994. Simulation of streamflow in a macroscale watershed using general circulation model data. *Water Resour. Res.* **30**, 1547-1559.
- Mekis, É. 2005. Adjustments for trace measurements in Canada. Preprints, 15th Conf. on Applied Climatology, Savannah, Georgia, Amer. Meteor. Soc., J3.7. [Available online at <http://ams.confex.com/ams/pdfpapers/92155.pdf>.]
- Mekis, É. & Hogg, W.D. 1999. Rehabilitation and analysis of Canadian daily precipitation time series. *Atmos. Ocean* **37**(1), 53-85.
- Mekis, É. & Hopkinson, R. 2004. Derivation of an improved snow water equivalent adjustment factor map for application on snowfall ruler measurements in Canada. Preprints, 14th Conf. on Applied Climatology, Seattle, WA. Amer. Meteor. Soc., 7.12. [Available online at <http://ams.confex.com/ams/pdfpapers/68724.pdf>.]
- Metcalf, J.R., Ishida, S. & Goodison, B.E. 1994. A corrected precipitation archive for the Northwest Territories. In: Mackenzie Basin Impact Study Interim Report No. 2 (ed. By Cohen, S.J.). Environment Canada, pp. 110-117.
- Nash, J.E. & Sutcliffe, J.V. 1970. River flow forecasting through conceptual models: Part 1 – a discussion of principles. *J. Hydrol.* **10**, 282-290.
- Thorne, R. & Woo, M.K. 2006. Efficacy of a hydrologic model in simulating discharge from a large mountainous basin. *J. Hydrol.* **330**, 301-312.
- van der Linden, S. & Woo, M.K. 2003. Transferability of hydrological model parameters between basins in data-sparse areas, subarctic Canada. *J. Hydrol.* **270**, 182-194.
- Woo, M.K. & Steer, P. 1979. Measurement of trace rainfall at a High Arctic site. *Arctic.* **32**, 80-84.
- Woo, M.K., Thorne, R. & Szeto, K.K. 2006. Reinterpretation of streamflow trends based on shifts in large-scale atmospheric circulation. *Hydrol. Processes* **20**, 3995-4003.
- Woo, M.K., Thorne, R., Szeto, K.K. & Yang, D. 2008. Streamflow hydrology in the boreal region under the influences of climate and human interference. *Philos. T. Roy. Soc. B.* **363**, 2251-2260.

THE EFFECTS OF CLIMATE CHANGE ON WATER BODIES OF THE NORTH
EUROPEAN PART OF RUSSIA

N. Fialtov
Northern Water Problems institute,
Karelai, Russia
nfialtov@rambler.ru

It was created database of the high latitude lakes situated in North West of Russia and determined the effects of climatic parameters (including atmospheric indexes) on water ecosystems. The aim of the work is to improve the predictions of the feedback mechanism of lakes on climate changes. The regular inherent hydrophysical, chemical-biological and meteorological observations are conducted on a few tens of water bodies in the North of European part of Russia. Meanwhile, understanding of functioning of morphologically variable lakes under changing climatic conditions still remains insufficient and presents a fundamental problem.

The important goals of the study in the framework of NRB activities is to compare the impacts of climate change on northern water resources and to estimate the possible changes of water ecosystems on the territories of Russia, Finland, Sweden, Norway, US and Canada.

JÖKULHLAUPS AND SEDIMENT TRANSPORT IN WATSON RIVER, KANGERLUSSUAQ, WEST GREENLAND

B. Hasholt¹, A.B. Mikkelsen¹, N.T. Knudsen²

¹ *Department of Geography and Geology, University of Copenhagen, 1350 Copenhagen K, Denmark.*

² *Department of Geology, Aarhus University, 8000 Aarhus C, Denmark.*

**Corresponding author: e-mail: bh@geo.ku.dk*

ABSTRACT

During three years out of the four year observation period (2007-2010) jökulhlaups have been observed. At a gauging station located on a rock threshold near the outlet of Watson River discharge and sediment transport has been monitored during the jökulhlaups. Stage rose up to 5.3 m and a maximum discharge of 1431 m³ s⁻¹ was recorded. The three jökulhlaups were very different, indicating the different influences of weather and englacial drainage conditions. Although the jökulhlaups represented some of the extreme discharge and sediment transport rates, their share of the annual discharge and sediment transport were less than 2 %. The jökulhlaups at Kangerlussuaq may be dangerous to tourists and may destroy roads, bridges and local water supply. Normally jökulhlaups occur without notice many places in Greenland because of the sparse population, but the possible occurrence should be taken into account when building hydro power stations or mining installations. The frequent occurrence of jökulhlaups may represent a new cycle caused by climate change.

KEYWORDS

Jökulhlaups, discharge, sediment transport, Kangerlussuaq, Greenland

INTRODUCTION

Jökulhlaups have been observed and described at Kangerlussuaq as early as in 1984 by Sugden *et al* (1985) and it is probably the most well observed jökulhlaup location in Greenland. In a recent publication by Russell *et al.* (2011) a complete review of the research efforts at the location is given. A key issue in this publication is the survey of the ice margin lake that has been tapped several times. Because of the robust determination of the lake volume, corrected for refill rate and movements of the ice front forming the ice dam, it is possible to recalculate the accurate volumes of water released during the jökulhlaups. Furthermore hydrodynamic calculations of the peak discharges are presented, which indicate that the peak discharges are much higher than predicted by the Clague-Mathews relationship (Clague & Mathews 1973) and that a substantial attenuation of peak discharges occurs downstream. Russell *et al.* (2011) also discuss possible trigger mechanisms which they relate to ice thickness and changes in glacier movements and mass balance. But also glacier hydrology and the development of the englacial drainage system is described as very important for the onset and timing of the jökulhlaup. Finally they indicate that the jökulhlaup in 2007 represents the beginning of a new cycle of jökulhlaups at Kangerlussuaq. Information about sediment transport and deposition is given in Russell *et al.*(1990) and Russell (2007, 2007). The collapse of a moraine ridge is described in relation to a jökulhlaup in 1988 and

sedimentology of deposits on a delta and a valley-confined sandur is investigated, but no continuous measurements of sediment transport during the jökulhlaups are available.

The present investigation was initiated in 2007, the main objectives were to monitor the freshwater and sediment input to the fjord in order to elucidate the hydrodynamics of the fjord and to provide background information for an interpretation of the sediment column deposited in the fjord. The 31st August 2007 a jökulhlaup occurred. Because of the installation of stage recorders and sediment concentration sensors related to the project, we were able to monitor the complete jökulhlaup event. A description of the discharge and sediment transport during the jökulhlaup in 2007, based on the preliminary stage discharge relationship, was given by Mernild *et al.* (2008). Later also the discharge and sediment transport during the jökulhlaup in 2008 has been described in Mernild & Hasholt (2009). Russel *et al.* (2011) have pointed out that the accumulated discharge based on our calculation is significantly lower than what he finds from measurements of volume changes in the lake responsible for the jökulhlaup. He also indicates that an inadequate stage discharge relationship may be the cause for this discrepancy.

As planned our investigations have continued through 2009 and 2010. The year 2010 was characterized by a prolonged and intense runoff period resulting in the highest record of both accumulated discharge and sediment transport for the four year period. Furthermore a new jökulhlaup occurred the 11th September. During the summer flood periods in both 2009 and 2010 a field assistant from the Department of Geography and Geology has been in Kangerlussuaq and has measured discharge and collected water samples for providing a better coverage of the high stages in the stage discharge relationship and for calibration of the sediment concentration sensors. Based on the newly obtained data a revised stage discharge relationship is established and used here.

The objectives of this study are: 1. To provide a revised description, with a high time resolution, of stage and discharge during the three jökulhlaup events. 2. To provide a revised description of the sediment concentration and sediment transport during the jökulhlaups to compare with the accumulated annual transport. 3. To describe the weather conditions before and during the jökulhlaups in order to identify possible causes to the onset and the timing. 4. To investigate effects within the fluvial system. 5. To evaluate the possible effects of climate change on the occurrence of jökulhlaups in the area and in Greenland.

STUDY AREA

The drainage area (9743 km²) of Watson River at Kangerlussuaq stretches from the fjord at the west coast of Greenland all the way to the ice divide on the Greenland ice sheet (GrIS), Figure 1. The outlet from the river is close to 67°00' N latitude; 50°40' W longitude and is located 22-35 km downstream from the GrIS terminus. The river has two main tributaries; the northern Sandflugtsdalen and the southern Ørkendalen. The river drains at least 4 different lobes of the GrIS, of which the Russell Glacier and Leverett Glacier drains into the tributary Sandflugtsdalen. Sandflugtsdalen is the valley system where the jökulhlaups have been observed. The lake which has been emptied during the jökulhlaups is seen on Figure 1. The drainage area is dominated by GrIS (9168 km²). The ice-free area (575 km²) (Hasholt *et al.* 2011) consists of gently rolling bed rock hills, up to about 500 m.a.s.l., with a thin cover of

glacial material. River and lake valleys are cut through this landscape by previous glacial erosion. The vegetation is sparse and consists mainly of grass and scrub.

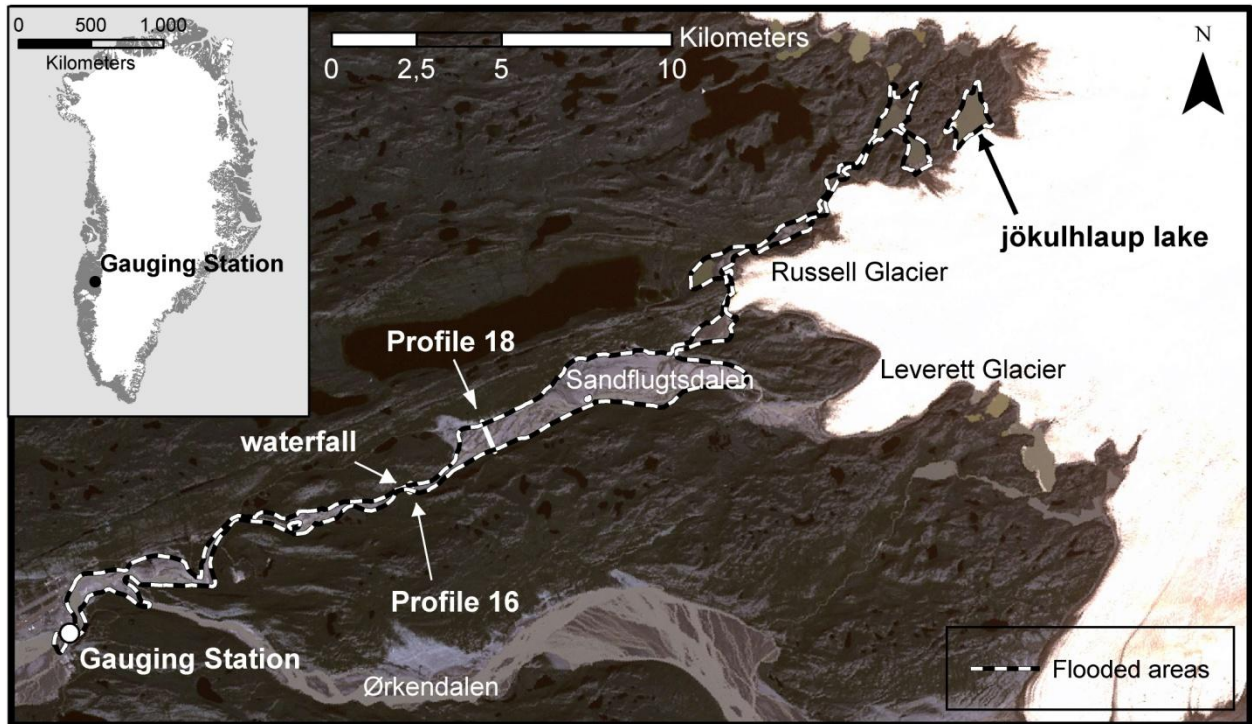


Figure 6: The Figure shows a Landsat 7 image of the area together with the mentioned places in the text. The dashed lines are outlining the extent of the flooded areas during the jökulhlaup 31st August 2007. The study area location is shown in the index map in the upper left corner.

Mean annual temperature, relative humidity and wind speed are respectively -10.9°C , 64 % and 5.3 m s^{-1} according to Mernild *et al.* (2010). Here also a corrected mean annual total precipitation of 246 mm for the period 1978/1979-2007/2008 is given. According to Born & Böcher (2001) the climate is characterized as Low Arctic. The ice-free area is dry as demonstrated by the presence of saline lakes, (Hasholt and Anderson 2003). The location of the equilibrium line at this part of the GrIS varies from 1370-1780 m.a.s.l. (van de Wal *et al* 2005; Broeke *et al* 2008).

METHODS

The monitoring station for discharge and sediment transport is located on a rock threshold south of the Kangerlussuaq Airport, see Figure 1. Stage is recorded with pressure transducers corrected for barometric pressure and discharge is measured with the float method at all stages utilizing the fixed cross section profile provided by the rock threshold. At very low stages the discharge has been measured with ordinary current meters and at high stages it has been measured with ADCP (Acoustic Doppler Current Profiler) in 2010. The sediment concentration is found from daily manual water samples, supplied by automatic pump sampling when manual sampling was not possible. The sediment concentration found in the water samples has been used for calibration of the recording transmissometers and optical backscatter sensors used to describe the sediment concentration at 5 to 10 minute intervals. For further details about the monitoring program, see Hasholt *et al.* (2011).

In the spring 2008 the Sandflugtsdalen valley system has been surveyed in order to identify maximum stages from the jökulhlaup the 31st August 2007 and to find tracks of related erosion and deposition in the fluvial system. A number of cross sections have been established with a Trimble 4000 GPS used for the location of datum points from where the profile has been surveyed using a Topcon theodolite with a distance meter without need for a reflector – it is then possible to measure the distance to solid objects on both sides of the river without crossing the river. In 2010 a pressure transducer was installed upstream a waterfall, see Figure 1. By comparing with records from the gauging station it is possible to find attenuation and travel time of the flood wave during the jökulhlaup in 2010.

RESULTS

2007

The stage began to rise the 26th August and until late the 31st August a diurnal variation was clearly visible. The stage rose abruptly the 31st August from 16 m.a.s.l. at 0400 hrs. up to 20 m.a.s.l. at 1400 hrs, see Figure 2a. Discharge, sediment transport and weather are shown in Figure 2a, b and c. In Table 1 the data from the three jökulhlaups are shown. The total volume of water originating from the jökulhlaup was $25.5 \cdot 10^6 \text{ m}^3$ which is only 0.7 % of the annual runoff. The sediment transport caused by the jökulhlaup was $83 \cdot 10^3 \text{ t}$ or 1.2 % of the annual transport, indicating an increased concentration of sediment related to the jökulhlaup (see Table 1).

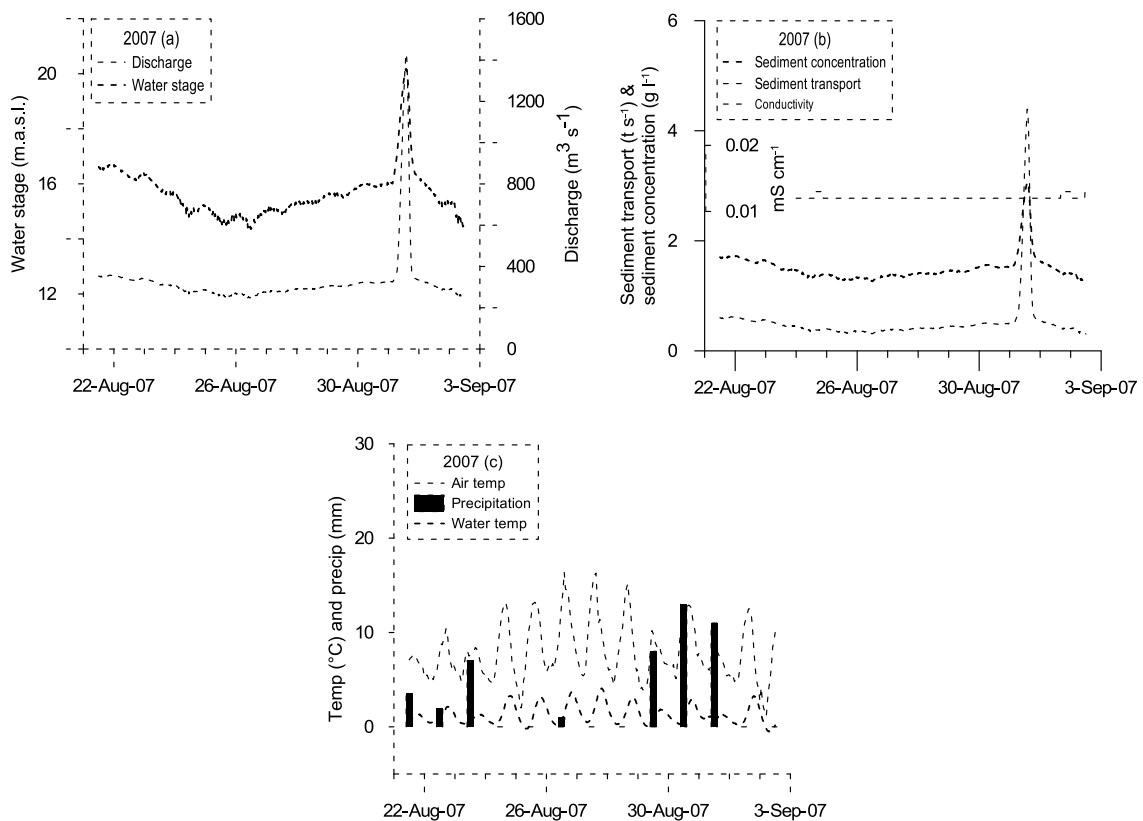


Figure 7: (a) The gauged water stage above the reference datum (mean sea level) and discharge during the 2007 Jökulhlaup. (b) Sediment transport (solid line with a distinct peak),

sediment concentration (dashed line) and the conductivity are shown here. (c) Air temperature, precipitation (DMI) and water temperature at the gauging station.

Table 5: The table selected values in connection to the observed Jökulhlaups. The water stage is listed as stage above the stage above the datum where zero flow is occurring.

	2007	2008	2010
Start (date & time)	31-08-07 04:00	31-08-08 04:40	11-09-10 13:20
End (date & time)	01-09-07 01:20	01-09-08 01:00	12-09-10 09:20
Duration (hours)	21.3	20.3	20
Max stage - total (m above H0)	10.4	5.3	8.1
Increase from start (m)	4.1	3.3	5.3
Max discharge including baseflow ($\text{m}^3 \text{s}^{-1}$)	1431	276	523
Max Jökuhl discharge ($\text{m}^3 \text{s}^{-1}$)	1103	156	373
Total volume caused by jökuhllaup ($\times 10^6 \text{ m}^3$)	25.5	3.6	8.4
Drainage volume from Russel <i>et al.</i> 2011 ($\times 10^6 \text{ m}^3$)	39.1	12.9	-
Discharge share of total for the year (%)	0.69	0.13	0.15
Max transport (t s^{-1})	4.4	0.7	1.3
Max concentration (g l^{-1})	3.06	2.59	2.55
Total transport caused by jökuhllaup ($\times 10^3 \text{ t}$)	82.8	14.4	22.4
Trans. share of total for the year (%)	1.16	0.29	0.19

This is also clearly seen in Figure 2b and in the hysteresis curve in Figure 3a. It is seen that the sediment concentration is the same at the same discharge at rising and falling stage, this indicate that the sediment supply from the fluvial system is adequate to account for the increased transport capacity during the flood. The conductivity of the water does not change significantly during the jökulhlaup indicating that all water is melt water from the GrIS. The diurnal temperature variation of the water was dampned to maximum of 1 °C as seen in Figure 2c, indicating the large input of cold water. The rise in stage is congruent with a period with rising temperature, all days are above the freezing point and daily maxima above 15 °C are recorded. A period with heavy rainfall seems to trigger the event.

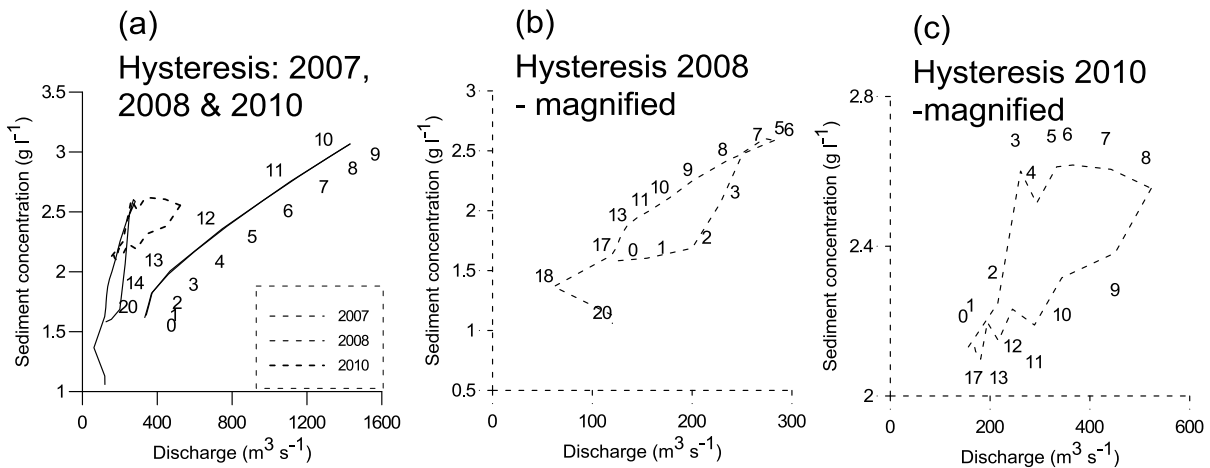


Figure 8: Hysteresis curves for the jökulhlaup events. (a) Here the hysteresis curve for the 2007 event is plotted with numbers corresponding to the time from start (hours). The 2008 and 2010 jökulhlaups are plotted as well. (b) The 2008 hysteresis curve are here magnified and plotted with time labels (hours). Note the counter clock wise sequence. (c) The same as (b) except from the clock wise sequence.

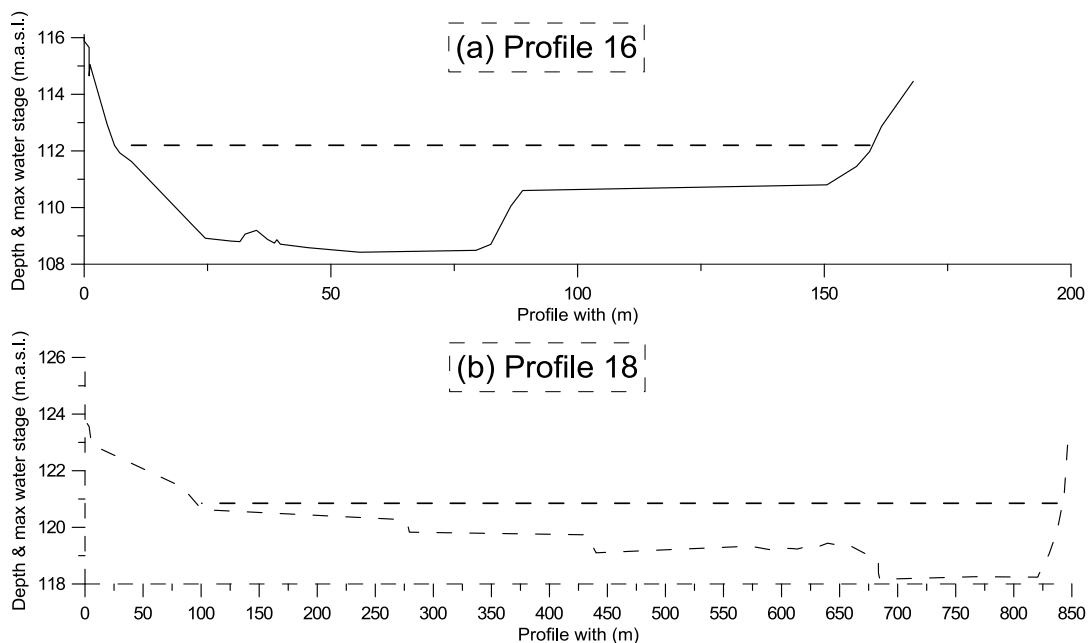


Figure 9: Maximum water stage in two cross sections of the river.

The lake from where the jökulhlaup originated was the same lake as described earlier by Russel. The lake has been drained through a tunnel within the ice originating near the south west end of the lake. The water level in the lake dropped 49.2 m and the released volume of water was $39.1 \pm 0.8 \times 10^6 \text{ m}^3$. The tapping of the lake caused severe flooding in Sandflugtsdalen (see Figure 1). Large ice blocks were deposited above the tourist road and the vegetation were torn apart and removed to the bare rock at narrow cross sections at the ice margin. In flat areas the inundation was indicated by debris of vegetation and by larger particles deposited on the vegetation. Bank erosion was observed in narrow sections cut

through glacial deposits. Several meters were eroded in an old terrace 10 km upstream the gauging station. The maximum stage during the jökulhlaup is seen on two cross sections in Figure 4.

2008

The stage rose abruptly the 31st August within a period with low slightly falling stage. The exact stage before the onset of the jökulhlaup is not known because the stage was below the pressure sensor. The stage raised up to 15.2 m.a.s.l (see Figure 5a). The estimated total volume of water originating from the jökulhlaup was $3.6 \times 10^6 \text{ m}^3$ or 0.1 % of the annual runoff (see Table 1). The sediment transport was $14 \times 10^3 \text{ t}$ or 0.3 % of the annual total. The concentration rose steeply up to a concentration of 2.6 g l^{-1} (see Figure 5b) indicating an uptake of sediment from the fluvial system. The hysteresis curve (Figure 3b) has an anticlockwise pattern indicating that the sediment in the water has not settled during the falling phase. The conductivity when the sensor was under water is seen in Figure 5b. The water temperature is again low during the jökulhlaup. The temperature started to rise the 30th August with a diurnal amplitude of up to $15 \text{ }^\circ\text{C}$, indicating a clear sky and thereby increased melting because of the short wave radiation. The precipitation prior to the jökulhlaup was only 2 mm and had no influence of the triggering of the jökulhlaup. Probably parts of the englacial drainage system from the 2007 event have been intact and when the water reached a certain level in the lake the water entered and expanded the old drainage system. There were no significant effects in the fluvial system because the stage was below the previous high stages from 2007.

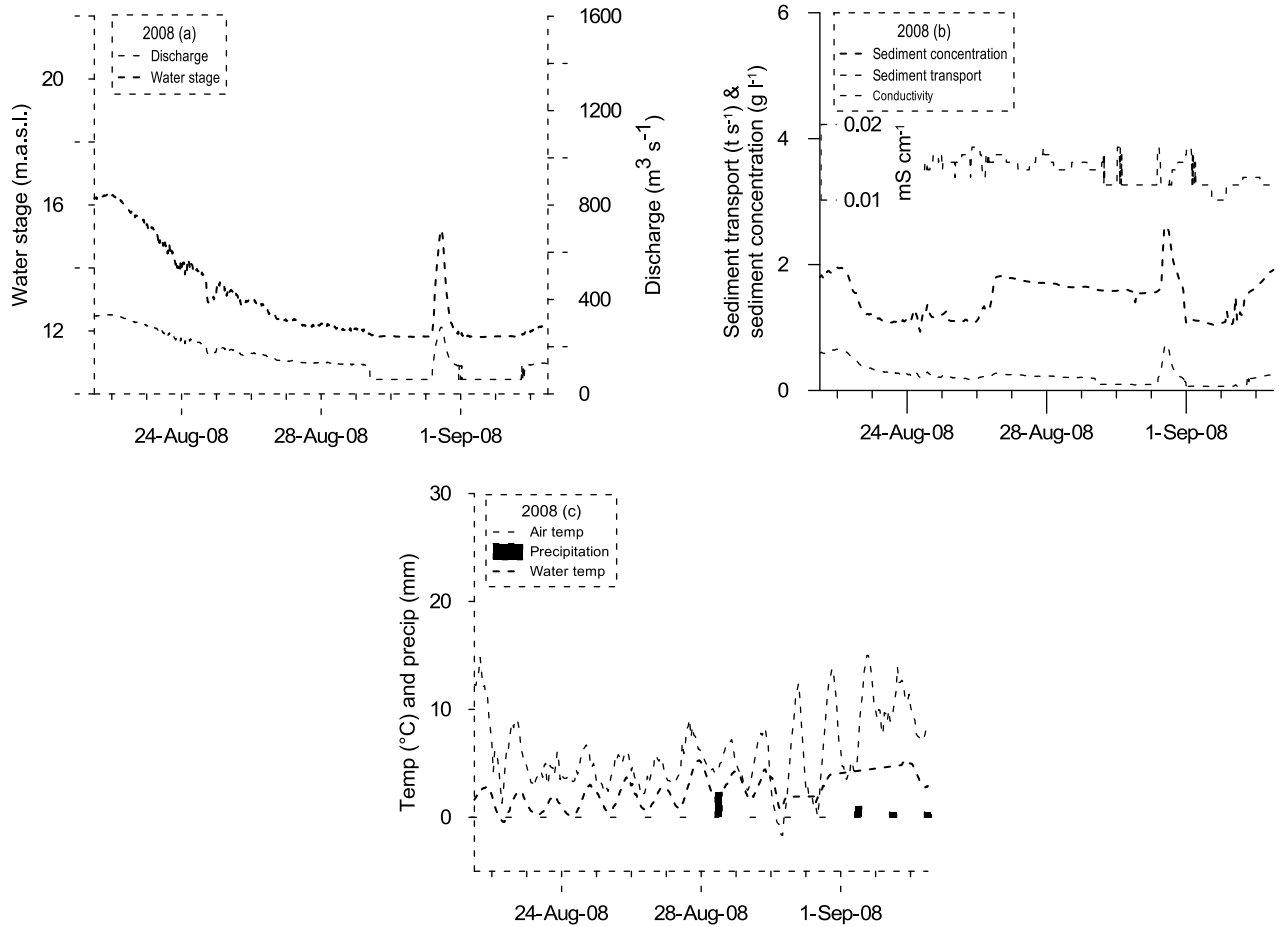


Figure 10: The gauged water stage above the reference datum (mean sea level) and discharge during the 2007 Jökulhlaup. (b) Sediment transport (solid line with a distinct peak), sediment concentration (dashed line) and the conductivity are shown here. (c) Air temperature, precipitation (DMI) and water temperature at the gauging station.

2010

This year was characterized by a very high discharge throughout the summer resulting in a record high annual discharge. After a recession period of about 10 days the water stage rose abruptly from about 13:20 the 11th September until it culminated at 21:20, see Figure 6a. The volume of water related to the jökulhlaup was about $8.4 \times 10^6 \text{ m}^3$ or 0.2 % of the annual discharge. The amount of sediment was $22 \times 10^3 \text{ t}$ equal to 0.2 % of the annual transport, see Table 1. The sediment concentration is seen in Figure 6b, it raised steeply to a value of 2.6 g l^{-1} and dropped to the same level as before the jökulhlaup just after the stage was low again. The hysteresis curve (Figure 3c) show a clockwise rotation because the concentration is lower during the falling stage than during the rising stage at the same discharge, this indicate that the sediment supply is limited, probably because sediment has been flushed out of the river system during the summer floods. The conductivity shows a clear drop during the jökulhlaup indicating a contribution of water with low conductivity from the proglacial lake into a fluvial system in recession where water from the floodplain is seeping into the river after having been in contact with the sediment for a longer period thus extraction solubles from the sediment. The jökulhlaup occurred during a period with relative low but positive temperature, see Figure 6c. There was a minor amount of precipitation prior to the jökulhlaup. This has

probably delivered enough water to raise the water in the proglacial lake to a critical level. As there was no tapping from the lake in 2009 the englacial drainage system has probably partly deteriorated near the bottom so that the water could not escape. The lake level rise until it reaches a level where it can drain into and expand the remnants of the drainage system from the large jökulhlaup in 2007.

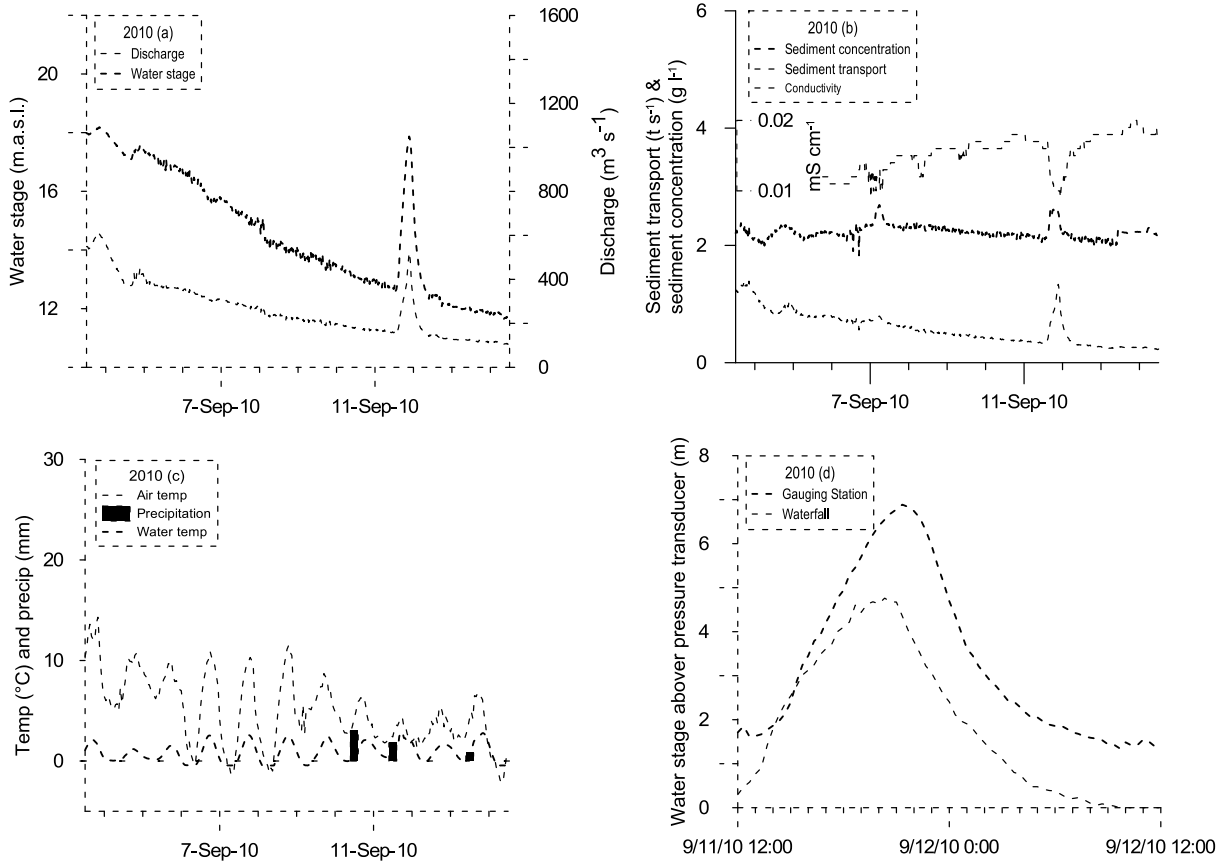


Figure 11: The gauged water stage above the reference datum (mean sea level) and discharge during the 2007 Jökulhlaup. (b) Sediment transport (solid line with a distinct peak), sediment concentration (dashed line) and the conductivity are shown here. (c) Air temperature, precipitation (DMI) and water temperature at the gauging station. (d) The delay of the flood wave from the waterfall to the gauging station.

DISCUSSION AND IMPLICATIONS

It is clearly demonstrated that jökulhlaups have occurred over a longer time span at Kangerlussuaq. Russel *et al.* 2011 suggests that a new cycle of jökulhlaups is experienced; this may be caused by the changing warmer climate resulting in larger amounts of melt water. The occurrence of the jökulhlaup in 2010 support the hypothesis of cyclicity in the way that the big event in 2007 have created an englacial drainage system that can be used and kept open by a series of minor jökulhlaups as long as the movement of the Greenland ice sheet keep the ice margin at a position where it close the bottom drainage of the valley forming the proglacial lake.

The morphological effects of the jökulhlaup have been inundation of large areas resulting in deposition of ice rafted sediment and debris in the vegetation far from the normal flood plain. However, the main effect has been erosion in the bed and banks, increased sediment transport and later deposition in areas with low slope (sandurs and the coastal delta). An indication of such deposition is observed at the gauging station at the bridges near the mouth of the Watson River. The bottom of the river was raised 1.5 – 2 m after the occurrence of the jökulhlaup in September 2010. As the concentration of sediment in the water from the proglacial lake is quite low, estimated $< 0.1 \text{ g l}^{-1}$ the high concentrations above the base level must be a result of erosion in the bed and the banks of the river. The maximum concentrations related to the jökulhlaups are clearly lower than maxima related subglacial outlets or summer floods, partly because the observed jökulhlaups have occurred late in the runoff season when the fluvial system may be more or less flushed out depending on the magnitude of the summer flood. The amount of sediment transported by the jökulhlaups is less than 2 % of the annual transport it is therefore assumed that it will be very difficult to identify layers related to jökulhlaups in the deposits on the bottom of the fjord, so layers with an increased amount of coarse grains are probably more related to drifting of ice from the bed and banks during the freeze up during autumn and ice break up during spring. Except for increased erosion at selected locations the morphological effects of jökulhlaups near Kangerlussuaq are limited. The sudden rise of the water may endanger the tourism if tourists are trapped by the water at low lying locations. It may also be a danger to the technical installations related to the town and airport because high stages may damage the bridges and break the drinking water pipeline that cross Watson River.

Jökulhlaups have been monitored at other locations in Greenland. At the Mittivakkat glacier at least two jökulhlaups were recorded in 1958 by Valeur (1959). Discharge was recorded, the maximum of $80 \text{ m}^3 \text{ s}^{-1}$ is 4 – 10 times higher than later recorded annual maxima. No simultaneous observations of sediment transport were available, but later observations by Hasholt (1976) and Busskamp & Hasholt (1996), of the fluvial system indicated that pebble and stone size material could only be transported all the way from the glacier to the marine delta during jökulhlaups or by ice rafting. It could also be observed that the jökulhlaup eroded in terminal moraine deposits within the valley. Other documented observations of jökulhlaups are from the research station Zackenberg in North East Greenland (Hasholt *et al* 2008). Here jökulhlaups have occurred several times, endangering the work at the field station and causing bed erosion in the river. The amount of sediment transport related to the jökulhlaups was here up to 82 % of the total annual load. In this case deposits from jökulhlaups may be used as markers in the sediment column deposited in a lake and on the marine delta, maybe even in the fjord.

In 2008 two persons were killed by a glacial outburst in front of Kangerluarsuk Sermia - no observations of magnitude of discharge were available (Internet 1, 2). Fortunately this is the only known incident where people were killed.

A survey of lakes having a potential for creating jökulhlaup was carried out by Weidick and Olesen (1978). The investigations showed several locations along the margin of the Greenland Ice Sheet in South West Greenland. It was also demonstrated huge volumes of water could be released, the largest volume was $5\text{-}6 \text{ km}^3$. A recent survey carried out by Asiaq/GRAS near

the capital Nuuk also demonstrated the potential of using satellite observations for monitoring of ice dammed lakes and their tapping (Tøttrup *et al* 2011). Because of the sparse population, mainly living in towns along the coast, very few jökulhlaups are actually observed in Greenland. The threat against humans is therefore limited, however the possibility should be taken into account at tourist locations and when establishing new technical installations such as mining facilities and hydro power stations.

ACKNOWLEDGMENTS

The project is sponsored by KVUG (Kommissionen for Videnskabelige Undersøgelser i Grønland) grant No.07-015998, grant No.09-064628 and grant No.2138-08-0003 and FNU (Forskningsrådet for Natur og Univers) grant No.272-07-0645. The project is included as part of the Danish IPY program as project No.104 and No. 317, and it is further included as partner in the SEDIBUD monitoring program.

REFERENCES

- Born, E. and Böcher, J. 2001 *The ecology of Greenland*. Ministry of Environment and Natural Resources in Nuuk.
- Broeke, M. v. d., Smeets, P., Ettema, J., and Munneke, P. 2008 Surface radiation balance in the ablation zone of the west Greenland ice sheet. *Journal of Geophysical Research*. **113**, 1-14.
- Busskamp, R. and Hasholt, B. 1996 Coarse bed load transport in a glacial valley, Sermilik, South East Greenland. *Zeitschrift für Geomorphologie*. **40**(3) 349-358.
- Clague, J. J. and Mathews, W. H. 1973 The magnitude of jökulhlaups. *Journal of Glaciology*. **16** (2), 209-216.
- Hasholt, B. 1976 Hydrology and transport of material in the Sermilik Area 1972. *Geografisk Tidsskrift*. **75**, 30-39.
- Hasholt, B. and Anderson, J. 2003 On the formation and stability of oligosaline lakes in the arid, low arctic area og Kangerlussuaq, south-west Greenland. *Northern Research Basins - 14th international symposium and workshop*. pp 41-48.
- Hasholt, B., Larsen, M., A., D., Mikkelsen, A., B., and Holtegaard Nielsen, M. Runoff and sediment and dissolved loads from the Greenland ice sheet at Kangerlussuaq, West Greenland, 2007 to 2010. *Journal of Glaciology*. (Submitted).
- Hasholt, B., Mernild, S. H., Sigsgaard, C., Elberling, B., Petersen, D., Jakobsen, B. H., Hansen, B. U., Hinkler, J., and Sjøgaard, H. 2008 Hydrology and Transport of Sediment and Solutes at Zackenberg. *Advances in Ecological Research* **40**, Elsevier. pp 197-221.

Internet: <http://www.naturvidenskab.net/img/pressemeddelelser/52.pdf> (visited 28-04-2011).

- Mernild, S. H. and Hasholt, B. 2009 Observed runoff, jökulhlaups and suspended sediment load from the Greenland ice sheet at Kangerlussuaq, West Greenland, 2007 and 2008. *Journal of Glaciology*. **55**(193), 855-858.
- Mernild, S. H., Hasholt, B., Tidwell, K., and Kane, D. L. 2008 Jökulhlaup observed at Greenland ice sheet. *Eos*. **89**(35), 321-322.
- Mernild, S. H., Liston, G. E., Steffen, K., van den Broeke, M., and Hasholt, B. 2010 Runoff and mass-balance simulations from the Greenland Ice Sheet at Kangerlussuaq (Søndre Strømfjord) in a 30-year perspective, 1979-2008. *Cryosphere*. **4**(2), 231-242.
- Russell, A., Carrivick, L., Ingeman-Nielsen, T., Yde, J., and Williams, M. 2011 A new cycle of jökulhlaups at Russel Glacier, Kangerlussuaq, West Greenland. *Journal of Glaciology*. **57**(202), 238-246.
- Russell, A. J. 2007 Controls on the sedimentology of an ice-contact jökulhlaup-dominated delta, Kangerlussuaq, west Greenland. *Sedimentary Geology*. **193**(1-4), 131-148.
- Russell, A. J. 2009 Jökulhlaup (ice-dammed lake outburst flood) impact within a valley-confined sandur subject to backwater conditions, Kangerlussuaq, West Greenland. *Sedimentary Geology*. **215**.1-4, 33-49.
- Russell, A. J., Aitken, J. F., and De Jong, C. 1990 Observations on the Drainage of An Ice-Dammed Lake in West Greenland. *Journal of Glaciology*. **36**(122), 72-74.
- Sugden, D. E., Clapperton, C. M., and Knight, P. G. 1985 A Jökulhlaup Near Søndre Strømfjord, West Greenland, and Some Effects on the Ice-Sheet Margin. *Journal of Glaciology*. **31**(109), 366-368.
- Tøttrup, C., Mätzler, E., Petersen, D., Larsen, M. and Naamansen, B. 2011 A satellite perspective on jökulhlaup in Greenland. pp. 1-56. Asiaq/GRAS Report 2011-15. Project no. B35-08.
- Valeur, H. 1959 Runoff studies from the Mitdluagat Gletcher in SE-Greenland during the late summer 1958. *Geografisk Tidsskrift*. **58**. 54-65.
- van de Wal, R. S. W., Greuell, W., van den Broeke, M. R., Reijmer, C. H., and Oerlemans, J. 2005 Surface mass-balance observations and automatic weather station data along a transect near Kangerlussuaq, West Greenland. *Annals of Glaciology*. **42**. 311-316.
- Weidick and Olesen 1978 Hydrologiske bassiner i Vestgrønland. 1-160., GGU 1978.

A Satellite Perspective on Jökulhlaup in Greenland

Eva Mätzler¹, Bo Naamansen¹, Morten Larsen^{1*}, Christian Tøttrup², Dorthe Petersen¹
and Kisser Thorsøe¹

¹ Asiaq – Greenland Survey, P.O. Box 1003, 3900 Nuuk, GREENLAND

² GRAS, c/o Dept. of Geography and Geology, University of Copenhagen, Øster Voldgade 10, 1350
Copenhagen K, DENMARK

*Corresponding author, e-mail: mol@asiaq.gl

ABSTRACT

Methods to locate potential jökulhlaup lakes and to assess the volume of the water discharges only by remote sensing techniques were developed. In an area of 16,000 km² east of Nuuk in West Greenland the method for locating potential jökulhlaup lakes was tested and for two known jökulhlaup lakes the volume of the water discharges were assessed.

To locate potential jökulhlaup lakes a time sequence of LANDSAT archive data covering the area was investigated with spectral mapping techniques. The investigations showed how the LANDSAT data can be used to map surface water, glacial ice, and surface temporal anomalies. By GIS analysis, the mapped themes were used to identify potential jökulhlaup lakes. It was found that the method is applicable for use in another connection.

For assessing the volume of the water discharges, the bathymetries for jökulhlaup lakes were mapped from stereo images acquired by the ASTER satellite sensor and thereby defining the relations between the lake surface areas and the volumes of water stored in the lakes. Annual lake areas outlined from LANDSAT images were combined with the area-volume relations to describe the change over time in the volume of water in the lakes and thereby the volume released during jökulhlaups. The results of the volume assessments were validated against recordings from a hydrological station in the downstream lake. The validation underpinned the credibility of the method and as the method relies on satellite data that are readily available the, method is applicable for use in a wider context.

KEYWORDS

Jökulhlaup; remote sensing; hydrology; Arctic; Greenland

1 INTRODUCTION

Ice dammed lakes are a very common phenomenon in Greenland. The lakes are formed where water collects in depressions under a glacier or along a glacier margin. When the water level in the lake reaches a critical level a jökulhlaup is possible to occur. Jökulhlaup is an Icelandic term that has been adopted by scientists. A jökulhlaup is a very intense flood where a subglacial or proglacial water reservoir releases a large amount of water abruptly.

Jökulhlaup influences ecosystems and human activities in downstream areas. Settlements or towns are potential catastrophe areas if hit by a jökulhlaup. Luckily, in Greenland, this is not the foremost concern as no permanent settlements are located in areas of potential jökulhlaup drainage, at least not at the moment. That said, knowledge making us able to predict jökulhlaup, thereby protecting human life, is always crucial.

In a more general perspective, global warming is likely to influence both the magnitude and the frequency of jökulhlaup.

A hydro power perspective initiated this work. In Greenland there are a number of potential hydro power areas where jökulhlaup lakes exist close by or within the catchment area. In these cases the consequence of jökulhlaup on any constructions and the possible exploitation of the water resource from the jökulhlaup lake have to be considered during the design process. It is therefore important to know the magnitude and frequency of jökulhlaup in each area.

The primary aim of the work was to develop a method to locate ice dammed lakes and determine the quantity of water discharged by jökulhlaup primarily based on satellite data. The secondary aim was to initiate a transfer and accumulation of knowledge and expertise to Greenland within the discipline of remote sensing.

The work was funded by KVUG (The Commission for Scientific Research in Greenland (*Kommissionen for Videnskabelige Undersøgelser i Grønland*)) under the Danish Ministry of Science, Technology and Innovation.

2 STUDY AREA

The study area consists of a large area in the vicinity of Nuuk called the *project area* and a smaller area containing two known ice dammed lakes, *Lake North* and *Lake South* in connection with the reservoir lake named *Isortuarsuup Tasia (Lake ISTA)*. This area is called the *ISTA area*. The project area and the ISTA area together with Nuuk can be seen in Figure 12.

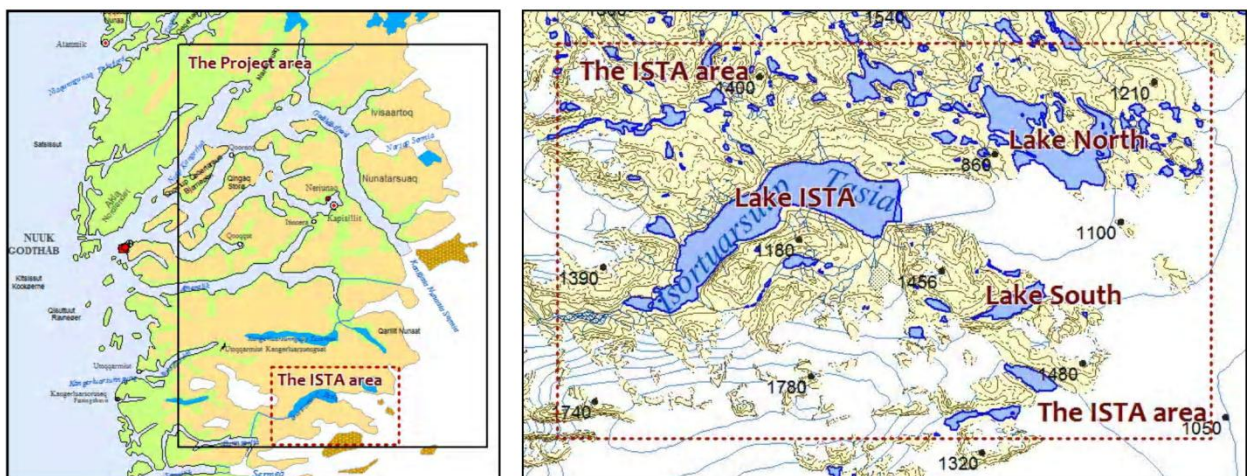


Figure 12 The project area and the ISTA area

It is known that Lake North and Lake South regularly empties into Lake ISTA and as Lake ISTA is a potential reservoir for hydro power, hydrological investigations has been carried out in the area and several of the jökulhlaup have been monitored. Therefore the area of interest for the assessment of volumes is *Lake North* and *Lake South* in the ISTA area, whereas the project area is well suited for method development for identifying lakes with jökulhlaup potential.

3 LOCATE POTENTIAL JÖKULHLAUP LAKES

In order to locate potential jökulhlaup lakes a four-task approach was used. In the three first tasks a lake theme, a glacier theme, and a surface anomaly theme was mapped using well

tested remote sensing classification techniques. The mapping was based on a time series of LANDSAT satellite data in the late summers in the period 2003 to 2009. In the fourth task a spatial location analysis with the three maps were performed in a GIS to find potential jökulhlaup lakes.

Mapping lakes

For the lake mapping the Tasseled Cap transformation was used. The Tasseled Cap transformation performs an orthogonal transformation of the original LANDSAT data into a new three-dimensional space, consisting of a *Brightness* index, a *Greenness* index, and a *Third* component related to soil moisture or *Wetness* (Chuvieco & Huete 2010). Especially brightness and wetness are strongly associated with water surfaces, and a simple threshold was used to classify water as any surface area with a brightness index less than 0.4 and a wetness index larger than 0.

The lake classification was enhanced by a simple rule stating that a pixel only was water, if it was classified as water in 5 out of 6 years in the LANDSAT time series.

Mapping glaciers

The mapping of glaciers from multi-spectral imagery involved discriminating between ice and other surface types. It was difficult to map glaciers for an individual year due to difficulties in separating glacier ice from other types of ice and snow. In addition debris covered ice caused confusion with non-ice areas. The areas of confusion tend to differ from year to year, so it was assumed that a better glacier classification could be achieved by using the surface long-term spectral characteristics as given by the Tasseled Cap parameters.

In the approach to map glaciers an output image was produced as the average of the Tasseled Cap parameters from the time series of LANDSAT satellite data in the late summers in the period 2003 to 2009. The image was used as input for an unsupervised classification with 50 spectral classes. The spectral classes were thematically coded into glacier-ice and non glacier-ice. After labeling, the classified image was filtered in order to remove speckle noise using a median filter.

Mapping surface temporal anomalies

The vegetation index approach Normalized Difference Vegetation Index (NDVI) was used for the mapping of surface temporal anomalies. It has been shown that NDVI is sensitive to the presence, density, and condition of vegetation (Tucker 1979; DeFries & Townshend 1994; Huete et al. 2002). Furthermore NDVI also provides valuable indications of land cover categories. By design, the NDVI varies between -1.0 and +1.0. Areas containing a dense vegetation canopy will have positive values (0.3 to 0.8), while soils tend to generate rather small positive NDVI values (0.1 to 0.2). Free standing water will tend to have very low positive or even slightly negative NDVI values. Clouds and snow fields will be characterized by negative NDVI values.

Since NDVI relates to the present land cover, multi-temporal NDVI images were used to identify surface temporal anomalies, i.e. surface areas that change over time. NDVI anomalies were calculated from the difference between NDVI at a given date and the long-term mean NDVI. The long-term mean NDVI was calculated from the images in the LANDSAT time series.

Potential jökulhlaup lakes were mapped using NDVI anomalies based on the assumption that a lake that empties, will have both strong positive or negative anomalies due to discharge or refill. Yearly anomalies for two known jökulhlaup lakes were compared with anomalies for

two reference lakes where jökulhlaup are known not to occur. The comparison showed significant difference between the anomaly for the jökulhlaup lakes and the reference lakes.

Spatial location analysis

For the GIS analysis the mapped lake theme, the glacier theme, and the surface anomaly theme were converted to polygons. By definition the potential jökulhlaup lakes borders the glacier margin. In the GIS analysis all lakes polygons located in the vicinity of a glacier, who also shared area(s) with a surface anomaly, were selected. Without any restrictions such a selection returned many hundreds of potential jökulhlaup lakes, making it necessary to include an area size threshold to filter out smaller and less significant anomalies. The threshold was set at 250,000 m² and 20 potential jökulhlaup lakes with changes of 250,000 m² or more in area size were selected in the test area east of Nuuk.

Discussion

The method showed good results for the project area. The collection of reliable data from several years took time; but the data could be used in the further analysis.

Ice covered lakes were difficult to classify in the remote sensing approach. Further development in discriminating between glacier and lake ice is advisable. Setting the threshold for the area anomaly is of great importance and it must be defined according to the goal of each project. The time series, i.e. the number of years to be analyzed is also significant. A jökulhlaup for a given lake can occur only every 10th year or even less frequent. For this reason it must be considered to get data from a longer time series. However, in this project the remote sensing approach with a time series of six years had no problems in locating Lake North, which is known to empty every nine years.

4 ASSESSMENT OF THE WATER VOLUMES

The method for assessing the volume of the water discharges quantifies the volume of water contained in the lakes from just before and just after the jökulhlaups. For this purpose bathymetries, surface areas and an area-volume relations for the lakes were needed.

Determining lake bathymetries

Measurements of lake bathymetries for most lakes in Greenland have not been carried out, and also not for Lake North and Lake South. Instead the bathymetries of the lakes were determined from a digital elevation model (DEM) extracted from satellite stereo images. For the extraction a set of ASTER stereo images from August 8, 2004 were chosen.

The ASTER sensor system is designed to allow along-track optical stereo data acquisition at a 15 m spatial resolution for each ASTER scene. These stereo pairs were used to create a DEM using a stereo autocorrelation procedure and applying the principle of the parallax effect. The parallax effect is based on the fact that the image stereo pair will show a pixel displacement in the satellite flight direction that is proportional to the pixel elevation (Welch et al. 1998). A cross-correlation method was used to evaluate this displacement, and transform it into elevation values.

Determining surface areas of the lakes

In the determination of the lake surface areas higher accuracy of the surface areas was needed than in the mapping of the lakes. Therefore three different pixel based classification

techniques, and a manual digitization of lake borders were tested. The pixel based classification techniques included unsupervised classification, supervised classification, and an index based classification.

In general a semi-automatic index based classification, where regions with problems were corrected manually, was the most consistent and fastest method. The index based classification was based on the *Brightness* index and the *Wetness* index from the Tasseled Cap transformation.

Lake surface areas for the two lakes were determined for a time series of LANDSAT satellite data in the late summers in the period 1999 to 2010. The determined lake surface areas for Lake North are seen in Figure 13. In the figure a jökulhlaup is seen by the abruptly change in the lake surface area in September 2002.

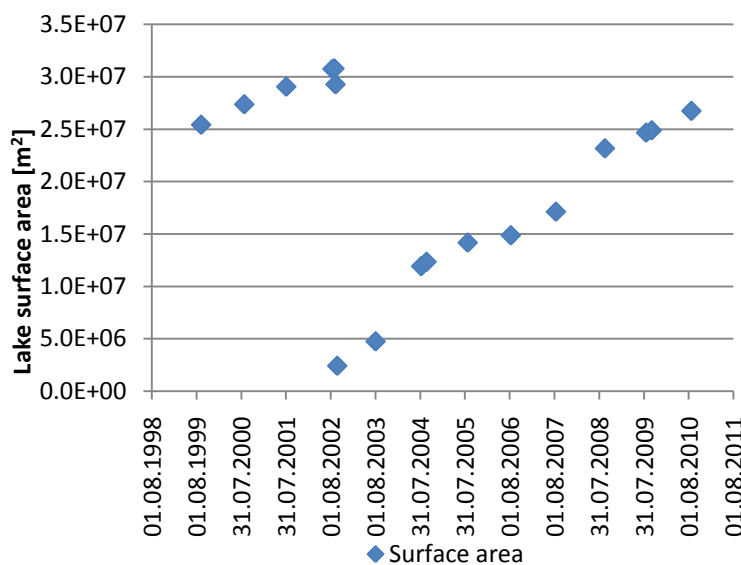


Figure 13 Digitized lake surface areas for Lake North

Determining the area-volume relations

An area-volume relation is a site-specific, empirical relation which describes the volume of water stored in the lake as a function of the lake surface area.

The area-volume relations were derived by estimations of surface areas and volumes from the lake bathymetries for potential water levels at 1 m increments. The surface areas were estimated as the total area of cells in the bathymetries with elevations below the potential water level. The volumes were estimated as the surface areas multiplied with the difference between the potential water level and the average elevation of cells below the potential water level in the bathymetries.

By deriving the area-volume relation from the DEM it was assumed that the water surface area increases with the water level, and that the volume in the lake increases with the water surface area, i.e. the volume of water *hidden* under an overhanging or floating glacier front is assumed negligible. Furthermore, as the DEM not was extracted when the water level in the lakes were at its absolute minimum, the estimated volumes only represent the volume above

the water level in the lakes when the DEM was extracted. The area-volume relation for Lake North is seen in Figure 14.

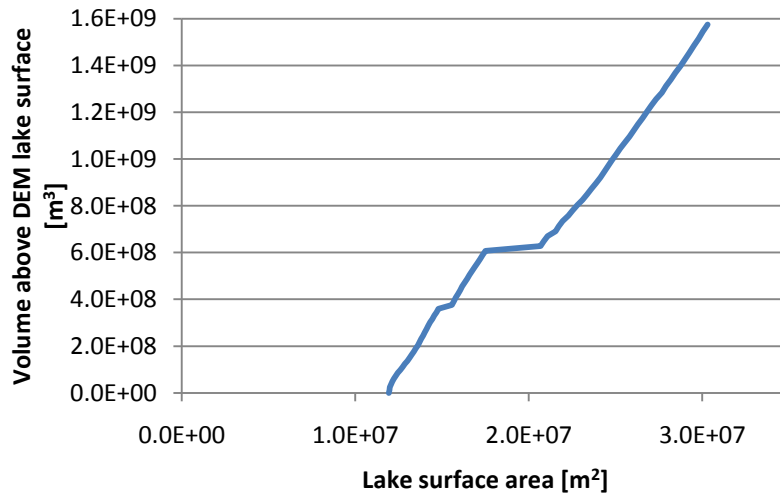


Figure 14 The area-volume relation for Lake North

In order to estimate the total volume of water released during a jökulhlaup it was necessary to evaluate the volume between the absolute minimum water level in the lakes and the water level in the DEM. The volumes were estimated by determination of the water fill rate for the lakes. The fill rates were determined from the changes in the lake volumes and the accumulated number of positive degree days (i.e. the sum of mean daily temperatures above 0° C). The volume of water in Lake North as a function of accumulated positive degree days is seen in Figure 15. A good correlation between the lake volume and the accumulated number of positive degree days is seen. By the slope of the linear regression lines fill rates of $2.17 \cdot 10^5$ m³/pos. degree day and $2.08 \cdot 10^5$ m³/pos. degree day are seen before and after the jökulhlaup in September 2002.

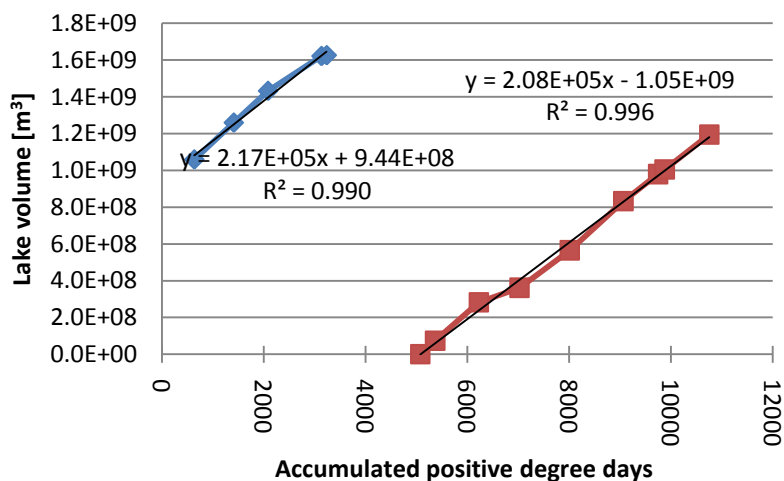


Figure 15 Volume of water in Lake North as a function of accumulated positive degree days

By the fill rate and the accumulated number of positive degree days in the years after a jökulhlaup, the volume difference between the water level in the extracted DEM and the

absolute minimum water level after the jökulhlaup was estimated by extrapolation. From the determined lake surface area just before the jökulhlaup and the area-volume relation the water volume above the water level in the DEM was estimated. The total volume of the water discharge from the jökulhlaup was estimated as the sum of the volume below and above the water level in the extracted DEM.

Validation of the volume assessment

The two jökulhlaup lakes are downstream connected with the reservoir lake Lake ISTA; see Figure 12. Hydrological investigations of Lake ISTA were initiated in 1975 and since 1976 the water level has been continuously monitored by an automatic hydrometric station. The measured water level time series has been converted to a discharge time series by use of a stage-discharge relation for Lake ISTA.

By integrations of the water balance equation for Lake ISTA, containing the measurement from the hydrometric station, the water released during the jökulhlaups was estimated. The water volumes from the water balance equation were used for validation of the remote sensing based method.

Results

In the period 1999 to 2010 three jökulhlaup occurred in the ISTA area. Lake North was emptied ones, in September 2002. Lake South was emptied twice, in August 2003 and in September 2007. The volumes of the water discharges from the three jökulhlaups were estimated by the developed remote sensing method and the water balance equation for Lake ISTA; see Table 6. By the estimations with the remote sensing method about 80 % of the water volumes were above the water level in the DEM in the three jökulhlaup events. The last 20 % were estimated by extrapolations with the rate filling method.

Table 6 Estimated volumes of water [m³] released during jökulhlaups

	Lake North	Lake South	
	September 2002	August 2003	September 2007
Remote sensing method	1.85·10 ⁹	0.28·10 ⁹	0.18·10 ⁹
Water balance equation	1.98·10 ⁹	0.29·10 ⁹	0.19·10 ⁹
Difference	7 %	0.4 %	2 %

The validation with the water balance equation showed, that the method gave very reliable results for the two test lakes in the ISTA area, even though the method has challenges and limitations.

The main challenges encountered were:

- To obtain ASTER stereo images immediately after a jökulhlaup event to extract the best possible DEM (i.e. when the lake water level is low) and when this was not possible to estimate the volume of water below the DEM water level.
- To derive reliable surface areas from LANDSAT images without ice or shadows on the lake, debris on bordering glaciers or clouds.

The optimal satellite data to assess lake volumes and to classify lake areas are:

- Cloudless images obtained immediately after the jökulhlaup event.
- Images obtained at the end of the melting season, where snow and ice cover and seasonal lake ice are minimal.
- Images obtained in mid-summer, where cast shadows are minimal.

The conditions described are somewhat contradictory explaining the challenge in data acquisition well. In reality selecting images to outline lake areas or to generate a DEM is almost never optimal due to adverse weather conditions (frequent clouds, early snow) and the narrow time window with optimal conditions.

Shadows influences also the quality of DEM extraction and challenges the assessment of lake volumes. Cloud covers, debris covered glaciers, and floating ice on lakes are additional challenges in outlining lake surface areas.

The method is less accurate for potential jökulhlaup lakes with a steep bathymetry. Here, the differences in lake surface areas over time would be small even when the volume of water in the lake changes dramatically. Thereby a small error in the lake surface area will give a large error in the calculated volume.

The smaller the lake, compared to the grid size of the DEM and spatial resolution of the images used to evaluate the surface area, the higher the uncertainties of the results.

5 CONCLUSION

The primary aim of the project was to develop methods to locate potential jökulhlaup lakes and to determine the quantity of water discharged by jökulhlaup based primarily on satellite data.

Remote sensing is a suitable and cost-efficient way to provide temporal, consistent and synoptic land surface information. The present study has demonstrated how satellite images in combination with relative simple analytical techniques can comply with the primary aim of the project.

Identifying lakes with jökulhlaup potential

The work showed how multi-temporal LANDSAT image data can be used to map surface water, glacial ice, and surface temporal anomalies (i.e. surface areas that change over time). When combined in a GIS, the mapped themes can be used to identify potential jökulhlaup lakes characterized as surface water bodies that border a glacier while also being associated with a surface area change.

Ice covered lakes are difficult to classify in the remote sensing approach. Further development in discriminating between glacier and lake ice is advisable.

Assessing the volume of water released during jökulhlaup

The magnitude of a jökulhlaup depends largely on the quantity of water draining the ice dammed lake, i.e. the water discharge volume. In the work it was shown how the bathymetry for a jökulhlaup lake can be mapped from stereo images acquired by the ASTER satellite sensor and thereby defining the relation between the lake surface area and the volume of water stored in the lake.

The stereo images obtainable for the project area were not in the immediate time after a jökulhlaup, making it necessary to develop a method to extrapolate the volume to the lowest observed water level (i.e. the smallest lake surface area).

Annual lake areas outlined from LANDSAT images were combined with the area-volume relation to describe the change over time in the volume of water in the lake and thereby the volume released during jökulhlaup.

The results from three known jökulhlaup events were validated against recordings from a hydrological station in the downstream Lake ISTA.

As the validation underpins the credibility of the method, and as the method relies on satellite data that is readily available for many parts of the world, we recommend its application in a wider context, i.e. Greenland as well as other places.

ACKNOWLEDGEMENT

The project group would like to express our thanks to KVUG for giving us the opportunity and the resources to produce this work and to learn about remote sensing in the process.

LIST OF REFERENCES

- Chuvieco, E. & Huete, A. (2010). *Fundamentals of Satellite Remote Sensing*. CRC Press.
- DeFries, R.S. & Townshend, J.R.G. (1994). NDVI-Derived Land-Cover Classifications at A Global-Scale. *International Journal of Remote Sensing*, 15, 3567-3586.
- Huete,A., Didan,K., Miura,T., Rodriguez,E.P., Gao,X. & Ferreira,L.G. (2002). Overview of the radiometric and biophysical performance of the MODIS vegetation indices. *Remote Sensing of Environment*, 83, 195-213.
- Tucker,C.J. (1979). Red and Photographic Infrared Linear Combinations for Monitoring Vegetation. *Remote Sensing of Environment*, 8, 127-150.
- Welch, R., T. Jordan, H. Lang, and H. Murakami, 1998. ASTER as a source for topographic data in the late 1990's, *IEEE Transactions on Geoscience and Remote Sensing*, 36:1282–1289.

A Hydrology, Hydro-Climatology and Sediment Research Program related to the
Canadian Oil Sands development

T.D. Prowse¹

**¹*Water and Climate Impacts Research Centre, Environment Canada and University of
Victoria, Victoria, BC, Canada
terry.prowse@ec.gc.ca***

The Oil Sands of western Canada has undergone significant industrial development in recent years and is forecast to expand further. To ensure that such development proceeds in an environmentally sustainable fashion, environmental monitoring plans have been recently developed by Environment Canada in collaboration with Alberta Environment and other private and academic scientists. The recently released *Integrated Oil Sands Environmental Monitoring Plan* includes four components: a) water quality (Athabasca River mainstem and tributaries), b) air quality, c) terrestrial biodiversity and habitat, and d) an expanded geographical extent program for water quality and quantity, aquatic biodiversity and effects, and acid-sensitive lakes. The primary goal of the first component was to quantify and assesses the sources, transport, loadings, fate, and types of oil sands and other industrial and municipal contaminants into the Athabasca River system. Specifically, it was targeted at obtaining a better spatial and temporal quantitative understanding of the key physical/chemical “stressors” affecting the system, specifically including: hydrology, hydro-climatology, hydraulics, and sediment dynamics.

Although the Oil Sands developments are located in the lower reaches of the Athabasca River, an understanding of the hydrological and climatic conditions affecting the overall Athabasca catchment is required because of the strong control the upper part of the catchment has on downstream river flow. Approximately 55% of the Athabasca River flow exiting the lower Athabasca River as it enters the Peace-Athabasca Delta originates from flow entering upstream of the developments. Hence, to quantify and characterize the downstream flow regimes, evaluations are needed of the upstream major source-water hydrologic regimes and types (e.g., nival, pluvial and glacial regimes). Specifically, focus needs to be placed on the importance of each regime to seasonal flow contributions, their sensitivity to variations in current and future climatic drivers, and potential to generate extreme events within the lower Athabasca (e.g., low flows and floods). A broader study of sediment dynamics (i.e. erosion, transport and deposition) is also needed because it can be a significant driver of contaminant transport as many contaminants partition strongly to fine sediments. A focus also needs to be placed on river-ice dynamics because they are known to produce floods and sediment fluxes that far exceed those possible under open-water conditions, and also play a major role in other physical and chemical processes associated with, for example, mixing regimes, flushing flows and background chemistry.

This presentation outlines an integrated field-based and modelling research program currently being designed and implemented by Environment Canada water-research scientists to address the above scientific needs. Given the multiple, cold-regions foci of the program, and the dual *Symposium & Workshop* structure of the *Northern Research Basins* meetings, a workshop focused on taking advantage of the notable NRB circumpolar expertise in cold-regions hydrology to define “best practices” that could be used in such a research program will follow the presentation.

Multi-dataset time series of Arctic and sub-Arctic snow extent and snow water equivalent

Chris Derksen^{1*} and Ross Brown²

¹*Climate Research Division, Environment Canada, Toronto, Ontario, M3H 5T4, CANADA*

²*Environment Canada @ Ouranos Inc. Montreal, Quebec, CANADA*

**Corresponding author, e-mail: Chris.Derksen@ec.gc.ca*

ABSTRACT

Time series of Arctic (land area north of 60, excluding Greenland) snow cover cover extent (SCE), duration (SCD), and snow water equivalent (SWE) anomalies relative to a 1988-2007 reference period were calculated to investigate trends and variability during the satellite era. SCE and SCD anomalies (spanning 1967-2010) derived from the NOAA snow chart Climate Data Record (CDR) showed significant reductions (lower SCE; shorter SCD) in the May/June period consistent with warming spring temperatures across high latitudes. The 2010 season marked the lowest SCE and shortest SCD in the satellite era for the North American and Eurasian sectors of the Arctic. Monthly averaged snow water equivalent (SWE) time series were derived for 1988 through 2010 from satellite passive microwave derived data (including empirical algorithms and an assimilation technique using radiative transfer modeling), the Canadian Meteorological Centre (CMC) daily gridded global snow depth analysis, and ERA-40 atmospheric reanalysis. The individual datasets exhibited considerable spread in the absolute mean monthly SWE estimates, however, the anomaly series showed significant agreement in April (the month of peak pre-melt SWE). The SWE time series indicated inverse trends over Eurasia (increasing SWE) versus North America (decreasing SWE) until 2003, after which the trend over North America changed sign and SWE anomalies in both regions trend positive.

KEYWORDS

Snow cover; snow water equivalent; remote sensing; time series analysis

1 INTRODUCTION

Reliable information on snow cover across the Arctic and sub-Arctic is needed for climate monitoring, for understanding the Arctic climate system, and for the evaluation of the representation of snow cover and snow cover feedbacks in climate models. Multiple snow cover data sources are available (for example, from satellite observations, analyses of surface measurements, and output from atmospheric reanalysis) however monitoring snow cover across the Arctic region is complicated by strong local controls on snow cover, frequent cloud cover, and large gaps and biases in surface observing networks. It is beneficial, therefore, to consider multiple sources of snow information (for example, from satellite observations, analyses of surface measurements, and output from atmospheric reanalysis) both to address the uncertainties associated with individual datasets, and to understand how various snow cover related variables are inter-related. These variables include snow cover extent (SCE: the area covered by snow), snow cover duration (SCD: how long snow is on the ground), and snow water equivalent (SWE: the amount of liquid water stored in the form of snow).

Variability in SCE and SCD across high latitudes is primarily controlled by surface temperature anomalies during the snow cover onset and melt periods (Brown et al., 2007). Variability in SWE is more complicated because it responds to both temperature and

precipitation anomalies and varies with snow climate regime and elevation (Brown and Mote, 2009). Producing meaningful gridded SWE estimates across northern environments is also complicated by a high degree of spatial heterogeneity introduced by topographic and vegetative controls on snow metamorphic and (re)distribution processes (Pomeroy and Li, 2000; Sturm et al., 2001).

The objective of this study is to report updated time series of Arctic (land area north of 60, excluding Greenland) snow cover parameters, including:

1. Spring (April, May, June; 1967-2010) SCE from the NOAA snow chart Climate Data Record (CDR) maintained at Rutgers University (<http://climate.rutgers.edu/snowcover/>). Interpretation of this time series is made in the context of recent multi-dataset assessments of Arctic and Northern Hemisphere SCE reported in Brown et al (2010) and Brown and Robinson (2011), respectively.
2. Spring SCD (1967-2010), also derived from the NOAA snow chart CDR.
3. Multi-dataset April SWE (1988-2010) including two independent satellite derived datasets (described in Pulliainen, 2006, and Derksen et al., 2010), the Canadian Meteorological Centre (CMC) daily gridded global snow depth analysis (Brasnett, 1999), and ERA-interim atmospheric reanalysis (Simmons et al., 2007).

2 DATA AND METHODS

In this study we provide an update to the 1967-2008 SCE and SCD information presented in Brown et al. (2010) with the addition of SWE information in order to comprehensively address the characteristics of pan-Arctic terrestrial snow cover. A complete update of the Brown et al (2010) analysis using all the SCE data sources outlined in Table 1 is beyond the scope of this study. Instead, we focus on the recently released NOAA snow chart CDR (see Brown and Robinson, 2011). The CDR combines the original 190 km resolution NOAA snow charts (1967-1999; Robinson et al., 1993) with the 24 km resolution Interactive Multi-Sensor (IMS) snow product (1999-present) described in Ramsay (1998). Production of the CDR resulted in minor modifications to the IMS product, primarily by increasing the snow extent in mountainous areas. While consideration of the full suite of SCE datasets would be preferred, the assessment presented in Brown et al (2010) provides evidence that anomaly time series computed from the NOAA CDR agree well with the other SCE data records during the spring melt period.

Arctic SWE time series were derived for 1988 through 2010 using the datasets outlined in Table 2. Satellite passive microwave data are frequently used to retrieve terrestrial SWE, although the characteristics of Arctic snow cover increases the retrieval uncertainty when simple microwave brightness temperature difference algorithms are applied in a standalone fashion. These factors include heterogeneous sub-grid scale snow distribution, a distinctly multi-layered snowpack with dense, fine-grained wind slabs overlaying loose large grained depth hoar, and a high lake fraction (Derksen et al., 2009; 2010). In this study, we utilized a tundra-specific algorithm for North America that exploits the single frequency (37 GHz) brightness temperature response to SWE changes (see Derksen et al., 2010). SWE retrievals were also derived from the algorithm of Pulliainen (2006), which combines station observations of snow depth, forward passive microwave brightness temperature simulations, and satellite microwave measurements within an assimilation framework. This method was used to produce the recently released GlobSnow SWE data record (www.globsnow.info). Since 1999, the Canadian Meteorological Center (CMC) has produced an operational daily gridded global snow depth analysis (Brasnett, 1999) by combining climate station snow depth

observations with a background first guess field produced using a simple snow model forced by temperature and precipitation fields from the Canadian forecast model (Brasnett, 1999). The same methodology was applied in ‘hindcast’ mode by Brown et al (2003) to develop a snow depth and estimated SWE analysis over North America for the 1979-1997 period. SWE was also extracted from the ERA-interim atmospheric reanalysis. Snow depth, snow water equivalent, and snow density estimates in ERA-interim are generated by the forecast model and updated based on a Cressman analysis of station observations of snow depth and (when available) snow cover data from satellites (Drusch et al., 2004) Further details are provided in Dee et al. (2011).

Northern Hemisphere SCE values were compiled as monthly averages for April, May, and June, months when snow cover is largely confined to the Arctic. A single SCD value was calculated for the first and second half of each snow season, in order to isolate changes in the snow cover season due to variability in snow-on and snow-off dates. The SWE time series was derived for April which approximates the peak annual SWE across the Arctic. Standardized anomalies for all time series were calculated using a 1988-2007 reference period.

Table 1: Summary of SCE data sources utilized in Brown et al. (2010).

Description	Acronym	Period	Resolution	Data Source
Snow-off date from Arctic Polar Pathfinder Advanced Very High Resolution Radiometer (AVHRR) dataset	CCRS	1982-2004	5 km	Canada Centre for Remote Sensing (CCRS), Zhao and Fernandes [2009]
Daily snow depth analysis from in situ observations and a snow model	CMC	1998-2008	~35 km	Canadian Meteorological Centre (CMC), Brasnett [1999]
ERA-40 reanalysis daily snow depths	ERA-40	1957-2002	~275 km	European Centre for Medium-Range Weather Forecasts (ECMWF), Uppala et al. [2005].
ERA-40 reconstructed snow cover duration with temperature-index snow model of Brown et al. [2003]	ERA-40rec	1957-2002	~275 km (with 5 km empirical elevation adjustment)	Environment Canada (EC), Brown et al. [2010]
NOAA IMS daily 24 km snow/no-snow product	IMS-24	1997-2008	24 km	National Snow and Ice Data Center (NSIDC), Ramsay [1998]
NOAA IMS daily 4 km snow/no-snow product	IMS-4	2004-2008	4 km	NSIDC, Helfrich et al. [2007]
MODIS 0.05° monthly mean snow cover fraction (MOD10CM Version 5) product	MODIS	2000-2008	~5 km	NASA, Hall et al. [2006]
NCEP thaw index – snow-off date estimated from 0°C crossing date with NCEP1 Reanalysis daily temperatures	NCEP	1948-2008	~275 km	Earth System Research Laboratory, NOAA, Kalnay et al. [1996]
NOAA weekly snow/no-snow	NOAA	1966-2008	190.5 km	Rutgers U., Robinson et al., [1993]
Snow water equivalent from Scanning Multichannel Microwave Radiometer (SMMR, 1978-1987) and the Special Sensor Microwave/Imager (SSM/I, 1987-2008)	PMW	1978-2008	24 km	NSIDC, Savoie et al. [2009]
QuikSCAT snow-off date	QSCAT	2000-2008	~5 km	EC, Wang et al. [2008]

Table 2. Summary of SWE data sources.

Description	Acronym	Period	Resolution	Data Source
Passive microwave with forward model simulations and climate station observations	GlobSnow	1990-2010	25 km	Finnish Meteorological Institute, Pulliainen (2006)
ERA-interim reanalysis	ERA-int	1990-2010	~275 km	ECMWF, Simmons et al (2007), Dee et al. (2011)
Surface analysis + snow model	B2003	1990-1997	~35 km	EC, Brown (2003)
Surface analysis + snow model	CMC	1999-2010	~35 km	CMC, Brasnett (1999)
Passive microwave standalone	EC	1990-2010	25 km	EC, Derksen et al (2010)

3 RESULTS

SCD anomalies computed separately for the first (fall; Figure 1a) and second (spring; Figure 1b) halves of the snow year using the weekly NOAA CDR dataset provide information on changes in the start and end dates of snow cover. While the timing of the onset of snow cover (as captured by the fall SCD) shows little change over the satellite record, spring SCD anomalies (relative to the 1988-2007 reference period) exhibit a negative trend over the time series with a new record low spring SCD observed over both the North American and Eurasian sectors of the Arctic during 2010 (Figure 1b). This continues the trend to earlier spring snow melt over the Arctic identified from multiple datasets by Brown et al. (2010). Northern Hemisphere spring SCE for months when snow cover is confined largely to the Arctic (Figure 2), show increasingly negative trends as spring progresses, a tendency previously linked to the poleward amplification of SCE sensitivity to warming air temperatures (Déry and Brown, 2007).

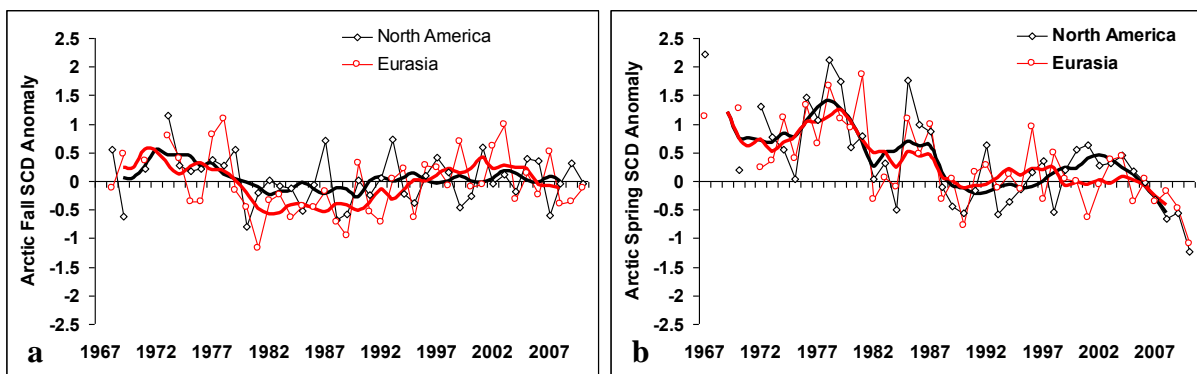


Figure 1. Arctic seasonal snow cover duration (SCD) anomaly time series (with respect to 1988-2007) from the NOAA snow chart CDR for (a) the first (fall) and (b) second (spring) halves of the snow season.

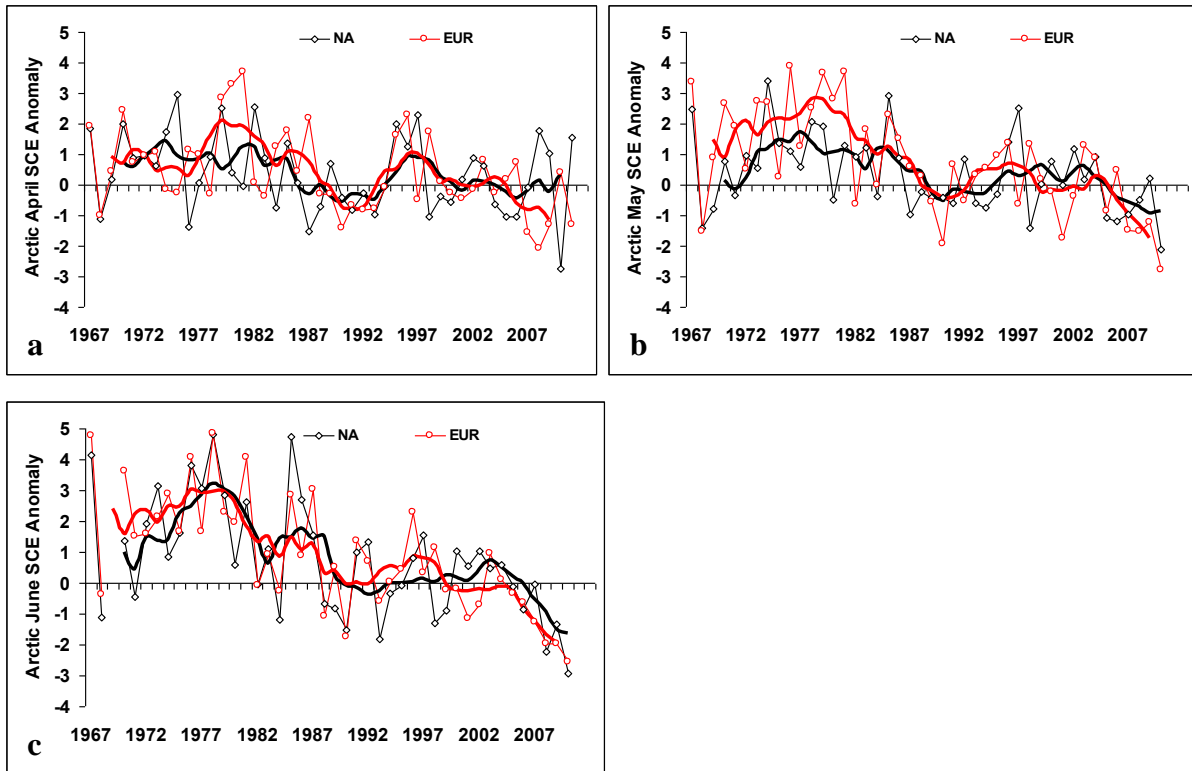


Figure 2. Arctic seasonal snow cover extent (SCE) anomaly time series (with respect to 1988-2007) from the NOAA snow chart CDR for (a) April (b) May and (c) June.

Evaluation of the April SWE climatologies for the four datasets in Table 2 with data in the 1998-2009 period (Figure 3) reveal large inter-dataset variance in SWE which was not unexpected, given the well documented challenges in characterizing SWE across the Arctic. The greatest inter-dataset differences were observed across the continental Arctic tundra of North America where the CMC and GlobSnow datasets have mean SWE values in the range of 50 to 100 mm, while the ERA-int and EC datasets have values in the range of 100 to 150 mm. The GlobSnow product is unable to capture SWE variability linked to topography over North America because a mountain mask is employed due to increased uncertainty in retrieval performance over complex terrain. The passive microwave derived products also do not retrieve the large coastal accumulations over eastern Baffin Island and Queen Elizabeth Islands, like due to the coarse resolution of the satellite microwave measurements and mixed land/sea grid cells in coastal areas. The CMC analysis produced notably lower SWE values than ERA-int although both products use similar data assimilation methodologies. Differences, therefore, must be related to different precipitation amounts in the forecast models or differing treatment of station snow depth observations.

In the Eurasian Arctic, the predominant feature characterized in all datasets is a region of high SWE across western Siberia. Stand-alone passive microwave retrievals have previously been shown to be anomalously low across this region (Clifford, 2010), so the ability of the GlobSnow, CMC, and ERA datasets to agree across western Siberia is notable. Other regions of peak SWE across northern Scandinavia and eastern Russia are also in agreement between the datasets.

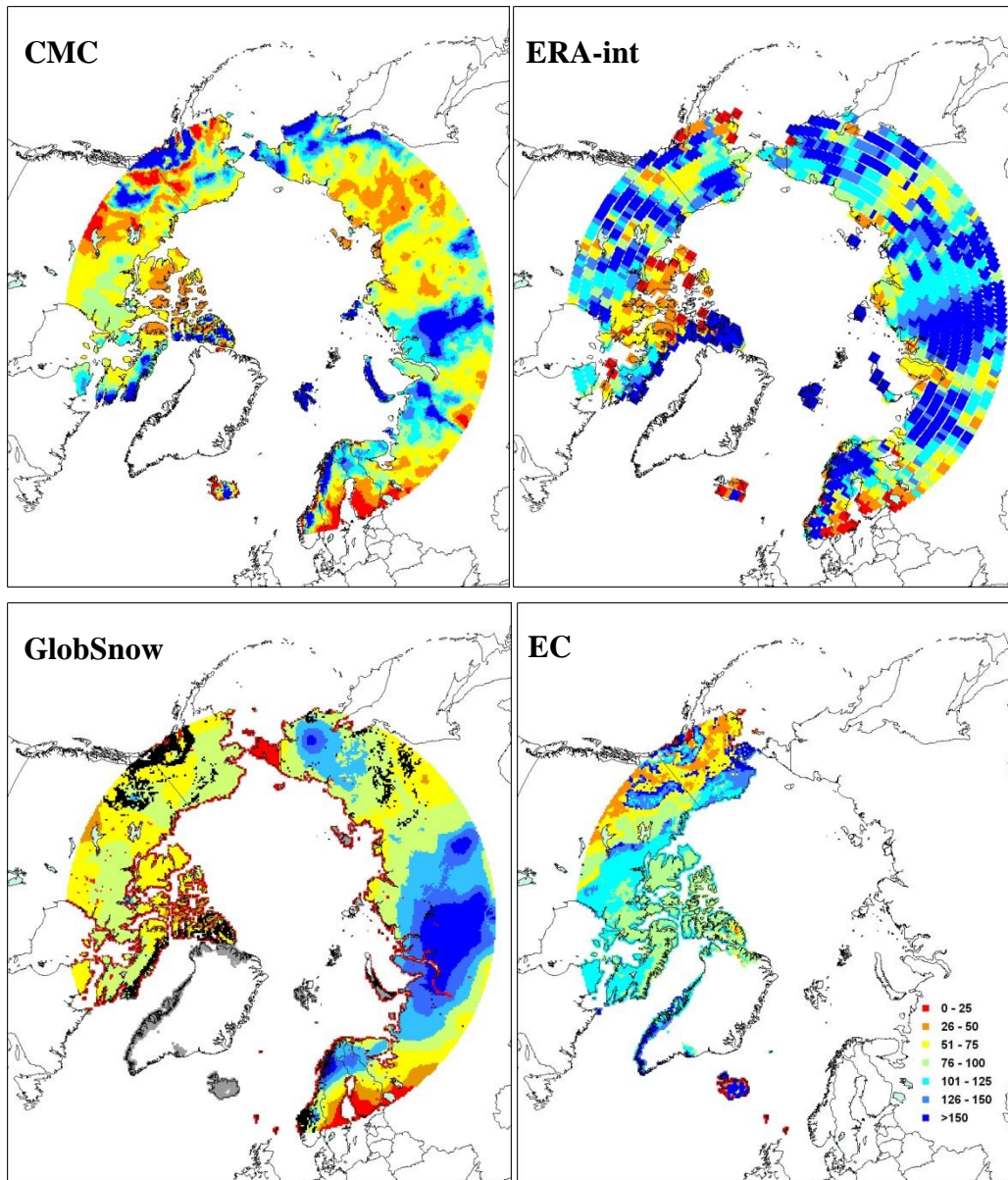


Figure 3. Spatial patterns of mean April SWE, 1998-2009 (mm) for the four data sources with overlapping data.

To further examine inter-dataset consistency, mean Arctic SWE values were computed for the months of March and April, 1988 through 2010 (Table 3). While all datasets consistently show peak SWE across the Eurasian Arctic occurs in March, the datasets are mixed whether peak SWE in the North American Arctic occurs in March or April. The ERA-int and CMC datasets show peak SWE during both March and April is higher in North America than Eurasia, which is not reflected in the GlobSnow dataset.

Multi-dataset Arctic SWE time series derived for 1988 through 2010 are shown in Figure 4. Prior to 2004, SWE anomalies across the North American Arctic were out of phase with Eurasia ($r=-0.49$), but the two sectors are both characterized by increasing SWE anomalies over the past 7 years ($r=0.67$). Composite differences (2004-2010 minus 1988-2003) in surface temperature and relative humidity at 700 mb from the NCEP/NCAR reanalysis were plotted in order to determine if changes in atmospheric parameters were consistent with the

SWE anomaly reversal over North America. These data (Figure 5) show that the 2004-2010 period was characterized by generally warmer temperatures and higher humidity (relative to 1990-2003) across the NA sector, consistent with the continental scale shift in SWE anomalies.

Table 3. Summary of mean continentally averaged Arctic SWE for March and April.

	ERA-int	CMC	GlobSnow	EC
March NA	243	112	83	85
April NA	230	114	73	99
March EUR	175	100	126	
April EUR	154	92	105	

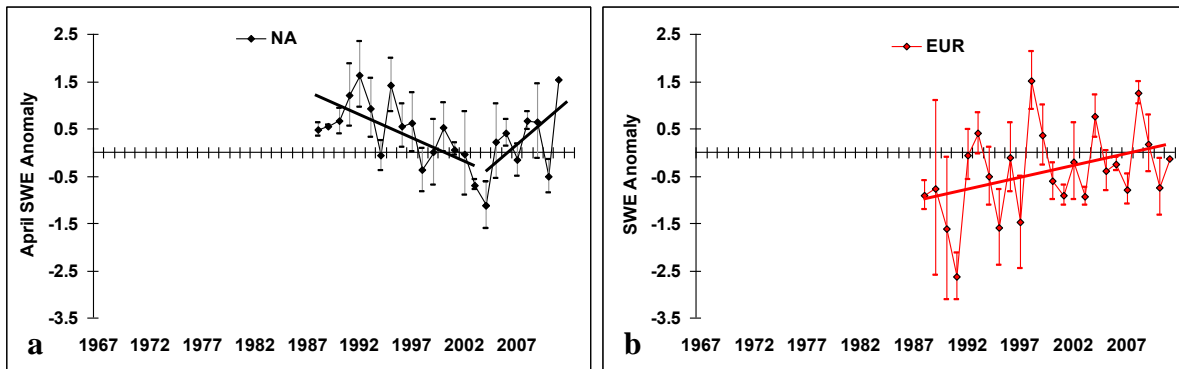


Figure 4. Time series of multi-dataset average monthly April snow SWE anomalies (+/- the standard error) relative to 1988-2007 period for (a) North America and (b) Eurasia. Solid lines denote the linear trend; the break point in the NA trend is 2004.

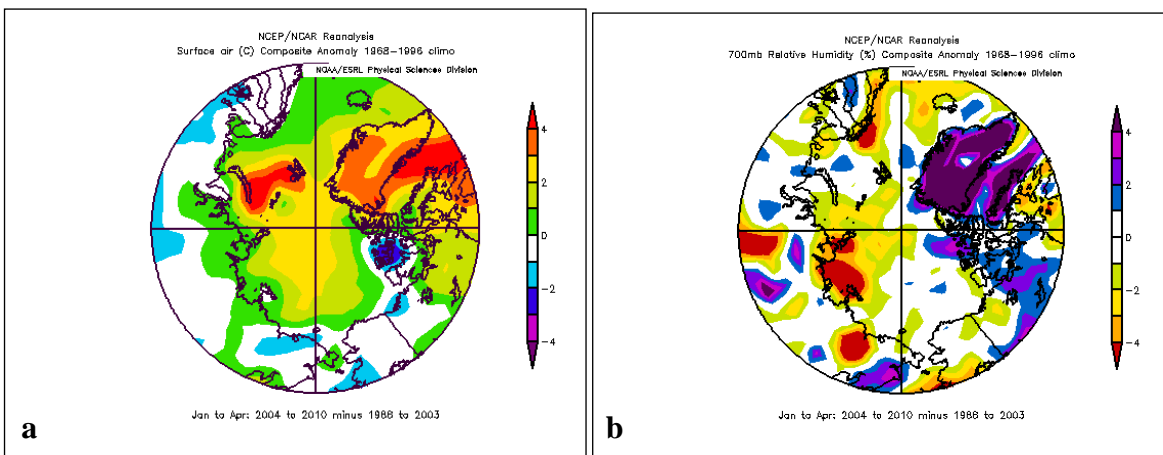


Figure 5. Composite anomalies of surface air temperature (a) and 700 mb relative humidity (b) for the January-April 2004-2010 minus 1990 to 2003.

The CMC and GlobSnow SWE datasets utilize climate station observations of snow depth within their analysis schemes, so a consideration when producing SWE time series is the quality and continuity in the reporting of station snow depth measurements. Observation quality is difficult to address, but a primary issue is the spatial representativeness of single point measurements when utilized to develop coarsely gridded products. A dataset of 2930 co-

located point snow depth and transect snow course measurements was compiled for Canada, spanning the winter seasons 1978/79 through 1992/93. These seasons were selected because the number of Environment Canada snow courses decreased sharply in the mid-1990's. Table 4 provides a statistical summary for all cases, and separated by land cover type. The root mean square error (RMSE) ranges from approximately 7 (prairie) to 18 (tundra) centimetres. The GlobSnow retrieval scheme utilizes a data assimilation approach, which requires that an observational variance be assigned to climate station snow depth. In current implementations, a variance of 150 cm² is applied to station snow depth observations - this value is appropriate given statistical assessment summarized in Table 4.

Table 4. Summary statistics for mean snow course versus single point climate station snow depth.

	R ²	RMSE (cm)	Mean Bias (cm)	Mean Depth (cm)	N
All data	0.68	9.3	-0.5	22.0	2930
Prairie	0.65	6.7	0.6	14.5	1485
Forest	0.69	10.1	-2.1	30.1	1276
Tundra	0.17	18.1	2.5	26.7	169

Temporal stability in the number of reporting stations (which would impact the spatial density of ground observations) was assessed by plotting the mean, minimum, and maximum number of daily snow depth observations for the Arctic in April (available from ECMWF) and utilized within the GlobSnow retrieval scheme. The mean number of stations reporting through the month of April varies by +/- 70 across Eurasia, and +/- 40 across North America (Figure 6). The impact of this variability on time series homogeneity remains to be determined, along with the impact of the transition from manual to automatic observations which occurred in many countries during the 1990's.

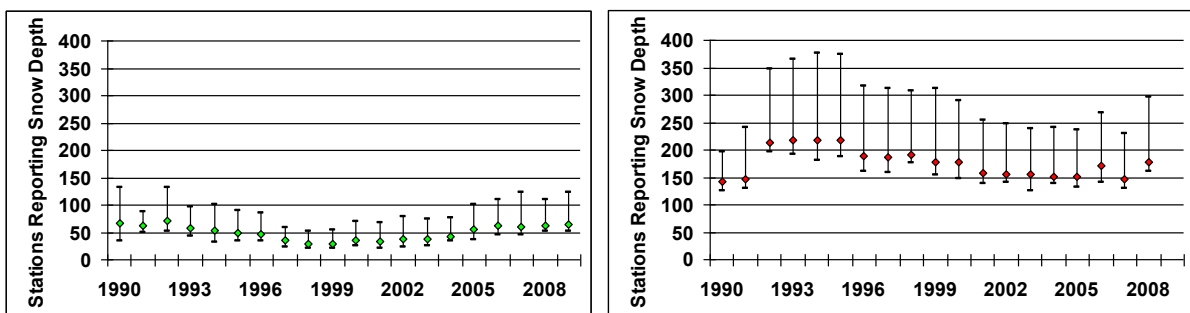


Figure 6. Mean (with maximum and minimum) number of land stations reporting snow depth in the month of April over the North American (left) and the Eurasian (right) sectors of the Arctic.

4 CONCLUSIONS

This study provides an update (through 2010) to the 1967-2008 Arctic SCE and SCD trends developed by Brown et al. (2010), with the addition of a multi-dataset SWE time series. Collectively, these data records provide a comprehensive overview of the state and variability of terrestrial snow cover through the satellite era at the pan-Arctic scale. SCD computed separately for the first (August–January) and second (February–July) halves of the snow year from the weekly NOAA snow chart CDR showed the timing of the onset of snow cover in fall changed little over the satellite record. A new record low spring SCD was observed over both the North American and Eurasian sectors of the Arctic during 2010. This continues the trend to earlier spring snow melt and extension of the growing season over the Arctic (Jia et al. 2008). The rate of decrease in Arctic June SCE since 1979 is actually similar to that observed for sea ice extent, as discussed in more detail in Brown et al. (2010).

Inter-dataset differences in absolute SWE values are relatively high: the individual datasets exhibited considerable spread in the timing and magnitude of pre-melt SWE estimates. The anomaly series, however, showed reasonable agreement from January through April, and indicated an increase in peak pre-melt SWE across Eurasia, in spite of the trend toward earlier snow melt and a shorter snow cover season. Prior to 2004, SWE anomalies across the North American Arctic were out of phase with Eurasia, but both sectors are characterized by increasing SWE anomalies since then. Over the past 10 years, the combination of continental wide increases in SWE coupled with reduced spring SCD is consistent with earlier peak stream flow, a more rapid recession limb, and higher peak runoff volume, as reported by Shiklomanov and Lammers (2009). Further work is required to better understand the differences in SWE evident between the various datasets.

ACKNOWLEDGEMENT

Thank-you to our data providers: National Snow and Ice Data Centre, ECMWF, NOAA Earth System Research Laboratory, Rutgers University Snow Laboratory, and the Canadian Meteorological Centre.

REFERENCES

- Brasnett, B. 1999 A global analysis of snow depth for numerical weather prediction. *J. App. Meteorol.* **38**, 726-740.
- Brown, R., Brasnett, B. and Robinson, D. 2003 Gridded North American monthly snow depth and snow water equivalent for GCM evaluation. *Atmos-Ocean*. **41**, 1-14.
- Brown, R., and Mote, P. 2009. The response of Northern Hemisphere snow cover to a changing climate. *J. Climate*. **22**, 2124-2145.
- Brown, R., Derksen, C. and Wang, L. 2010 A multi-dataset analysis of variability and change in Arctic spring snow cover extent, 1967-2008. *J. Geophys. Res.* doi:10.1029/2010JD013975.
- Brown, R., and Robinson, D. 2011 Northern Hemisphere spring snow cover variability and change over 1922–2010 including an assessment of uncertainty. *The Cryosphere*. **5**, 219–229.
- Clifford, D. 2010 Global estimates of snow water equivalent from passive microwave instruments: history, challenges and future developments. *Int. J. Remote Sens.* **31**, 3707–3726.
- Dee, D. P., Uppala, S. M., Simmons, A. J., Berrisford, P., Poli, P., Kobayashi, S., Andrae, U., Balmaseda, M. A., Balsamo, G., Bauer, P., Bechtold, P., Beljaars, A. C. M., van de Berg, L., Bidlot, J., Bormann, N., Delsol, C., Dragani, R., Fuentes, M., Geer, A. J., Haimberger, L., Healy, S. B., Hersbach, H., Hólm, E. V., Isaksen, L., Kållberg, P.,

- Köhler, M., Matricardi, M., McNally, A. P., Monge-Sanz, B. M., Morcrette, J.-J., Park, B.-K., Peubey, C., de Rosnay, P., Tavolato, C., Thépaut, J.-N. and Vitart, F. 2011 The ERA-Interim reanalysis: configuration and performance of the data assimilation system. *Quart.J.Royal .Met. Soc.*, **137**, 553–597. doi: 10.1002/qj.828
- Derksen, C., Toose, P. Rees, A. Wang, L. English, M. Walker, A. and Sturm, M. 2010 Development of a tundra-specific snow water equivalent retrieval algorithm for satellite passive microwave data. *Remote Sens. Environ.* **114**, 1699-1709.
- Derksen, C., Sturm, M. Liston, G. Holmgren, J. Huntington, H. Silis, A. and Solie, D. 2009 Northwest Territories and Nunavut snow characteristics from a sub-Arctic traverse: Implications for passive microwave remote sensing. *J. Hydromet.* **10**, 448-463.
- Dery, S., and Brown, R. 2007 Recent Northern Hemisphere snow cover extent trends and implications for the snow-albedo feedback. *Geophys. Res. Lett.* **34**, L22504, doi:10.1029/2007GL031474.
- Drusch M, Vasiljevic D, Viterbo P. 2004 ECMWF's global snow analysis: assessment and revision based on satellite observations. *J. Appl. Meteorol.* **43**, 1282–1294.
- Jia, G. Epstein, H. and Walker, D. 2009 Vegetation greening in the Canadian Arctic related to decadal warming. *J. Environ. Monit.* **11**, 2231–2238.
- Pomeroy, J. and Li, L. 2000 Prairie and Arctic areal snow cover mass balance using a blowing snow model. *J. Geophys. Res.* **105**, 26 619-26 634.
- Pulliainen, J. 2006 Mapping of snow water equivalent and snow depth in boreal and sub-arctic zones by assimilating space-borne microwave radiometer data and ground-based observations. *Remote Sens. Environ.* **101**, 257-269.
- Ramsay, B. 1998 The interactive multisensor snow and ice mapping system. *Hydrol. Proc.* **12**, 1537-1546.
- Robinson, D., Dewey, K. and Heim, R. 1993 Global snow cover monitoring: an update. *Bull. American Met. Soc.* **74**, 1689-1696.
- Shiklomanov, A. and Lammers, R. 2009 Record Russian river discharge in 2007 and the limits of analysis. *Environ. Res. Lett.*, **4**, 045015, doi:10.1088/1748-9326/4/4/045015.
- Simmons, A., Uppala, S. Dee, D. Kobayashi, S. 2007 ERA-Interim: New ECMWF reanalysis products from 1989 onwards. *ECMWF Newsletter No. 110 – Winter 2006/07*, 25-35.
- Sturm, M., McFadden J., Liston, G. Chapin, S. Racine C. and Holmgren, J. 2001 Snow-shrub interactions in Arctic tundra: a hypothesis with climatic implications. *J. Climate.* **14**, 336-344.

Thank you to our sponsors:

